drones

MDPI

Article

Simulation-Based Airspace Accessibility Analysis for Integrating Regional Unmanned Aircraft Systems into Non-Towered Airport Traffic Patterns

Tim Felix Sievers

Institute of Flight Guidance, German Aerospace Center (DLR), 38108 Braunschweig, Germany; tim.sievers@dlr.de

Highlights

What are the main findings?

- Simulation results show that UAS holdings can be considered as an effective deconfliction strategy in uncontrolled terminal airspace, as they can be frequently conducted in the lowest available holding altitude (i.e., 2500 ft AGL). However, in more congested settings with increased UAS traffic volumes (i.e., one approaching UAS every 15 min instead of 30 min), holding demand and delay propagation increases and holdings may expand into vertical altitude bands.
- Extending look-ahead times for conflict detection (i.e., 60/120/180 s) reliably increases how often and for how long UAS must hold (e.g., more holding cases and more holding orbits), illustrating the expected trade-off between safety and efficiency, where a more conservative conflict detection improves safety margins but reduces UAS throughput.

What are the implications of the main findings?

- UAS access to uncontrolled terminal airspace cannot be seen as a static challenge, as accessibility changes with traffic demand, expected traffic intent, and operational constraints (e.g., DAA capabilities). Therefore, operational UAS integration and required procedural separation schemes should be assessed at each airport individually, rather than assumed to work as a "one size fits all" approach.
- Longer look-ahead times to detect conflicts with manned aircraft enable more stable holding executions but reduce UAS throughput and increase delay propagation, implying that UAS operating schemes must balance safety and efficiency, especially in terminal environments with higher traffic densities.

Abstract

Unmanned aircraft systems for regional operations are assumed to frequently operate at non-towered airports, where routine integration remains challenging due to limited separation principles and partially observable manned traffic intent. This research investigates tactical procedures for integrating unmanned aircraft into non-towered airport environments, where unmanned aircraft must interact with manned traffic under procedural constraints. A simulation framework is developed that combines historical traffic data with standard traffic pattern procedures and rule-based decision-making to integrate unmanned aircraft at non-towered airports. The simulation logic includes detection of manned traffic activities, rule-based queuing, and airspace capacity constraints. By varying detection look-ahead times (60/120/180 s) and unmanned aircraft traffic rates (15/30 min), the simulation quantifies terminal airspace accessibility and derives metrics that capture throughput (no conflict versus deconflicted holding flights), delay propagation (holding minutes and holding orbit counts), concept feasibility (aborted/denied holdings), and

Academic Editor: Kimon P. Valavanis

Received: 16 January 2026
Revised: 13 February 2026
Accepted: 14 February 2026
Published: 17 February 2026

altitude band utilization. The results show a consistent safety versus throughput trade-off with longer look-ahead times increasing holding demand but reducing the share of aborted holdings, while higher traffic volumes amplify holdings and delay. Holdings are predominantly conducted in the lowest available holding altitude at 2500 feet above the ground, with occasional multi-layer use to handle traffic peaks.

Keywords: UAS; regional air mobility; airspace integration; non-towered airport; VFR traffic uncertainty; traffic pattern; holding stack; fast-time simulation

1. Introduction

New air mobility concepts, including the integration of Unmanned Aircraft Systems (UAS), are increasingly focused on Urban Air Mobility (UAM), with tightly managed operations around newly developed vertiports and highly structured air taxi corridors [1,2]. These concepts are considered relevant for short-haul passenger operations, one use case of many envisioned for future aviation. A second use case, Regional Air Mobility (RAM), is envisioned to deploy regional cargo UAS to leverage existing airport infrastructure and connect smaller communities with time-critical logistics [3,4]. In practice, these operations are expected to involve under-utilized airports without an operating Air Traffic Control (ATC) tower, referred to as non-towered airports in this work, where integration with manned traffic is considered one of the most demanding challenges of UAS integration [5–7]. However, to date, most of the research on UAS integration into terminal environments has focused on major towered airports under supervision of ATC [8–10].

Non-towered airports represent a unique operational environment. Unlike towered airports, which are often capacity constrained and therefore not ideal to integrate UAS on a larger scale, ATC does not provide separation and sequencing information to aircraft in the terminal airspace. Instead, pilots rely on visual self-separation, meteorological conditions, and radio traffic advisory (the latter being potentially incomplete, delayed, or even absent). As a result, traffic activities around non-towered airports are heterogeneous in behavior and equipment and depend on airport-specific integration procedures as well as individual pilot preferences and technique [11].

From a UAS perspective, this setting elevates both state uncertainty (what nearby aircraft are doing) and intent uncertainty (what nearby aircraft will do next), increasing uncertainty in conflict probability estimates and feasible trajectory planning. On the one hand, state uncertainty may be resolved through electronic conspicuity regulations (e.g., broadcasting current flight positions through certified transponders) [12] or the availability of Ground-Based Surveillance Systems (GBSS) [13] in the vicinity of a non-towered airport. However, resolving intent uncertainty, such as projecting reliable manned flight behaviors, remains a key challenge for UAS integration into uncontrolled terminal airport environments [14,15].

Therefore, Detect And Avoid (DAA) systems for UAS are currently being tested and certified to determine the likelihood of a loss of "DAA well clear" and to trigger avoidance guidance if needed by using surveillance-based state estimates (e.g., aircraft position and speed) [16–18]. However, the integration of UAS at non-towered airports becomes increasingly more complex if less predictable Visual Flight Rules (VFR) traffic is present.

VFR-flying aircraft separate according to "see and avoid" principles and generally use a schematic circular Traffic Pattern (TP) to approach a non-towered airport. In contrast, Instrument Flight Rules (IFR) traffic, which is subject to ATC services and requires a flight plan to be filed prior to their flight, follows fixed approach Waypoints (WPs) if an

Instrument Approach Procedure (IAP) is active. However, at many non-towered airports, especially in Germany, an IAP is not installed and VFR is the only operating mode under certain meteorological conditions. More importantly, at non-towered airports, sequencing and spacing between aircraft is the responsibility of the pilot, which in case of a UAS, is given to the Remote Pilot (RP) on the ground. Consequently, in the absence of an IAP, the RP will have to comply with current "see and avoid" principles, which poses another regulatory hurdle for UAS integration.

Increased intent uncertainty of VFR traffic, the lack of certified DAA systems for use in terminal airspace, and missing UAS operating schemes lead to a central dilemma for UAS integration into non-towered airport TPs: safety versus efficiency. Although conservative assumptions about VFR traffic behaviors and respective uncertainty considerations may ensure safe separation, airspace access may be considered infeasible or economically unattractive for regional cargo UAS use cases. In contrast, aggressive UAS integration strategies risk conflict probabilities in environments where VFR intent is inherently difficult to project due to individual spacing, sequencing, and TP maneuver preferences of manned traffic.

Therefore, this research aims to answer the following questions:

- First, how does the spatio-temporal traffic distribution in terminal airspace segments impact UAS integration into non-towered airport TPs?
- Second, how effective are UAS integration options into non-towered airport TPs based on standard integration procedures and holding maneuvers?

This paper argues that scalable UAS integration at non-towered airports requires a joint consideration of structured real-world traffic data using historical manned flight tracks, near-term intent prediction, and state-of-the-art DAA principles to achieve UAS operational feasibility. The contribution of this work is to move towards a holistic UAS integration framework by advancing and validating a UAS operating scheme that has been proposed by the author in previous joint research, see Ref. [11], conducted by the United States (US) National Aeronautics and Space Administration (NASA) and the German Aerospace Center (DLR). In Ref. [11], a holding stack concept for UAS is proposed above the airport-specific TP of non-towered airports, which is validated in this paper to assess interaction behaviors of UAS and manned aircraft in uncontrolled terminal environments.

The UAS holding stack concept presented in Ref. [11] is advanced by developing a simulation-based assessment framework, including a conflict detection logic and procedural deconfliction rules, to implement and evaluate the holding stack concept. Empirical validation is ensured by deriving the traffic environment and procedural baseline conditions from observed manned operations, enabling concept evaluation against realistic TP usage and manned traffic variability. This work proposes a simulation study to empirically assess when and how UAS can access uncontrolled terminal airspaces using standard TP approach procedures and holding options for UAS integration. The UAS holding stack concept is inspired by conventional traffic flow management techniques, where ATC assigns holding patterns to IFR traffic around major airports to manage delays and airspace saturation [19], for example.

This paper will provide background information on standard TP integration procedures, the proposed holding stack concept for UAS, and required UAS capabilities for terminal airspace integration in Section 2. Section 3 will explain the conceptual operating scheme for UAS integration that is used as a baseline architecture for this work and will derive the simulation principles and its design. In Section 4, empirical results on temporal and spatial manned traffic distributions at selected non-towered airports will be presented, and simulation findings will be analyzed and discussed. Finally, Section 5 will provide concluding remarks.

2. Background: Terminal Airspace Integration of Regional UAS

The scope of this research remains similar to that of the author's previous work, as Germany is considered highly relevant as an area for the potential introduction of initial cargo UAS operations [20]. Due to its central location in the heart of Europe, the high number of long-haul international flight connections and the presence of major cargo hubs (DHL at Leipzig/Halle (EDDP) airport and UPS at Cologne/Bonn (EDDK) airport), Germany is the busiest European country in terms of annual cargo flight movements. Despite Germany's relatively low share of cargo operations by regional aircraft (∼6%), which have a Maximum Takeoff Weight (MTOW) of up to 25 metric tonnes (t) [21], compared to Spain (∼22%) or Norway (∼29%) for example, Germany has the highest number of non-towered airports in Europe relevant for initial cargo UAS operations [22].

Since non-towered airports, by definition, do not have an operating control tower that provides ATC separation services for aircraft in the airport vicinity, their operating volume is relatively limited, and many non-towered airports are considered to be under-utilized. Regarding the initial integration of UAS at these airports, it can be argued that relatively low manned traffic volumes in terminal airspaces will potentially lead to fewer flight path conflicts with UAS. Compared to high-traffic-volume airport environments in controlled airspace, many European airports are already capacity constrained, and the introduction of new airspace entrants is expected to increase significant workload on ATC [8,9]. On the other hand, non-towered airport environments are usually subject to "see and avoid" separation principles, which lead to an increased uncertainty of flight intent due to the increased operational flexibility of VFR pilots [14].

Different types of retrofitted and newly developed UAS vehicles are expected to enter the cargo market in the next decade, including electric Vertical Takeoff and Landing (eVTOL) aircraft, fixed-wing aircraft, and hybrid solutions of different wing and propulsion configurations. Larger fixed-wing configurations are currently pioneering initial unmanned cargo operations in the regional aviation realm such as a retrofitted variant of the Cessna 208 Caravan (e.g., used by Reliable Robotics [23] or Merlin Labs [24]) or newly developed airframe designs (e.g., the "Nuuva V300" by Pipistrel [25]); see Figure 1.

(**a**) (**b**)

Figure 1. Examples of unmanned cargo aircraft: (**a**) Cessna 208 Caravan (Credit: Textron Aviation Inc.) [26] retrofitted by companies such as Reliable Robotics or Merlin Labs. (**b**) Concept design "Nuuva V300" by Pipistrel (Credit: Pipistrel d.o.o.) [25].

In Europe, these types of unmanned cargo operations will likely be conducted in the "certified" category as defined by the European Union Aviation Safety Agency (EASA) as operations with the "highest level of risk". UAS in this category will need to have a

type certificate and a certificate of airworthiness, similar to today's regulations for manned aviation. In addition, the UAS operator and the RP in charge of monitoring the UA will also require license and approval [27]. To date, civilian UAS operations of the "certified" category have not been established in Europe.

2.1. Standard Integration Procedures at Non-Towered Airports

In traditional airspaces, pilots can fly according to two main sets of flight rules: IFR and VFR. The pilot's decision on which flight rule to use depends on different factors, such as airspace class regulations, meteorological conditions, operational safety, and operational flexibility. Based on meteorological conditions during a flight, the pilot on board an aircraft can operate following IFR or VFR under Visual Meteorological Conditions (VMC) or be restricted to operate only under IFR in Instrument Meteorological Conditions (IMC) if equipped and trained appropriately. VMC is the only meteorological condition that allows pilots to fly their aircraft according to the principles of "see and avoid", namely VFR.

At non-towered airports, flying according to "see and avoid" principles, as envisaged by the International Civil Aviation Organization (ICAO) in Annex 2—Rules of the Air [28], is often preferred for operational efficiency. Generally, under VFR, pilots do not have to follow published procedures such as Standard Terminal Arrival Routes (STAR) or Standard Instrument Departure Routes (SID), which are commonly used by ATC to separate IFR aircraft via initial approach fix points in controlled terminal airspaces. In addition, VFR flights usually do not have to file a flight plan, in contrast to IFR flights, and communication and intent sharing with ATC are not required around non-towered airports, for example. In general, a VFR aircraft that approaches a non-towered airport following "see and avoid" principles usually follows a standard schematic airport TP to separate from other traffic and to remain predictable to other airspace users (see Figure 2).

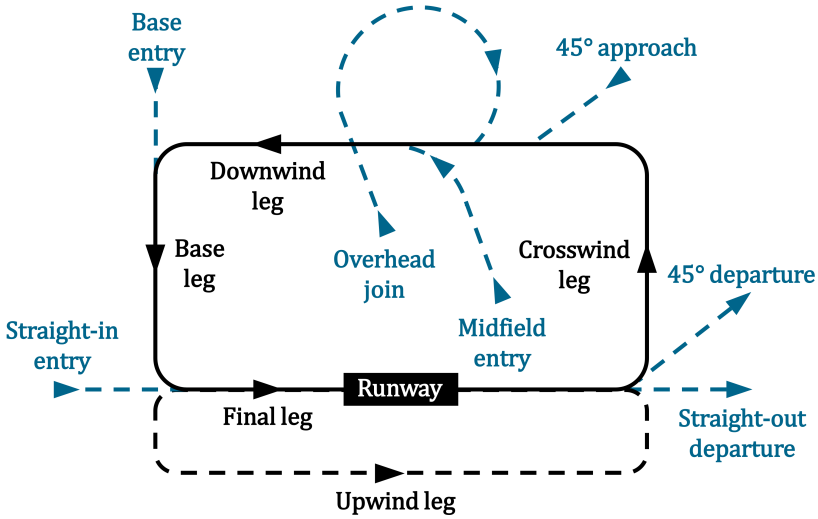

Figure 2. Standard airport TP scheme [29]—own depiction.

The standard airport TP consists of different legs, which are flown by pilots according to their personal preferences, meteorological conditions, airport topography, and in-flight behaviors of other airspace users in and around the TP. For a VFR aircraft, it is common to fly the airport TP counterclockwise and integrate into the TP via a 45° approach or via an overhead join into the downwind leg. Other entry and departure procedures can be seen in Figure 2. Based on the performance characteristics of the approaching aircraft, conventional TP altitudes (TPA) range from 500 ft (∼150 m) to 1500 ft (∼460 m) Above Ground Level (AGL). A detailed description of regulations and standard flight procedures in and around TPs can be found in Refs. [30,31].

2.2. UAS Holding Stack Concept

In the past, concepts have been proposed to overcome the dilemma of integrating airspace users who are incapable of executing a "see and avoid" approach at non-towered airports. Concepts such as the Small Aircraft Transportation System (SATS) program, which was carried out by NASA from 2001 to 2006, were intended to allow self-sequencing of manned aircraft using vertical holding areas at non-towered airports under IMC [32].

With the emergence of retrofitted and novel aircraft types in recent years, such as fixed-wing cargo UAS (e.g., developed by Reliable Robotics [23], Merlin Labs [24], and Pipistrel [25]), a revitalization of regional aviation and traffic at under-utilized non-towered airports is expected [3,4]. However, to date, airspace integration with manned traffic remains one of the most challenging UAS airspace integration problems [5–7]. Furthermore, there are only limited research and data available to quantify the behavior of manned aircraft and to derive UAS integration options and strategies for efficient and safe UAS integration in uncontrolled terminal airspaces [33,34].

An analysis and comparison of different (UAS) integration concepts at non-towered airports can be found in Ref. [11].

In previous joint research conducted by NASA and DLR, the author of this paper proposed a holding stack concept for UAS above the airport-specific TP of non-towered airports to deal with manned aircraft in uncertain airspace environments (see Ref. [11]). The concept proposes that if a UAS is unable to integrate into the airport TP due to uncertain manned traffic behavior or a Lost Command and Control Link (LC2L) (i.e., the Command and Control (C2) link between the UA and the RP is severed), the UAS will transfer into a circular holding pattern above the TP until it is safe to integrate into the airport TP and land (see Figure 3). From holding, the UAS is expected to integrate via a standard overhead join into the downwind leg of the TP and land at the airport (see Figure 4a).

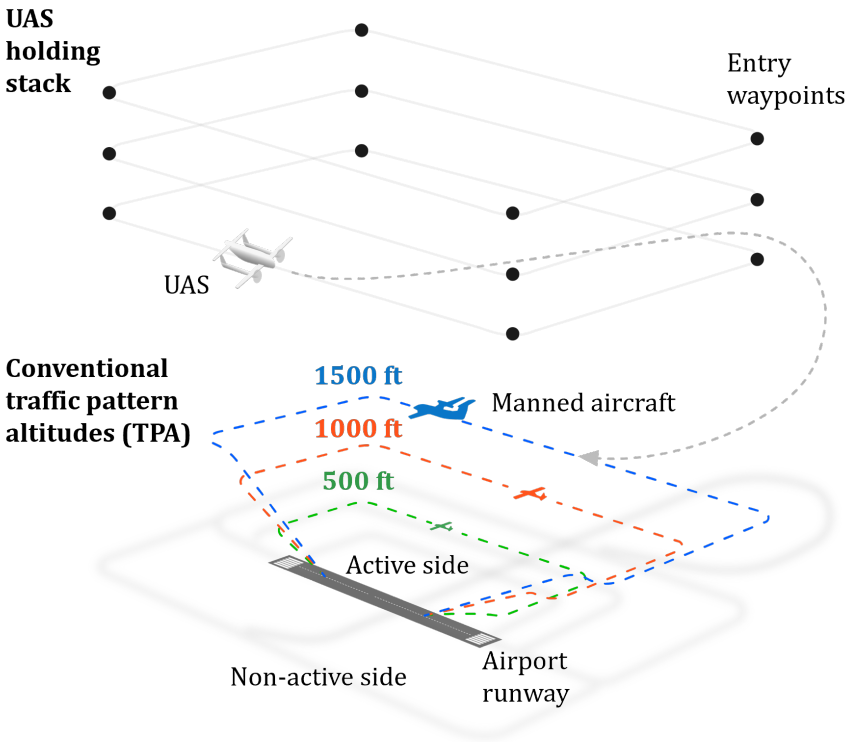

Figure 3. Conceptual scheme of the UAS holding stack above conventional TPA with UAS overhead join from holding into the TP; modified from Ref. [11].

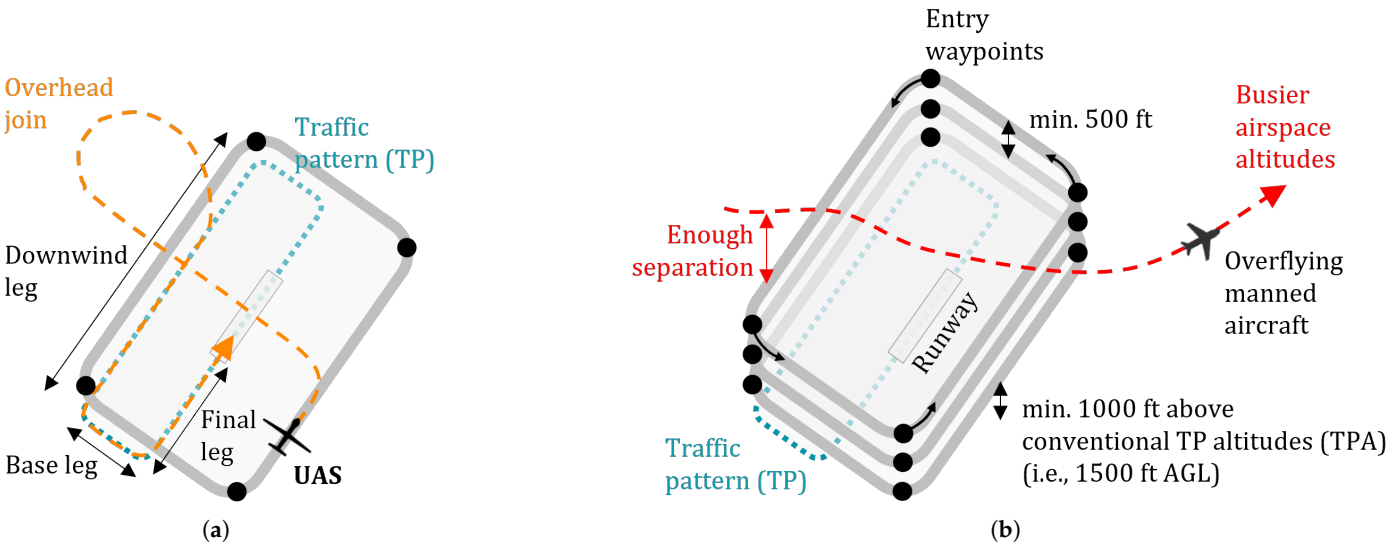

Figure 4. Conceptual design of the UAS holding stack above conventional TPA according to the dimension of the airport-specific TP (top view); modified from Ref. [11]: (**a**) UAS holding stack design with one layer (gray rectangle) with UAS overhead join approach from holding into TP towards runway (orange-dashed line). (**b**) UAS holding stack design with vertical layers (gray rectangles).

The size of the holding stack legs is supposed to be the size of the standard TP legs of the airport with extensions towards the non-active side of the airport by doubling its size. This allows the UAS sufficient time and space to integrate from the holding with other aircraft, if necessary (see Figure 4). In addition, the bottom layer of the holding stack will need to be vertically separated from the airport standard TP, while each holding layer will need to be separated from traffic streams; see busier airspace altitudes in Figure 4b.

The UAS holding stack concept is based on several assumptions, which are discussed in more detail in the following sections: "First, it is expected that policy makers and regulators will certify onboard DAA functions for UAS to enable safe separation from VFR aircraft in terminal environments. Second, to enable VFR-like operational flexibility and IFR-like airspace accessibility, authorities will have to adapt current flight rules or introduce new sets of flight rules to enable highly automated UAS operations at scale, especially in uncontrolled airspace. Third, traffic management concepts such as U-space and respective digital services will have to be certified and implemented to enable increasingly automated and cooperative airspace interaction between traditional airspace users and new airspace entrants" [11] (p. 46). For a detailed description of the UAS holding stack design, the conceptual UAS operating scheme, the interaction analysis of manned traffic behaviors to identify holding locations and UAS integration options, the application of the holding stack concept to different real-world non-towered airport environments, respective UAS integration hurdles, and the concepts limitations, see Ref. [11].

2.3. Required UAS Capabilities for Terminal Airspace Integration

Generally, it can be assumed that increased traffic around a non-towered airport will lead to higher overall traffic intent uncertainty and larger spreads of the flown airport TP. For an in-depth analysis of different flight metrics and their standard deviations to measure uncertainty of historical flight behaviors at non-towered airports, see Ref. [11]. UAS holding stacks are proposed to effectively resolve traffic situations with a high degree of uncertainty in traffic intent. In some traffic scenarios, holding might not be the most efficient conflict resolution strategy for UAS, but it provides a practical mechanism to trade efficiency for safety when interacting with manned aircraft. Efficient UAS trajectory

planning may require operating in airspace segments with high utilization by manned aircraft, for instance by directly integrating into the final leg of an airport TP, which may compromise flight safety. In contrast, routing the UAS through airspace segments with low interaction risk is likely to reduce efficiency and/or predictability of UAS behavior for other airspace users.

Operational integration of UAS into non-towered airport environments requires certain system capabilities of the UA, the RP station, the C2 link, and the overall traffic management. Required system capabilities to enable cooperative interaction of mixed traffic (i.e., manned and unmanned) can be achieved by traffic management concepts such as U-space, Europe's unmanned traffic management system. U-space defines technical and operational requirements within a regulatory framework to enable scaled airspace integration of UAS [35]. U-space and its digital services are anticipated to enable greater automation of UAS operations and improved connectivity between airspace users with the aim of increasing airspace capacity and accessibility. However, to date, U-space remains largely conceptual and is currently tested in pilot projects and experimental setups; see Ref. [36], for example. For more information on U-space and cooperative airspace access based on digital services, see Ref. [37] for the foundational Concept of Operation (ConOps) of the U-space architecture and Ref. [38] for a preliminary ConOps of U-space Flight Rules (UFR). For the role of the RP in the Terminal Maneuvering/Control Area (TMA) of an airport in controlled airspace and the different functionalities of the C2 link, see Ref. [39].

In the absence of UAS traffic management systems, additional means of detecting airspace users and corresponding solutions for procedural UAS integration are required, especially when integrating into complex non-towered airport environments. The following sections will elaborate on UAS capabilities such as DAA to enable safety-aware spacing and merging with manned traffic and UAS flight rules to enable "visual-like" flexibility in uncontrolled airspace.

2.3.1. UAS DAA Capabilities: Intent Prediction of Airspace Users

In today's Air Traffic Management (ATM) system, the prediction of an aircraft trajectory follows basic principles such as using cleared flight plans of IFR flights in controlled airspace environments, which are filed pre-flight along with separation assurances provided by ATC. However, in uncontrolled airspace, flight plans of VFR flights are usually not required, and ATC supervision is not guaranteed. Therefore, predicting VFR flight intent is subject to greater uncertainties, depending on the availability of flight information and the methods used to detect potential conflicts. In uncontrolled airspace, methods to predict aircraft trajectories are commonly based on the analysis of flight information by linear extrapolation of speed vectors or by investigating known flight plans [40]. Predicting trajectories by extrapolating the current aircraft position is known as dead reckoning navigation. This trajectory prediction approach can be particularly useful if the flight plans of aircraft are not available, but the current status data are [41]. In this context, the concept of state-based DAA refers to the detection and resolution of calculated conflicts based on the current state of the in-flight information of an aircraft [42,43]. However, the prediction of a conflict using state-based DAA is valid only for the look-ahead time in which the flight track status of an aircraft does not change [44].

During the last decade, research has been conducted to investigate various metrics for trajectory planning problems for traditional aviation and for different UAS use cases that face complex and uncertain traffic situations. Ref. [45] investigates the flexibility of an aircraft trajectory to mitigate the risk of constraint violation (i.e., separation, airspace, and traffic flow management constraints). They define a robustness and adaptability metric to measure the ability of an aircraft trajectory to remain feasible with no constraint violation

(i.e., robustness) and to regain feasibility in case of a constraint violation (i.e., adaptability). Analysis showed that applying trajectory flexibility results in reduced traffic complexity within self-organized traffic situations [45].

For UAS trajectory planning, Ref. [46] investigates trajectory feasibility and optimality metrics. The first includes performance-based parameters such as the maneuverability of an aircraft and constraints presented by airspace or operational limitations. The second refers to efficient trajectory planning considering minimum operational costs. Additionally, Ref. [47] presents two trajectory planning metrics for UAS operations in highly uncertain airspace environments. The first metric refers to the number of feasible UAS trajectories during the UAS flight, and the second metric to the robustness of these feasible trajectories. Consequently, Ref. [48] characterizes the effectiveness of trajectory planning metrics as flight survivability. The flight survivability originates in the military domain and describes the probability that the UAS has at least one feasible trajectory available to reach its destination [49]. In addition, Ref. [48] refers to the current situation of the UAS indicating the robustness of feasible trajectories. The UAS situation is distinguished by vehicle capabilities, environmental influences, operational policies, and flight dependent parameters such as different phases of flight [48,50]. However, current UAS flight survivability and flexibility formulations are typically evaluated using stochastic uncertainty models (e.g., Monte Carlo propagation) rather than being validated against context-specific historical manned flight track data (e.g., VFR TP behavior at non-towered airports) or in multi-aircraft scenarios (e.g., mixed traffic environments). Ref. [51] is the only identified research that proposes a VFR trajectory prediction model using historical traffic and weather data to forecast flight behavior around non-towered airports. However, Ref. [51] does not couple these predictions with the feasibility of UAS trajectories and operational constraints (e.g., DAA equipment) to compute reachable and conflict-free UAS trajectories along manned traffic.

To date, only a few studies have been presented using historical data sets to study feasible trajectories for UAS interaction with manned aviation around airports. However, these studies are exclusively focused on controlled terminal airspace environments. In the context of UAM, Ref. [52] uses historical aircraft and meteorological data to develop a probabilistic traffic model with spatial traffic distributions in the controlled terminal airspace of São Paulo-Guarulhos (SBGR) [52]. In addition, Ref. [53] introduces a data-driven approach to identify airspace segments in the terminal airspace for the integration of small UAS. Using historical Automatic Dependent Surveillance-Broadcast (ADS-B) data from manned flights for six days in 2018 and 2019, airspace segments below 500 ft (∼150 m) AGL were identified that had not been used by manned aircraft.

Studying UAS airspace integration at non-towered airports, Ref. [54] presents a NASA tool that generates TP approach trajectories based on user-defined scenario parameters to benchmark situational awareness, manned intent prediction, and trajectory planning. In its current form, the tool generates each UAS flight as a standalone trajectory; multi-aircraft interactions are not modeled, and conflicts are ignored. Moreover, the paper notes that the tool does not perform flight path feasibility checks such as validation against historical manned flight track data.

Additional simulation work for multi-UAS integration in terminal airspace focuses on controlled terminal airspaces by reducing the workload of the UAS operator and minimizing conflicts with ATC. In Ref. [55], a Tailored Trajectory Management (TTM) capability for UAS investigates conflicts up to a ∼20 min horizon and generates trajectory change proposals that the UAS operator would request from ATC rather than waiting for ATC to issue tactical instructions. However, the simulation study in Ref. [55] only focuses on UAS integration in controlled terminal airspace and does not model manned traffic uncertainty or trajectory planning in off-nominal situations, for example.

As a summarizing example, Figure 5 illustrates historical flight track data, colored by altitude AGL and centered to the airport runway, of the two busiest traffic days of 2022 around the German non-towered airport Juist (EDWJ). Both days represent peak times for terminal traffic, but the observed flight paths are highly variable and show limited repeatability from day to day below the conventional TPA (indicated in green colors) and above, i.e., 1500 ft (∼460 m) AGL. Historical flight data from August 13 (199 flight tracks) and August 14 (191 flight tracks), 2022 show significant differences in terms of turning points, flight path geometry, and altitude profiles. These daily variations indicate that at non-towered airports, flight intent is difficult to predict reliably given the limited number of recurring manned flight routes. As a result, intent uncertainty can be considered a key driver of reduced airspace accessibility for UAS, motivating robust UAS trajectory planning that can project a variety of feasible manned flight paths in uncontrolled terminal airspaces.

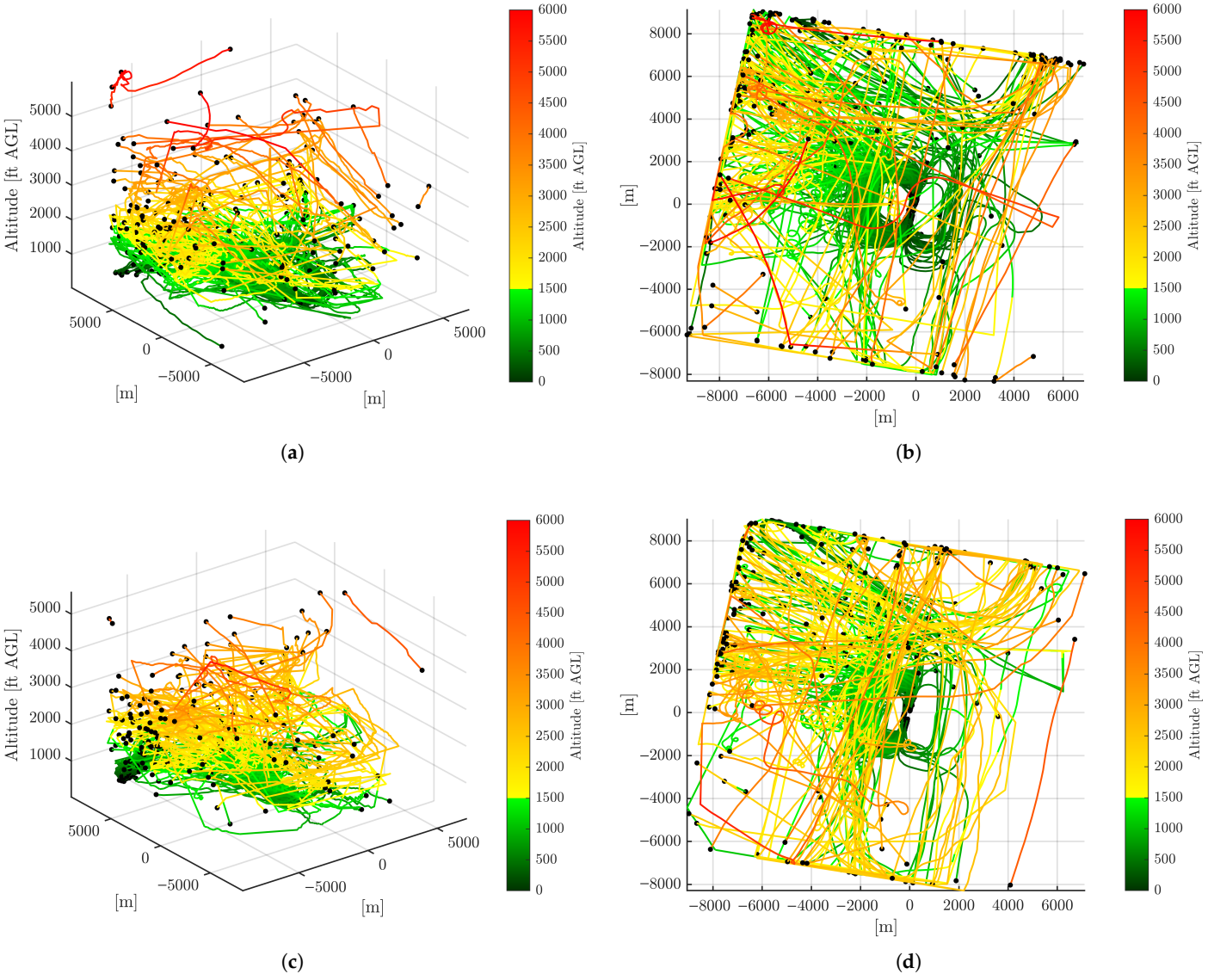

Figure 5. Runway-centered flight track data for the two busiest days at Juist (EDWJ), colored by altitude AGL. Saturday, 13 August 2022 with 199 flight tracks: (**a**) three-dimensional side view and (**b**) two-dimensional top view. Sunday, 14 August 2022 with 191 flight tracks: (**c**) three-dimensional side view and (**d**) two-dimensional top view.

It can be summarized that UAS trajectory feasibility is inherently linked to the intent prediction of other airspace users. It is challenging to translate surveillance data (e.g.,

aircraft positions) into feasible probabilistic forecasts of manned intent, which impact the set of reachable, conflict-free UAS trajectories. In uncontrolled terminal airspace, DAA functions can support these forecasts to estimate conflict probabilities and to plan operationally realistic interactions with manned traffic.

It becomes apparent that, for the civil airspace integration of UAS, especially in high-traffic scenarios with manned traffic, certified onboard DAA capabilities of UAS are required to enable operations beyond the current "see and avoid" principles [43]. DAA systems onboard regional cargo UAS are currently being developed and tested to autonomously detect and resolve in-flight conflicts with other airspace users en-route and in terminal airspaces [23,24]. However, integrated onboard DAA systems must provide the highest level of reliability by guaranteeing sufficient separation from other aircraft at any time. Therefore, they are currently considered more as an additional safety net for GBSS [37], which can support UAS integration by detecting non-cooperative airspace users and their current flight tracks around non-towered airports [13]. However, many non-towered airports are located in less busy regional areas and do not have access to surveillance radar systems.

In addition to integrated DAA capabilities on board the UAS and GBSS, U-space is intended to provide an ecosystem with flight information from all airspace users known to the U-space [35]. Digital U-space services could make use of historical flight data to predict the most probable flight path of manned aircraft according to their state-based flight information (i.e., using real-time electronic conspicuity traffic data) for a given time horizon. Traffic intent prediction could be implemented as part of tactical conflict detection and resolution U-space services to provide in-flight advisory and/or instruction services to the RP at non-towered airports. In U-space, tactical conflict management services will utilize performance-based information from different systems [56] and are expected to be deployed from the ground and not among airspace users [37]. This includes performance-based information from the UA and from Communication, Navigation, and Surveillance (CNS) and DAA systems, which can be used to provide dead reckoning navigation, the projected position of manned aircraft [38,56]. However, as mentioned above, U-space remains largely conceptual to date.

In summary, scaling UAS integration in complex environments, such as at non-towered airports, depends on the maturity and interoperability of several enabling technologies and operational procedures. In particular, onboard DAA systems for UAS are progressing through standardization and evaluation toward operational use. Complementary enablers, including GBSS and U-space services, are intended to support scalable mixed-traffic operations; however, implementation is still in its early stages. Finally, a holistic approach that assesses scenario-based airspace accessibility of UAS in realistic terminal environments using historical manned flight tracks, predicting near-term manned flight intent, and enforcing operational feasibility has not yet been demonstrated.

2.3.2. UAS Flight Rule Capabilities: VFR-like Flexibility and IFR-like Safety

Operational feasibility for UAS integration is fundamentally constrained by regulatory requirements, including flight rules and associated procedural responsibilities. Current flight rules pose a hurdle to the safe and efficient integration of UAS into uncontrolled airspace. The RP typically has no Visual Line Of Sight (VLOS) to the UA and therefore has to operate the UA Beyond Visual Line Of Sight (BVLOS). Consequently, the RP cannot "see and avoid" other aircraft in the vicinity of the UA, as envisaged by ICAO Annex 2—Rules of the Air [28]. As a result, regional UAS flying BVLOS are initially expected to operate according to today's IFR, especially in complex airspace environments with manned traffic such as around airports. As introduced in Section 2.1, in terminal airspaces, IFR enhance

procedural safety and predictability of arriving and departing aircraft, but reduce pilot operational flexibility such as spacing and merging with other aircraft around airport TPs.

Furthermore, the integration of UAS under IFR becomes more challenging, as many non-towered airports do not provide IAPs for IFR arrivals and departures. As a result, current flight rules would have to be revised to enable UAS flying BVLOS under "VFR-like flexibility" with "IFR-like safety", especially around non-towered airports. For an international comparison of procedural UAS airspace integration hurdles, such as IFR approaches in uncontrolled airspace, see Ref. [11].

In Germany, IFR arrivals and departures at non-towered airports are relatively infrequent in practice. Only 27 of ~400 non-towered airports in Germany, including a heliport, are supported by a Radio Mandatory Zone (RMZ), which is designed to improve operational safety in high-traffic-density environments and to support the safe integration of IFR flights at airports in uncontrolled airspace [20]. An RMZ requires all pilots to listen and communicate flight entries and exits via a Very High Frequency (VHF) radio link; ATC clearance is not required [31].

Figure 6 provides an overview of possible UAS integration options at a non-towered airport given the availability of flight rules (i.e., IFR and/or VFR), meteorological conditions (i.e., IMC or VMC), and different safety thresholds based on manned traffic volumes. Note that, for simplicity and due to a lack of regulations, these UAS integration options do not consider off-nominal flight situations, such as an LC2L.

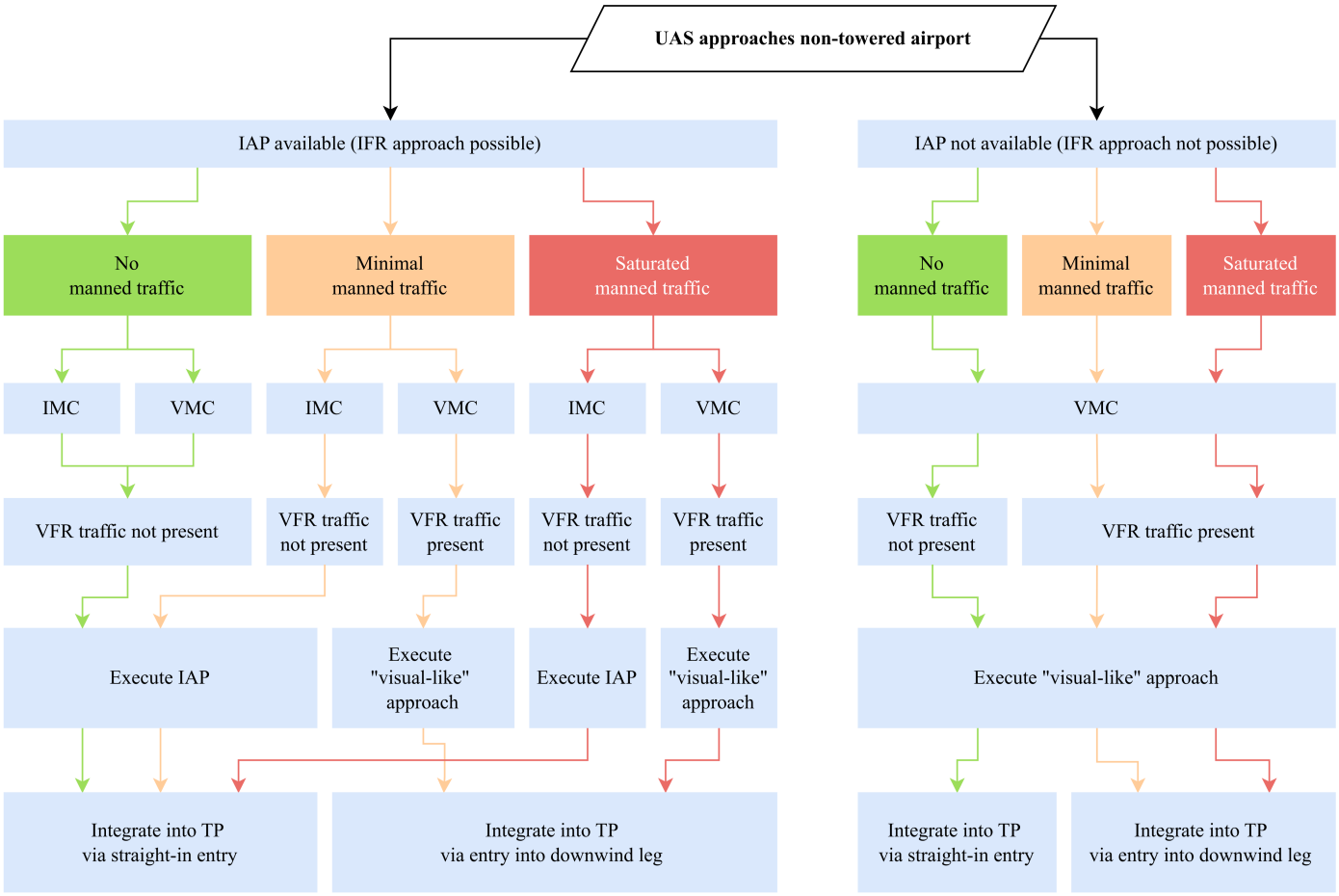

Figure 6. Overview of possible UAS integration options at a non-towered airport given the availability of flight rules, meteorological conditions, and safety thresholds based on manned traffic volumes.

"No manned traffic", "minimal manned traffic", or "saturated manned traffic" refer to the presence of manned traffic in the terminal airspace. "Minimal manned traffic" refers to

traffic volumes where UAS integration with manned aviation might be possible without flying deconfliction maneuvers and "saturated manned traffic" requires holding maneuvers by UAS, for example.

Assuming that a non-towered airport provides at least one IAP, UAS could operate in both IMC and VMC. The UAS would usually attempt to execute the IAP enabling "IFR-like safety", but it could also switch to "visual-like" rules to benefit from "VFR-like flexibility".

Given IAP availability, if "no manned traffic" is present in the terminal airspace, the UAS is expected to execute an IAP by flying a straight-in approach to land via the final leg of the TP. However, if there is traffic in the terminal airspace, such as VFR-flying aircraft in the TP, a straight-in approach is not recommended [30]. If "minimal manned traffic" is present in the terminal airspace, no VFR-flying aircraft would be allowed under IMC (only IFR-flying aircraft) and the UAS could execute the IAP, if needed, by following other preceding IFR aircraft.

Under VMC and "minimal manned traffic", such as VFR aircraft around the airport TP, the integration problem for a UAS becomes significantly more complex. In the TP, IFR traffic does not have priority over VFR traffic, and the aircraft that first enters the TP usually has right-of-way. For example, an aircraft that integrates via a 45° approach into the downwind leg has right-of-way over an aircraft that attempts to integrate via straight-in approach into the final leg. However, in practice, if sufficient spacing exists, an aircraft on a straight-in approach close to the final may merge ahead of other traffic and land first, provided this can be achieved safely and without disrupting established traffic in the TP.

In VMC with manned traffic around the TP, the UAS would execute a "visual-like" approach to benefit from "VFR-like flexibility" by following the preceding VFR aircraft into the TP, likely via the downwind leg of the TP. However, if traffic exceeds a pre-determined safety threshold (i.e., "saturated manned traffic" causing increased intent uncertainty) and VMC are given, the UAS is expected to hold until it is safe for the UAS to continue executing a "visual-like" approach by following the preceding VFR aircraft into the TP. Under IMC in a "saturated manned traffic" scenario (only IFR-flying aircraft present), the UAS will either hold somewhere close to the IAP or merge with other IFR aircraft to execute the IAP via a straight-in approach.

Assuming that a non-towered airport provides no IAP, UAS will initially only be able to approach the airport under VMC following a "visual-like" approach. If "no manned traffic" is present, the UAS can simply integrate into the airport TP, either directly via the final leg for operational efficiency or via a standard 45° approach or overhead join into the downwind leg for operational safety. Given a level of "minimal manned traffic" around the airport TP, the UAS is expected to integrate via the downwind leg to be predictable to other aircraft, likely following other preceding VFR aircraft into the TP. Exceeding a pre-determined safety threshold "saturated manned traffic", the UAS is expected to transfer into holding until VFR intent uncertainty is resolved and the UAS can safely space and merge with other VFR aircraft into the airport TP.

The required UAS capability to space and merge with other aircraft enabled by onboard DAA systems, GBSS and/or U-space services has been discussed in Section 2.3.1. However, numerical separation thresholds for UAS traffic encounters for different levels of safety-critical traffic volumes, especially in terminal airspaces, remain to be validated and are currently being investigated by industry and regulators [18,57]. Validation of separation thresholds in conjunction with traffic-dependent spacing and merging capabilities can be considered particularly important to enable UAS to perform "visual-like" approaches.

VFR pilots mainly apply visual separation to space their aircraft from other aircraft. Visual separation from another aircraft is based on the individual pilot's preference and experience on what they consider safe and appropriate. To obtain a numerical separation

threshold for mixed airspace encounters around non-towered airports, current DAA capabilities of Airborne Collision Avoidance System (ACAS) variants are discussed in the following paragraphs.

In manned aviation today, ACAS II is the only system that meets the ACAS ICAO Standards and Recommended Practices (SARPs) and is currently implemented as Traffic Alert and Collision Avoidance System (TCAS) II version 7.1 [58]. TCAS II identifies and displays time-based collision risks for an estimated closest point of approach which is triggered for intruder aircraft carrying operative transponders (e.g., Mode-S or Mode-C) [58,59]. TCAS II has specific operational requirements such as aircraft climb rates of 2500 ft (∼760 m) per minute and operational flight levels of above 1000 ft (∼300 m) AGL for conflict resolution advisories. Therefore, TCAS II is not utilized by smaller aircraft categories in the general aviation realm and by UAS that cannot meet operational requirements or operate in lower level airspace such as in urban environments or around airports [58,59].

In unmanned aviation, ACAS X variants (i.e., ACAS Xu and ACAS sXu) are supposed to provide guidance on collision avoidance to the RP in demanding airspace environments that host manned and unmanned traffic [60–62]. ACAS X variants are expected to enable safe DAA principles and separation guidance for UAS for different traffic encounters, especially in lower altitudes. Based on the recommendations of different studies on horizontal and vertical separation minima for UAS traffic encounters using ACAS X [17,63–65], it can be expected that a safety threshold will be applied using a Horizontal Miss Distance (HMD) of 2000 ft (∼610 m) and a Vertical Miss Distance (VMD) of 500 ft (∼150 m) to separate UAS from other aircraft, such as in low-altitude terminal airspaces. If these separation thresholds are violated, the encounter would be treated as a loss of the tactical "DAA well-clear" buffer, triggering alerting and separation guidance to restore appropriate spacing (e.g., through vertical or lateral maneuver recommendations). If separation continues to decline despite guidance, the conflict may transition into a last-resort collision avoidance stage, where more urgent advisories are required to prevent a collision.

Although these next-generation DAA systems can provide advanced tactical conflict detection and resolution services, they do not substitute the regulatory framework that defines responsibilities, separation minima, and right-of-way rules. This motivates the development of novel/additional flight rules enabling safe but flexible "visual-like" operations for UAS in uncontrolled airspace, particularly at non-towered airports where IFR availability for UAS operations is limited.

In recent years, concepts for flight rules have been proposed that address the UAS integration dilemma of "IFR-like safety" versus "VFR-like flexibility". These concepts include the proposal of Basic Flight Rules (BFR) and Managed Flight Rules (MFR) [66], Digital Flight Rules (DFR) [67], Tailored Flight Rules (TaFR) [68], Enhanced Flight Rules (EFR) [69], Low-level Flight Rules (LFR) and High-level Flight Rules (HFR) [6], U-space Flight Rules (UFR) [37,38], and Automated Flight Rules (AFR) [70]. Generally, these "new" flight rules share the same underlying objective of scaling UAS operations through digital cooperation (e.g., through surveillance, connectivity, intent exchange, and conformance monitoring) rather than relying exclusively on classical VFR "see and avoid" or ATC-centric IFR separation principles. Their main differences lie in the governance model that enables self-managed or automation-/service-managed flight planning and the extent to which trajectories are constrained by corridors or managed routes. However, these proposals are still purely conceptual and far from being implemented in practice.

3. Methodology

For the purpose of the concept and simulation study presented in this paper, this research is based on several operational and technological assumptions. It is assumed that UAS DAA systems (e.g., ACAS X variants) will be certified and functional for use in uncontrolled terminal environments and that manned flight intent can be successfully predicted given certain look-ahead times to enhance cooperative airspace access for both manned and unmanned aircraft. Similarly, UAS are expected to be able to fly and integrate into a conventional TP and to perform an automated landing. Furthermore, it is assumed that UAS will be able to merge and space with other traffic in and around the TP of non-towered airports, likely by applying "new" flight rules for UAS that enable "VFR-like flexibility" and "IFR-like safety" in uncontrolled terminal airspaces. Finally, the proposed simulation study builds on the holding stack concept discussed in Section 2.2 and aims to validate whether the proposed UAS operating scheme from Ref. [11] remains operationally feasible in a non-towered terminal environment with highly variable manned traffic.

3.1. Data Selection

Flightradar24 data are used to assess historical manned flight activities in and around non-towered airport environments for the latest year available, 2022. Flightradar24 collects data from several flight tracking sources such as aircraft with ADS-B transponders, the Open Glider Network using FLARM transponders, and by multilateration (MLAT) of the aircraft's position [71]. Data from Flightradar24 are used to analyze the three-dimensional position and time of aircraft, as well as the heading, speed, and callsign. Data were analyzed using internal DLR software to filter and sort flight tracks and to visualize traffic density heatmaps with QGIS (v3.38.0). All other data processing, simulation, and visualization tasks were performed in MATLAB R2024b–R2025b. Note that the data sets analyzed in this paper are not comprehensive, as not all airspace users transmit their flight information. However, the analyzed data sets can be considered to have a high indicative quality. A survey has demonstrated that 78% of manned airspace users in Europe carry an electronic conspicuity device such as ADS-B when flying in uncontrolled airspace [72].

Two German non-towered airports were chosen to assess manned aircraft activities and to derive UAS integration options into airport TPs. Juist (EDWJ) and Egelsbach (EDFE) are considered highly relevant for the initial integration of cargo UAS at airports in uncontrolled airspace due to their locations and their availability to operate commercial cargo [20]. Moreover, both airports provide different airspace environments in terms of topography, flight counts, and flight behaviors, present aircraft types, and airspace classes to challenge the proposed operating scheme for UAS integration into airport TPs.

First, the island airport Juist (EDWJ) was selected as an airport of interest because of its unique location in the German North Sea and its availability of commercial cargo operations. The initial use of unmanned air cargo can be expected to play an increasingly vital role in hard-to-reach areas, such as islands [21].

Juist (EDWJ) has two standard TPs north and south of its runway at a recommended TPA of 600 ft Mean Sea Level (MSL) (which is 592 ft or ∼180 m AGL); see Figure 7a. However, looking at Figure 8a, it becomes apparent that the southern TP has significantly higher TP activities (darker colors) than the northern TP (lighter colors). The southern TP is supposed to be primarily used by non-motor-driven glider aircraft, as indicated in the Visual Operating Chart (VOC) of Juist (EDWJ). In addition to the appearance of glider aircraft, the airspace environment of Juist (EDWJ) accommodates other types of airspace users, such as helicopter traffic streams towards offshore wind parks north of the island; see the dense linear traffic flow east of the airport TP in Figure 8a.

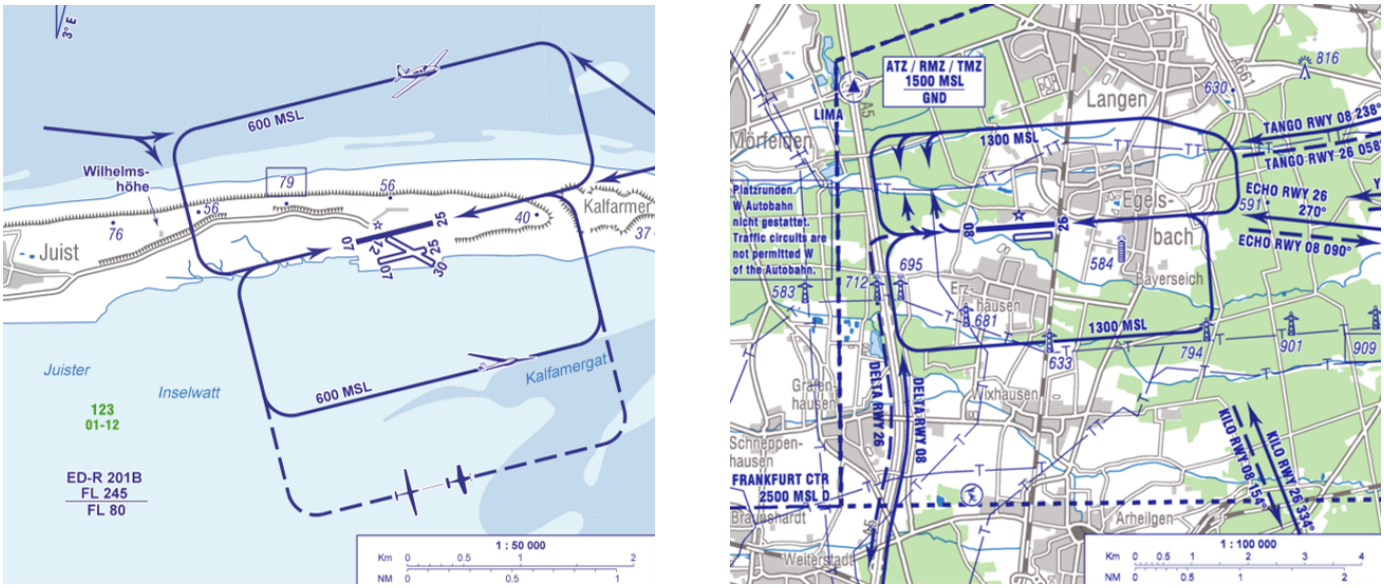

(**a**) (**b**)

Figure 7. VOC with indicated TP, recommended TPA, TP integration directions, and airspace classes [31]: (**a**) Juist (EDWJ) and (**b**) Egelsbach (EDFE).

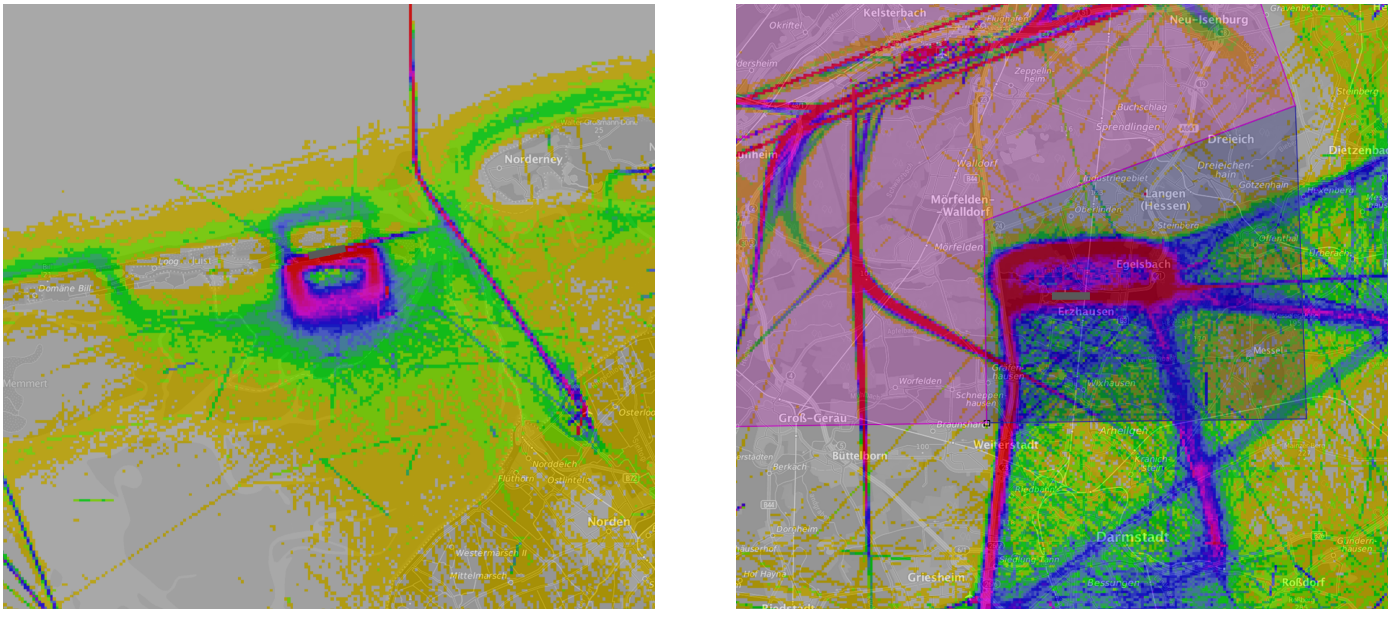

(**a**) (**b**)

Figure 8. Visualization of flight track data for (**a**) Juist (EDWJ) and (**b**) Egelsbach (EDFE) with its RMZ (blue-colored bounding box) and the Controlled Traffic Region (CTR) (purple-colored bounding box) of Frankfurt (EDDF). Traffic densities are visualized in an altitude band of 0–3000 ft (∼910 m) AGL with dark red indicating the highest and yellow the lowest flight track density.

Second, Egelsbach (EDFE) was selected as the other non-towered airport of interest. Egelsbach (EDFE) is the busiest non-towered airport in terms of annual flight movements out of ∼400 non-towered airports in Germany [20] and has the highest TP spread and deviation of manned aircraft flight times and flight distances of German airports assessed in Ref. [11]. In addition, Egelsbach (EDFE) has the most stringent airspace regulations of all German non-towered airports, operating an Aerodrome Traffic Zone (ATZ) and a Transponder Mandatory Zone (TMZ) around its airport in addition to its RMZ. An ATZ

serves as an airspace bounding box that is only allowed to be accessed if the pilot intends to land. Pilots entering a TMZ must carry an active transponder, such as ADS-B, on board their aircraft to share their flight information with other aircraft. Moreover, since 2024, Egelsbach (EDFE) has offered a special IFR to VFR flight rule change procedure for runway end 26 for arriving aircraft, ending in a VFR approach using different WPs towards the VFR arrival route "ECHO RWY (runway) 26" [31]; see right-hand side of the VOC in Figure 7b. The bounding box of the RMZ surrounding Egelsbach (EDFE) and the bordering CTR of Frankfurt (EDDF) can be seen in Figure 7b (dashed lines on the left and bottom side) and Figure 8b (RMZ as blue-colored bounding box and CTR as purple-colored bounding box).

The analysis of Egelsbach (EDFE) will stress test the UAS integration options developed and assessed in this paper. As introduced above, an ATZ, RMZ, and TMZ will likely help to support the integration of UAS operating under IFR. Furthermore, Egelsbach (EDFE) can be considered relevant for the introduction of cargo UAS due to its close proximity to the busiest German airport located in controlled airspace, Frankfurt (EDDF) and its availability of commercial cargo operations. Future cargo UAS flights to and from Egelsbach (EDFE) could relieve traffic load at Frankfurt (EDDF), with Egelsbach (EDFE) serving as a potential cargo feeder airport for the greater Frankfurt area.

Dense traffic flows of arriving aircraft can be seen south and east in the traffic heatmap of Figure 8b. West and north of Egelsbach (EDFE), the CTR of Frankfurt (EDDF) restricts flights from entering and interfering with aircraft departing and arriving at Frankfurt (EDDF); see Figure 7b. Similarly to Juist (EDWJ), Egelsbach (EDFE) has a northern and southern TP displayed in its VOC, with a recommended TPA of 1300 ft MSL (which is 915 ft or ∼280 m AGL). A detailed analysis of historical flight activities in and around the TP of both airports can be found in the author's previous research in Ref. [11]. Note that the airport-specific recommended TPA differs from the conventional TPA; the latter is usually between 500 and 1500 ft (∼150–460 m) AGL, see Section 2.1, whereas the recommended TPA can be found in VOCs, for example.

In the absence of a dedicated airspace zone such as an ATZ/RMZ/TMZ, German non-towered airports typically do not have airspace boundaries to identify the spatial boundaries of their terminal airspace. To assess manned traffic activities relevant for UAS integration at a non-towered airport, a terminal airspace bounding box was drawn around the runway of both airports of interest. The terminal airspace bounding box has the common dimension of an RMZ, which usually covers a size of ∼10 × 20 km. The spatial dimensions of the terminal airspace bounding boxes of Juist (EDWJ) and Egelsbach (EDFE) are illustrated in Figure 9 by the orange-dashed bounding box.

As seen in Figure 7, both airports have multiple standard TPs indicated in their VOC. Generally, the UAS will likely choose the TP based on the broader traffic activities in the terminal airspace, the ongoing TP activities, the approaching direction of the UAS and the wind directions. However, for initial UAS integration, choosing the TP that provides the greater operational safety might be of interest for the UAS operator.

To perform in-depth analysis and derive specific implications for TP integration of UAS, one TP has been chosen for UAS integration at each airport of interest. A TP bounding box called the "UAS TP integration area" was derived, marking the airspace where UAS are proposed to integrate into the airport TP. This area covers the respective TP and extends from the ground to the airport-specific recommended TPA plus an additional 1000 ft (∼300 m). This intends to also cover TP-approaching aircraft that integrate from 500–1000 ft (∼150–300 m) above TPA, for example via overhead join. Note that the UAS TP integration area of Egelsbach (EDFE) extends beyond the CTR of Frankfurt (EDDF) to capture traffic that occasionally crosses the CTR boundary before integrating into the TP of Egelsbach (EDFE).

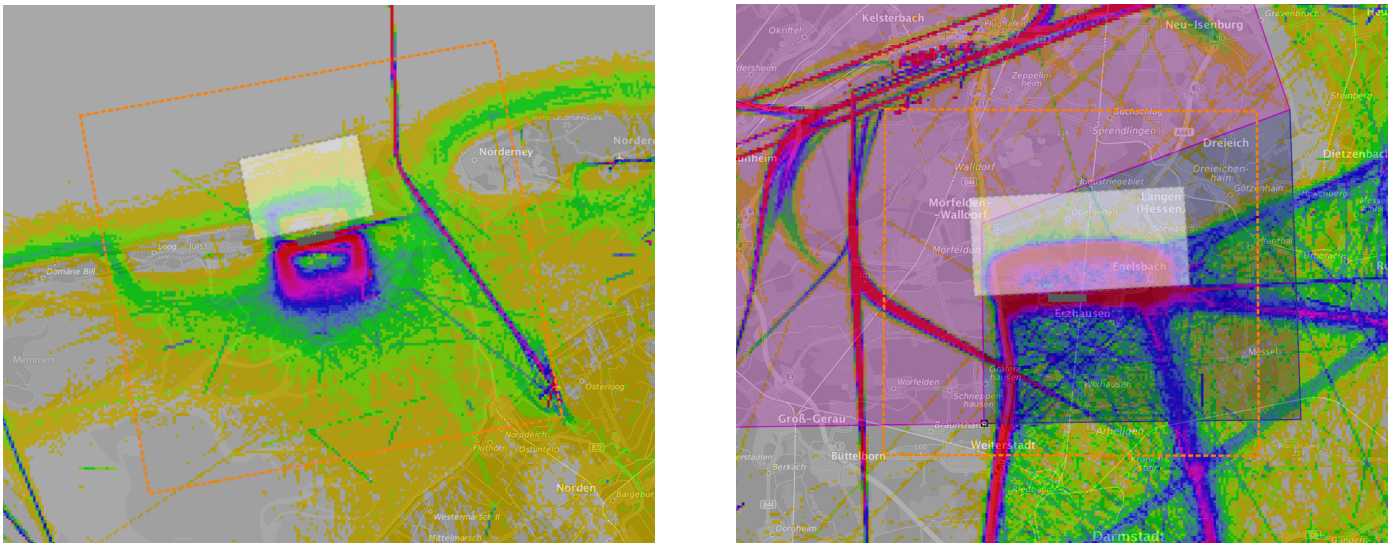

(**a**) (**b**)

Figure 9. Selection of flight track data in the terminal airspace (orange-dashed bounding box) and UAS TP integration area (transparent gray-dashed bounding box) for (**a**) Juist (EDWJ) and (**b**) Egelsbach (EDFE) surrounded by its RMZ (blue-colored bounding box) and the CTR (purple-colored bounding box) of Frankfurt (EDDF). Traffic densities are visualized in an altitude band of 0–3000 ft (∼910 m) AGL with dark red indicating the highest and yellow the lowest flight track density.

For Juist (EDWJ), motor-driven aircraft are expected to use the northern TP as indicated in the VOC; see Figure 7a. Similarly, the northern TP is less frequently used than the southern TP, likely resulting in fewer UAS interactions with manned aircraft when integrating into the TP. Consequently, the UAS TP integration area was placed around the northern TP to reduce manned aircraft interaction; see the transparent gray-dashed bounding box in Figure 9a with a size of ∼14 km^2.

For Egelsbach (EDFE), two TPs are displayed in its VOC with five specific VFR arrival and departure routes (i.e., DELTA, ECHO, TANGO, KILO, and YANKEE) that indicate TP utilization. Looking at the traffic heatmap of Egelsbach (EDFE) in Figure 9b, it can be clearly seen that the northern TP has significantly higher traffic densities than the southern TP, likely due to the recommended VFR arrival and departure routes that focus the northern TP. To comply with arrival recommendations, the UAS TP integration area was placed around the northern TP, see the transparent gray-dashed bounding box in Figure 9b with a size of ∼33 km^2.

Note that the UAS TP integration area does not cover the runway and final legs of the targeted TP. As discussed in Section 2.1, standard integration procedures into the TP often use an approach via the downwind leg, such as the overhead join or the 45° approach. To be predictable for other aircraft and to follow procedural recommendations, it is expected that UAS will follow these standard TP procedures. Similarly, aircraft flying the TP usually have right-of-way over other traffic in the vicinity of the TP. Therefore, the UAS TP integration area and analysis of historical manned aircraft behavior focus on the airspace segment that captures the majority of TP traffic, such as aircraft that either fly the TP downwind leg directly or merge into the pattern in close proximity to it.

Table 1 provides an overview of ATC separation and ATC clearance regulations in different airspace classes around Juist (EDWJ) and Egelsbach (EDFE), historical traffic volumes, and their airport-specific altitude limits [31].

Table 1. Airspace classes, airspace regulations, and traffic count at airports of interest.

				Juist (EDWJ)	**Egelsbach (EDFE)**
Airspace Class		**ATC Separation**	**ATC Clearance**		
Controlled airspace	Class C	IFR to V/IFR	V/IFR	>FL100	>2500 ft MSL
	Class D	IFR to IFR	V/IFR	–	1500 ft MSL to 2500 ft MSL
	Class E	IFR to IFR	IFR	2500 ft AGL to FL100	–
Uncontrolled airspace	Class G	No	No	Ground to 2500 ft AGL	Ground to 1500 ft MSL (RMZ, ATZ, TMZ)
Airport-specific recommended TPA				600 ft MSL (592 ft AGL)	1300 ft MSL (915 ft AGL)
Size [km^2]		Terminal airspace		∼200	∼200
		UAS TP integration area		∼14	∼33
Number of annual flights [1] [flights]		Terminal airspace		12,696	63,290
		UAS TP integration area		2789	6810

[1] Flights are counted in an altitude band of 0–3000 ft (∼910 m) AGL.

Both airports of interest are surrounded by uncontrolled Class G airspace, where operations are conducted without ATC separation or clearances. Above that, at Juist (EDWJ), Class G transitions into controlled Class E airspace starting at the upper limit of Class G. Here, IFR flights require ATC clearance and receive separation services, while VFR flights operate without separation or clearances. In contrast, Egelsbach (EDFE) operates controlled Class D airspace above its Class G airspace, with Class C airspace starting at 2500 ft MSL. Within Class C, all aircraft require ATC clearance and IFR traffic is separated from both IFR and VFR traffic.

3.2. Conceptual Operating Scheme for UAS Integration at Non-Towered Airports

As mentioned earlier, there is no official operating scheme for UAS integration at non-towered airports under IMC or VMC, especially for UAS integration into the airport TP with VFR traffic. The author of this work has proposed a conceptual operating scheme for UAS integration into non-towered airport environments in previous research, see Ref. [11] and a brief introduction of the concept in Section 2.2, but the options for integrating UAS will have to be based on regulations that have not yet been introduced.

As discussed in Section 2.3.2, different UAS integration options can be expected to depend on different levels of traffic and intent uncertainty critical to the safety of UAS integration. For initial integration of UAS into non-towered airports, if there are traffic activities close to the airport TP, it is likely that the UAS will follow the preceding aircraft into the TP or that the UAS will loiter until the TP is empty. Consequently, if traffic (uncertainty) in the terminal airspace, especially around the TP, exceeds a pre-determined threshold, which again is subject to ongoing safety regulations, the UAS is expected to go into holding and to monitor ongoing traffic activities before integrating into the TP of the airport.

In Ref. [11], the author of this paper has proposed and analyzed different quantitative measures to assess manned aircraft behavior. Juist (EDWJ) and Egelsbach (EDFE) were identified as potential locations for the implementation of UAS holding layers above the TP due to the airport's surrounding airspace classes and historical manned flight behaviors in different altitde bands. Other non-towered airports such as Schoenhagen (EDAZ), for example, were considered not "ideal" as initial candidates to introduce UAS holdings

above the airport TP. Schoenhagen (EDAZ) has significant shares of IFR flights above its airport TP at altitudes between 3000 ft (∼910 m) and 6000 ft (∼1830 m) AGL [11]. These traffic streams follow an IAP designed for IFR aircraft that approach the capital airport of Germany, Berlin (EDDB), from the south-east towards runway ends 07L or 07R [31].

This paper expands on the author's previous research in Ref. [11] and proposes a simulation-based UAS integration study to assess safety and efficiency aspects of UAS integration into non-towered airport TPs. The simulation study applies look-ahead times and spatial separation minima, as well as deconfliction holding maneuvers, to mitigate safety-critical interaction with other aircraft to validate and scale the UAS holding stack concept introduced in Section 2.2.

The simulation study proposes that once a UAS is the only aircraft in the UAS TP integration area, it will have right-of-way to approach the airport runway. This requirement is in accordance with current TP integration principles, which require aircraft to "conform with or avoid the pattern of traffic formed by other aircraft in operation" [73] (p. 29) and to sequence accordingly. Consequently, no other aircraft should enter the airspace of the TP (i.e., UAS TP integration area) within a defined time period (i.e., look-ahead times t_i with $i = 1, \ldots, N$). In addition, no other aircraft should interfere with the UAS trajectory within a defined volume around the UAS (i.e., spatial separation minima; green cylinder around the UAS in Figure 10) until the UAS TP integration area is reached.

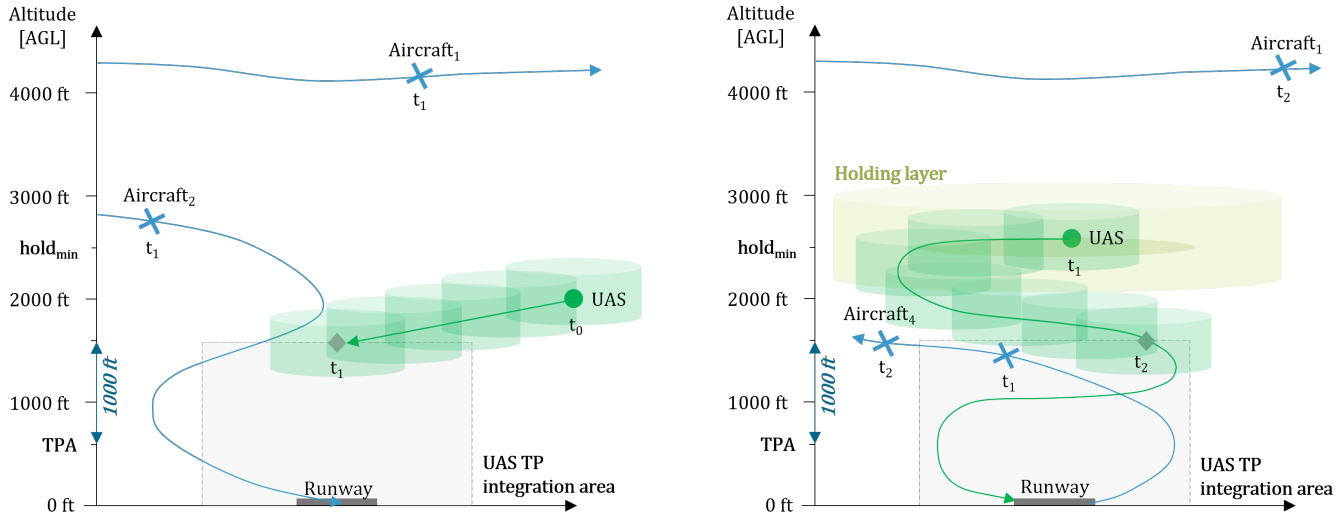

Figure 10. Illustration of UAS TP integration options using look-ahead times, spatial separation minima, and deconfliction holding maneuvers (dimensions are not to scale): (**a**) TP integration without holding. (**b**) TP integration via holding.

If at least one other aircraft is projected to appear in the UAS TP integration area, see Figure 11a Aircraft$_3$ and Aircraft$_4$ indicated as red crosses at t_1, once the UAS reaches the area and/or another aircraft is predicted to violate the safety bound of the UAS trajectory (red cylinder around UAS at t_1 due to Aircraft$_4$ at t_1), the UAS is expected to enter holding above the airport TP (light green wide cylinder labeled "holding layer"). Consequently, the UAS holding should be at an altitude that is deconflicted from other traffic present in the terminal airspace (Aircraft$_2$ at t_1), see Figure 11b. However, in case of aircraft present in the UAS TP integration area, see Figure 11c Aircraft$_3$ at t_1, and the UAS cannot find a place to hold due to other aircraft in altitude bands above the airport TP (red-lined light green wide cylinders due to interference with Aircraft$_2$, Aircraft$_5$, and Aircraft$_1$), the UAS will terminate its TP integration approach (i.e., holding denied). On the other hand, the

UAS will also terminate its TP integration approach (i.e., holding aborted), see Figure 11d, if aircraft are present in the UAS TP integration area and holding layers are available (light green wide cylinders at t_1–t_3), but the UAS cannot access these holding layers due to aircraft interference with the UAS trajectory into holding (see red cylinder around UAS at t_A due to Aircraft$_6$ at t_A).

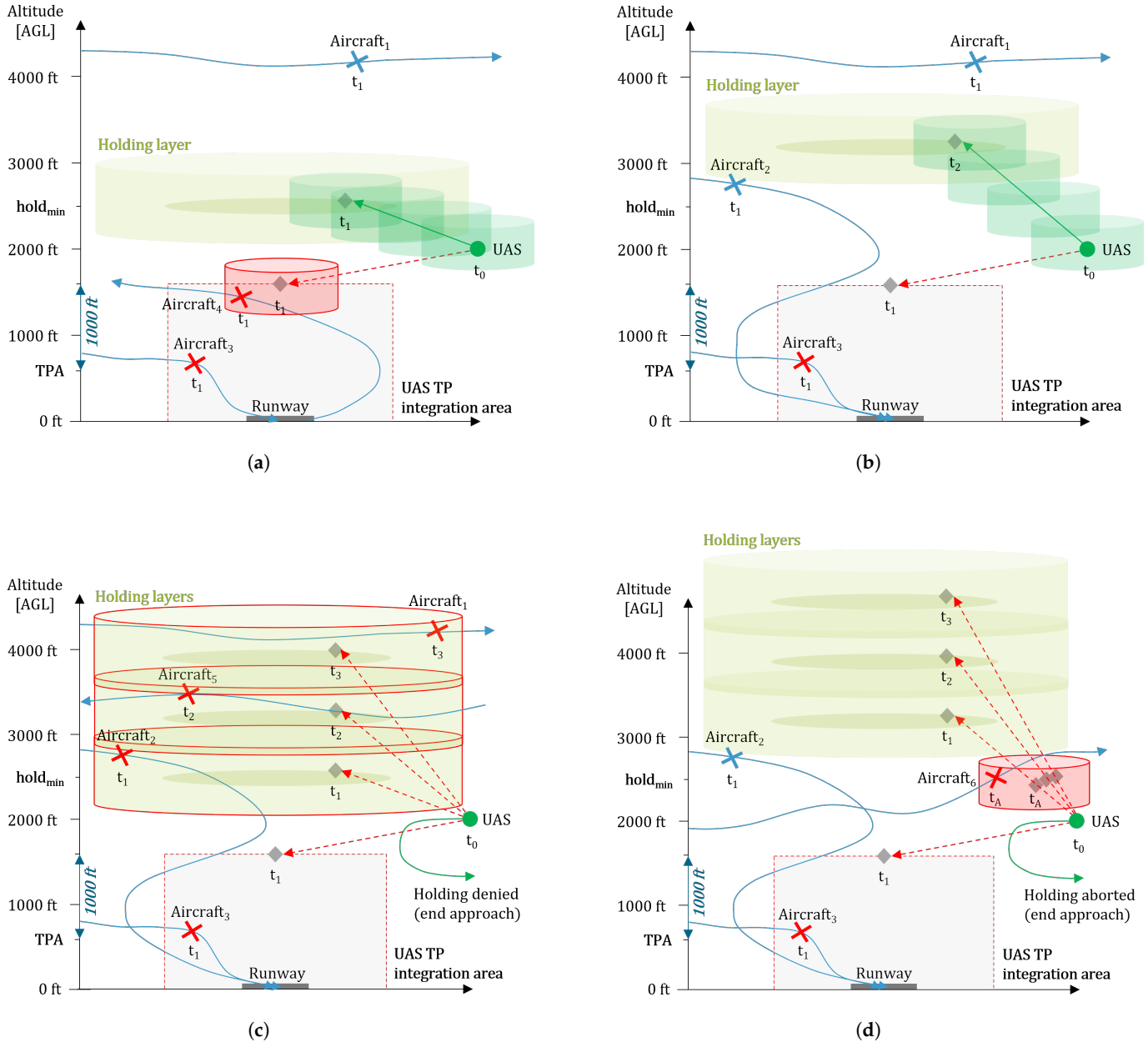

Figure 11. Illustration of UAS TP integration options using look-ahead times, spatial separation minima, and deconfliction holding maneuvers (dimensions are not to scale): (**a**) TP integration with holding at hold$_{min}$ due to detected conflicts in UAS TP integration area. (**b**) TP integration with holding above hold$_{min}$ due to a detected conflict in UAS TP integration area. (**c**) No TP integration due to conflicts and denied holding. (**d**) No TP integration due to conflicts and aborted holding.

The procedural UAS integration options visualized in Figures 10 and 11 might not represent the most efficient way of UAS integration. However, to overcome the trade-off between efficiency and safety, as discussed in Section 2.3, holdings might be an initial UAS integration option to enhance operational safety in uncertain environments while remaining relativity efficient by staying close to the airport TP. At the same time, especially

for the introduction of new airspace entrants, applying a standard integration scheme for UAS is likely to increase acceptability and predictability by other airspace users.

Consequently, the simulation study applies a standard TP operating scheme for UAS integration. The UAS will integrate into a TP, located north of the runway for the airports of interest (i.e., UAS TP integration area; transparent gray-dashed bounding box in Figure 12a,d), approaching the TP from the south.

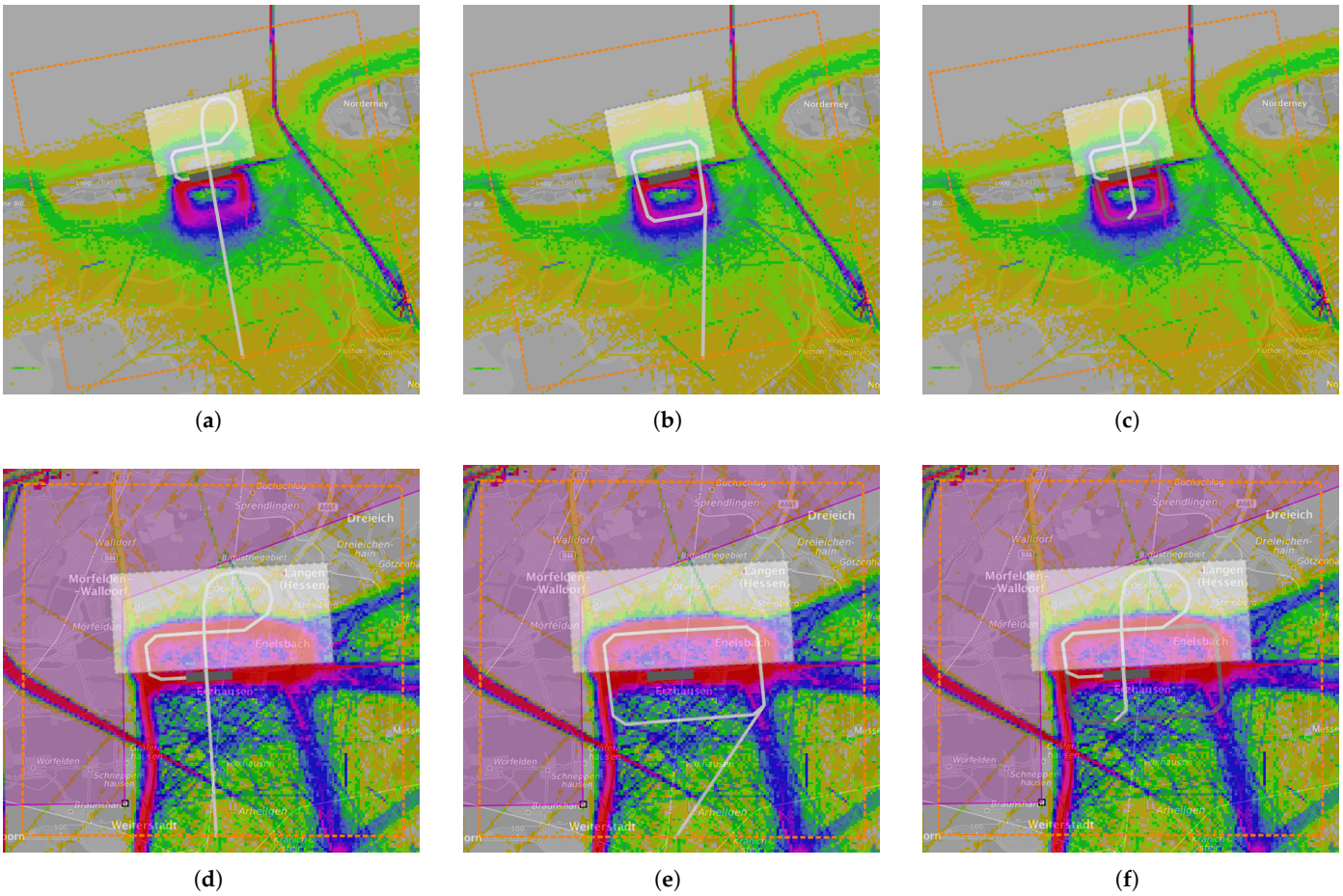

(**a**) (**b**) (**c**)

(**d**) (**e**) (**f**)

Figure 12. Traffic densities in the terminal airspace (orange-dashed bounding box) and the UAS TP integration area (transparent gray-dashed bounding box) with UAS TP integration options (light gray trajectories). Traffic densities are illustrated in an altitude band of 0–3000 ft (∼910 m) AGL with high TP activities indicated by darker colors and low TP activities indicated by lighter colors. (**a**) Juist (EDWJ) and (**d**) Egelsbach (EDFE): UAS trajectory from terminal airspace entry via overhead join into airport TP towards runway. (**b**) Juist (EDWJ) and (**e**) Egelsbach (EDFE): UAS trajectory from terminal airspace entry via holding entry into holding. (**c**) Juist (EDWJ) and (**f**) Egelsbach (EDFE): UAS trajectory from holding via overhead join into airport TP towards runway.

In this work, the standard overhead join approach is proposed for UAS integration into the established TP and to improve situational awareness by monitoring wind conditions and TP traffic from overhead before descending to the recommended TPA. In case of projected TP activities (see Figure 11b) or separation violation towards TP (see Figure 11a), the UAS will transfer to holding; see Figure 12b,e. From holding, if the TP and the planned UAS trajectory towards TP remain conflict-free, the UAS will proceed via overhead join from holding into TP downwind leg towards runway; Figure 12c,f.

The simulated UAS trajectories and their WPs are shown in Figures 13–15, illustrated using the dimensions of Juist (EDWJ) and exemplary altitudes from different viewpoints. Key WPs relevant to algorithmic decision-making on UAS behavior are highlighted in red.

The role of the key WPs in the simulation is explained in the following Section 3.3. Based on the proposed UAS operating scheme, four interacting UAS trajectories are derived for the simulation study that are considered relevant for integrating UAS at non-towered airports:

`DIR` (Direct) : UAS arrival trajectory ($\texttt{DIR}_{\texttt{WP1}}$ to $\texttt{DIR}_{\texttt{WP2}}$) and overhead join into TP downwind leg without holding ($\texttt{DIR}_{\texttt{WP2}}$ to RWY);

`EHLD` (Entry Holding) : UAS entry trajectory into UAS holding layer ($\texttt{EHLD}_{\texttt{WP1}}$ to $\texttt{EHLD}_{\texttt{WP4}}$);

`HLD` (Holding) : UAS holding trajectory (circuit starting at $\texttt{HLD}_{\texttt{WP1}}$), also referred to as UAS holding layer or holding orbit;

`REJ` (Rejoin) : UAS rejoin trajectory from UAS holding layer into overhead join ($\texttt{REJ}_{\texttt{WP1}}$ to $\texttt{REJ}_{\texttt{WP3}}$).

The UAS trajectory from terminal airspace entry via overhead join into airport TP, if no holding is required, is called `DIR` trajectory; see Figure 13. $\texttt{DIR}_{\texttt{WP1}}$ marks the entry WP into terminal airspace and $\texttt{DIR}_{\texttt{WP2}}$ marks the start of the UAS overhead join. The `DIR` trajectory consists of nineteen WPs, which enable realistic turning angles of the UAS and trajectory geometries.

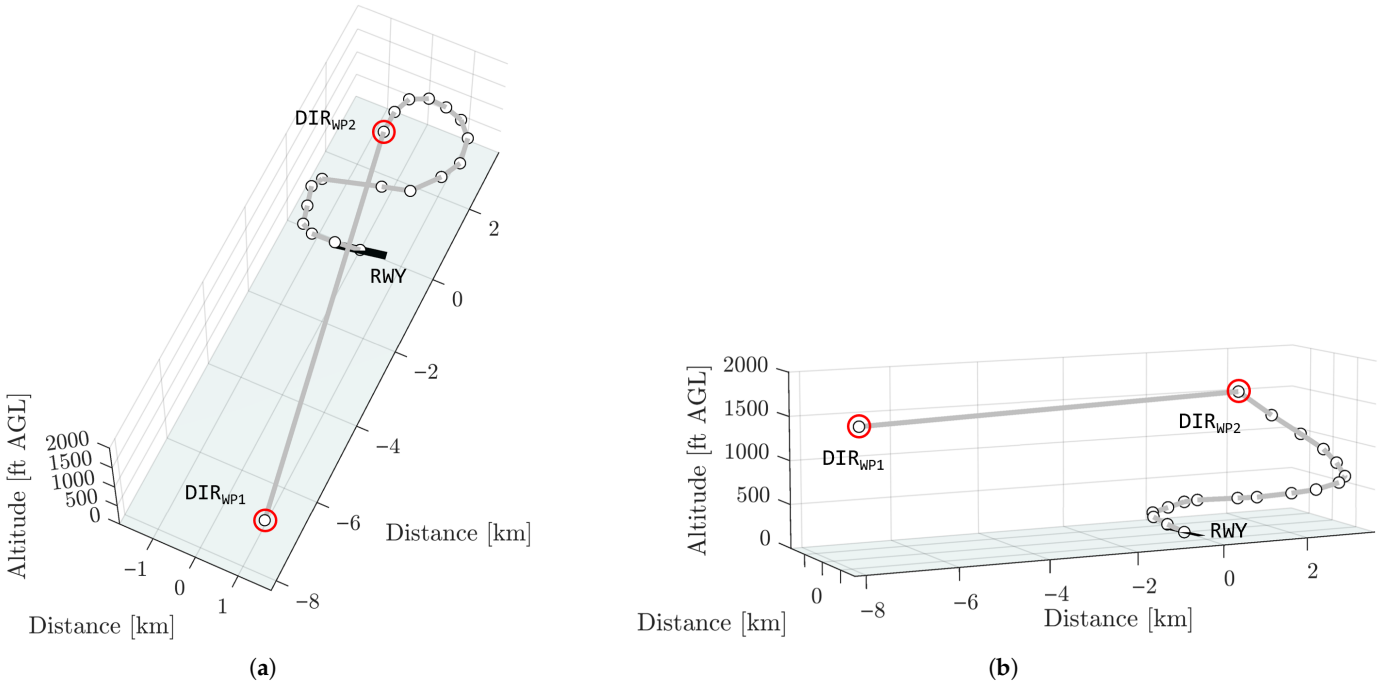

Figure 13. UAS trajectory and key WPs from terminal airspace entry via overhead join into airport TP downwind leg towards runway, using the dimensions of Juist (EDWJ): (**a**) top view and (**b**) side view.

If the UAS is required to hold above airport TP, the UAS will transfer to the `EHLD` trajectory, starting at $\texttt{EHLD}_{\texttt{WP1}}$. `EHLD` consists of four WPs. Note that $\texttt{EHLD}_{\texttt{WP1}}$ is the same initial WP as $\texttt{DIR}_{\texttt{WP1}}$; see Figure 14. From $\texttt{EHLD}_{\texttt{WP1}}$, the UAS will enter holding at $\texttt{HLD}_{\texttt{WP1}}$, which marks the beginning of the holding trajectory, `HLD`. Note that $\texttt{HLD}_{\texttt{WP1}}$ is the same WP as the final `EHLD` WP, $\texttt{EHLD}_{\texttt{WP4}}$. The circular holding trajectory `HLD` consists of twelve individual WPs.

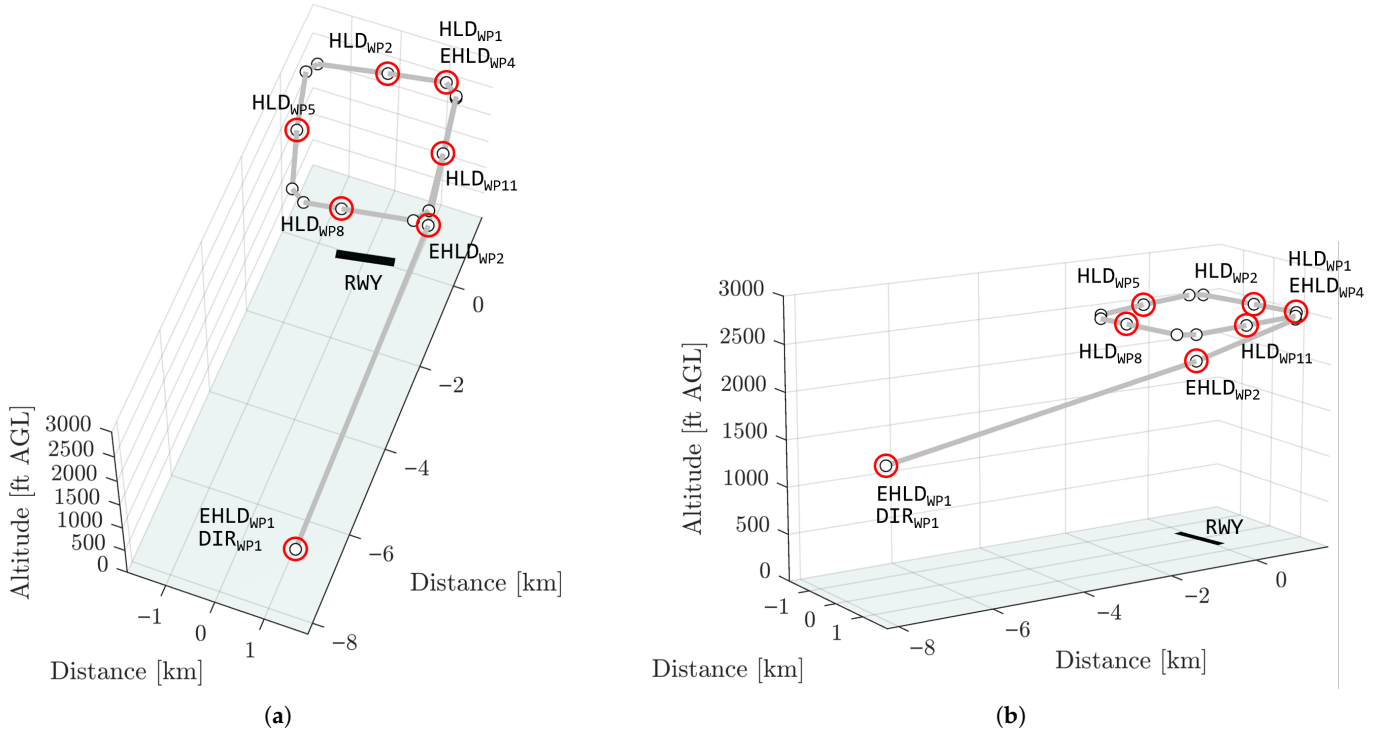

Figure 14. UAS trajectory and key WPs from terminal airspace entry via holding entry into holding above TP, using the dimensions of Juist (EDWJ): (**a**) top view and (**b**) side view.

If the UAS is allowed to rejoin from HLD towards the airport TP, it will leave HLD at HLD$_{WP8}$, initiating the beginning of the REJ trajectory at REJ$_{WP1}$. REJ consists of three WPs. From REJ$_{WP1}$, the UAS will descend steadily to initiate the overhead join approach into the airport TP similar to DIR, while the final REJ$_{WP3}$ also represents DIR$_{WP2}$; see Figure 15. Reaching REJ$_{WP3}$, the UAS continues the overhead join approach of DIR through the TP downwind leg to the airport runway.

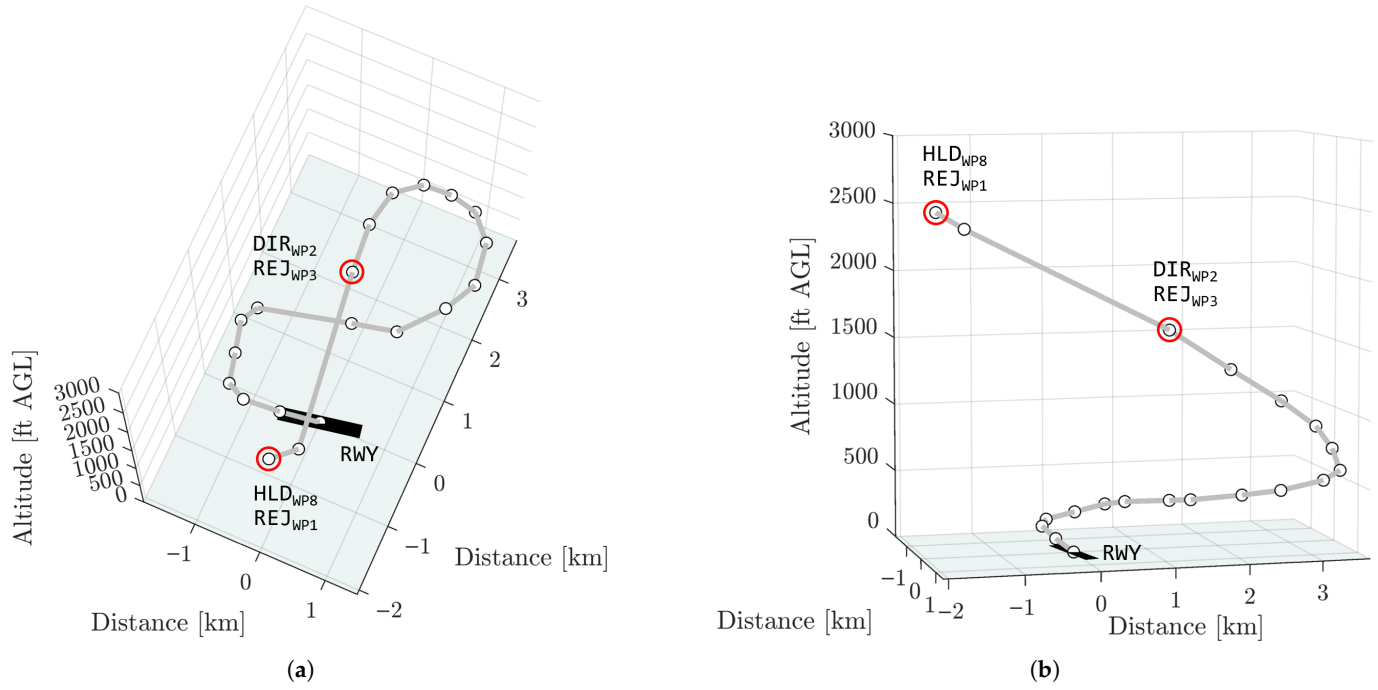

Figure 15. UAS trajectory and key WPs from holding via overhead join into airport TP downwind leg towards runway, using the dimensions of Juist (EDWJ): (**a**) top view and (**b**) side view.

Illustrated UAS trajectories using the dimensions of Egelsbach (EDFE) and exemplary altitudes from different viewpoints are shown in Appendix A.1 in Figures A1–A3.

3.3. Design of Fast-Time Simulation for UAS Integration into Non-Towered Airport TP

The simulation study is based on an algorithmic decision-making approach to validate the proposed UAS integration concept using historical manned flight data in different altitude bands of the terminal airspaces of Juist (EDWJ) and Egelsbach (EDFE). A fast-time simulation approach was chosen to evaluate the operational UAS integration concept, proposed in Section 3.2, at scale using different UAS traffic volumes and look-ahead times of manned traffic activities. The simulation intends to evaluate the following key aspects:

1. **UAS TP accessibility using standard integration procedures**
   The simulation evaluates TP accessibility by applying standard TP integration procedures such as the overhead join approach to UAS trajectories approaching non-towered airports. Using historical manned flight track data, the simulation identifies altitude band usage of manned traffic. For each UAS arrival, the algorithm assesses whether the UAS can safely and legally enter the TP without causing spatial and/or temporal conflicts with manned aircraft. The algorithm uses a conflict taxonomy, altitude-based deconfliction rules, and timing constraints to determine whether the UAS can access the TP. TP accessibility is then quantified as the share of UAS approaches that can proceed directly to the TP without requiring holding.
2. **UAS holding layer availability across altitude bands**
   Using historical manned track data, the simulation identifies the availability of vertical holding layers above the TP that could be used to temporarily sequence UAS arrivals. The holding layer allocation algorithm incrementally evaluates candidate holding layers, beginning at a pre-defined base altitude, and checks each layer for potential conflicts with manned traffic as well as with the projected UAS trajectory to that layer. A holding layer is identified if a conflict-free altitude exists within a minimum and maximum altitude band range. By varying UAS traffic volumes, the simulation quantifies how available airspace altitudes and conflict-free layer assignment rates change as a function of manned traffic volumes and their altitude band usage.
3. **Slot-based UAS throughput across altitude bands**
   The simulation calculates potential UAS throughput by assigning holding slots and entry/exit gates to UAS based on "First-In/First-Out" (FIFO) sequencing principles and conflict detection. The UAS allocation process ensures that UAS are separated and deconflicted both spatially (via holding layers) and temporally (via slot assignment). UAS throughput capacity emerges from the interplay between available conflict-free holding layers, minimum vertical separation, and merge constraints associated with the TP entry. By applying replicable UAS sequencing behavior, the simulation identifies feasible UAS operating patterns that avoid manned interaction.
4. **UAS conflict probability under varying look-ahead times**
   The simulation examines conflict detection performance for different look-ahead times by applying a time-based detection window to each UAS approach. Within this window, the algorithm evaluates potential encounters between the UAS and manned aircraft based on altitude band occupancies and projected trajectory intersections. Varying look-ahead times determine how early conflicts are detected, which in turn affects UAS holding assignments, UAS trajectory feasibility, and ultimately UAS TP accessibility. By investigating varying UAS traffic volumes and look-ahead settings, the simulation provides quantitative insights for deconfliction strategies, sequencing effectiveness, and operational limits for integrating UAS with manned traffic.

The simulation study relies on a set of simplified operational assumptions regarding UAS flight performance and environmental conditions. These assumptions are intended to ensure comparability between different simulation runs by isolating the effects of the proposed conflict detection logic, holding layer assignment, and sequencing rules from UAS specific performance variations.

UAS performance assumptions are based on the performance characteristics of a Cessna 208 Caravan aircraft, which is used for initial regional unmanned cargo operations by companies such as Reliable Robotics [23] and Merlin Labs [24]. In the simulation, UAS are assumed to fly a constant indicated airspeed during all TP legs, holdings and holding transitions, and descents into the TP. UA acceleration or deceleration phases are not modeled. Vertical transitions such as from holdings into the TP are based on a maximum Rate Of Climb (ROC) and Rate Of Descent (ROD). Vertical performance variations or wind impacts are not considered.

$$\begin{aligned} \text{Steady indicated airspeed } (v_{\text{avg}}) &= 90\,\text{kn } (\sim 2.78\,\text{km per min}); \\ \text{Maximum rate of descent } (r_{\text{ROD}}) &= 800\,\text{ft } (\sim 240\,\text{m}) \text{ per min}; \\ \text{Maximum rate of climb } (r_{\text{ROC}}) &= 1200\,\text{ft } (\sim 370\,\text{m}) \text{ per min}. \end{aligned}$$

The geometries of the UAS trajectories, the limits of the lower and upper holding layer altitude, and UAS trajectory separation thresholds (i.e., HMD and VMD) are assumed constant throughout the simulation. As explained in Section 2.3.2, in collision avoidance research, UAS trajectories are expected to be protected by a cylindrical safety volume around the UA to effectively separate from other airspace users. Accordingly, this research applies a simplified standard safety volume around the UA as a tactical deconfliction layer to drive holding and sequencing decisions. This simplified standard safety volume is based on the DAA capabilities of current ACAS X variants, using an HMD of 2000 ft (∼610 m) and a VMD of 500 ft (∼150 m). The safety volume is projected around the simulated UAS trajectory and is evaluated against historical manned trajectories to detect separation violations. A separation violation (i.e., a conflict) occurs if another aircraft violates the safety volume around the UA; see Figure 11b. Geometrically, the horizontal separation is computed as the great-circle distance between the UAS and manned aircraft positions, and the vertical separation as the absolute altitude difference.

Historical manned tracks are synchronized to the simulation timeline and aligned with the UAS evaluation times via linear interpolation in time, where necessary, for example by linearly interpolating position and altitude at the required track states between two recorded samples. Conflict detection is updated every 5 s and applied to the current UAS state and over look-ahead horizons of 60, 120, or 180 s, which forecasts near-term conflicts and can trigger tactical actions such as holding.

UAS are strictly sequenced in FIFO order, and dynamic prioritization or trajectory negotiation is not modeled. Using different look-ahead horizons changes how far ahead the simulation checks for potential conflicts and, therefore, affects the resulting conflict assessment in space and time.

$$\begin{aligned} \text{Horizontal miss distance (HMD)} &= 2000\,\text{ft } (\sim 610\,\text{m}); \\ \text{Vertical miss distance (VMD)} &= 500\,\text{ft } (\sim 150\,\text{m}); \\ \text{Look-ahead time } (t_{\text{look-ahead}}) &\in \{60, 120, 180\}\,\text{s}. \end{aligned}$$

In addition, the simulation assumes a deterministic arrival schedule for UAS operations depending on the scenario. A periodic arrival structure allows for the analysis of UAS sequencing behavior, holding layer occupancy over time, and the evolution of queuing dynamics using different levels of UAS traffic demand. UAS arrivals occur only within an

operational time window between 08:00 AM and 6:00 PM local time. For each day of the year, UAS arrivals are scheduled at the top of the hour, followed by subsequent arrivals at fixed time intervals. UAS arrivals are not generated outside the 08:00 AM to 6:00 PM time window, and UAS will be released from holding at 6:00 PM local time, if necessary.

$$\text{Sequence of scheduled UAS arrival times } (\Delta t_{\text{UAS}}) \in \{15, 30\} \text{ min};$$
$$\text{Scheduled UAS arrival times } (t_{\text{UAS}}) \in \{08{:}00\,\text{AM},\ 08{:}00\,\text{AM} + \Delta t_{\text{UAS}},\ \ldots,\ 6{:}00\,\text{PM}\}.$$

Using 15 min and 30 min sequences of scheduled UAS arrival times is a pragmatic assumption to assess modest encounter rates and sequencing requirements of UAS around the airport TP. These two sequences are expected to be consistent with current demand (or even exceed hourly demands) at non-towered airports where traffic volumes are generally relatively low (see the following Section 4.1). Therefore, two to four UAS arrivals per hour are considered feasible in this simulation study, with the 30 min sequence representing a conservative low-complexity baseline, while the 15 min sequence testing whether the same procedures still work under a moderate increase in interaction frequency.

In summary, the look-ahead times (60/120/180 s) and UAS arrival intervals (15/30 min) are scenario parameters to compare different operating conditions and are not intended as fixed operational requirements. The selected look-ahead times represent preliminary tactical decision times for terminal UAS interactions and align with commonly used look-ahead times in conflict detection logic [74,75]. For example, NASA's DAIDALUS (Detect and Avoid Alerting Logic for Unmanned Systems) provides a reference implementation of the functional requirements of the RTCA, Inc. DO–365 series "Minimum Operational Performance Standards (MOPS) for Detect and Avoid (DAA) Systems" to predict potential violations of a defined DAA separation buffer within specified look-ahead horizons and provides conflict alerting and resolution guidance [16,75].

Furthermore, the simulation distinguishes between two UAS interaction conditions with respect to other UAS, "not assigned" and "assigned". Under "not assigned", UAS plan and fly their approach as if other UAS were not present and the separation logic only considers conflicts with manned traffic. This is expected to reflect the introduction of initial UAS operations where UAS volumes are low or unknown and simplifies the analysis to "one UAS at a time" interacting only with manned aircraft. Therefore, potential conflicts between UAS are ignored. Under the "assigned" condition, if a conflict is detected, UAS are assigned to a specific holding layer altitude that is chosen to avoid both manned traffic and other UAS. Interactions between UAS are explicitly modeled as newly arriving UAS must find a conflict-free holding layer given the already assigned UAS.

However, inherent in this simulation is the assumption that manned traffic can be detected, especially non-cooperative VFR aircraft without a transponder, and that there exist safety thresholds at which, for example, the TP is "not accessible" to UAS and UAS are required to hold. In this work, real-time traffic monitoring is expected to be provided to the RP via GBSS, such as a local low-altitude radar close to the non-towered airport to provide traffic information about manned aircraft, and/or via digital services from U-space to provide information about other UAS.

3.3.1. Decision-Making Process "Commit Holding Above TP"

Figure 16 provides a flow chart that describes the UAS decision-making process to integrate directly into airport TP or initiate to hold in the event of an occupied TP or projected conflicts with the UAS trajectory. Note that for simplicity, the UAS TP integration area is abbreviated as UAS TP area in the following flow charts to enhance readability. After entering the terminal airspace (i.e., at $\texttt{DIR}_{\texttt{WP1}}$), the UA RP is provided with information on other UAS activities. The UAS is expected to integrate into the terminal airspace at an

altitude of 1000 ft (∼300 m) above the airport-specific TPA to have sufficient separation from potential traffic in the TP, which is consistent with current TP integration principles [30,31].

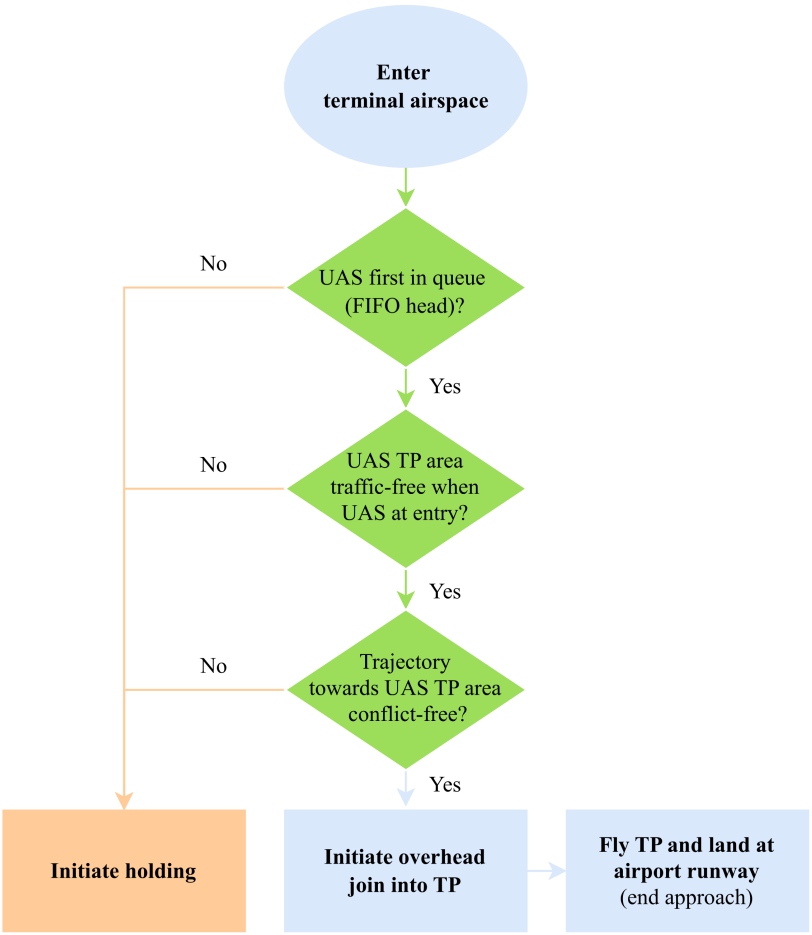

Figure 16. UAS decision-making flow chart "commit holding above TP".

The communication flows of airspace users, especially between different UA and their RPs, are beyond the scope of this paper. However, unmanned traffic management systems such as U-space could provide the required digital ecosystem and related services to monitor airspace activities and take responsibility for orderly traffic flows, provide sequencing information to UAS on arrival, departure and hold, and detect and resolve tactical conflicts of UAS trajectories with other manned/unmanned aircraft; see Ref. [37] for the U-space architecture and exemplary digital services. As mentioned earlier, different functionalities of the UAS C2 link and the role of RP in a TMA can be investigated in Ref. [39].

If there is at least one UAS in a holding layer above the TP (only under the "assigned" condition), the UAS will sequence behind the other UAS according to the FIFO principle. Therefore, the UAS will always initiate to hold if another UAS is holding ahead of the newly arriving UAS (i.e., "initiate holding"; see Figure 16). If there is no UAS in holding, the RP will be notified if the UAS TP integration area is traffic-free at UAS entry (i.e., at $\mathtt{DIR}_{\mathtt{WP2}}$). At the same time, the UAS trajectory towards the UAS TP integration area (i.e., $\mathtt{DIR}_{\mathtt{WP1}}$ to $\mathtt{DIR}_{\mathtt{WP2}}$) is checked for conflicts with other airspace users. If there is projected traffic in the UAS TP integration area and/or a projected conflict with the UAS trajectory, the UAS will initiate to hold. Otherwise, if the UAS TP integration area remains free and the UAS trajectory has no conflicts, the UAS will initiate an overhead join once it reaches $\mathtt{DIR}_{\mathtt{WP2}}$, fly the TP and approach the runway.

3.3.2. Decision-Making Process "Pick Holding Layer Above TP"

After the UAS decision-making process initiates to hold, a holding layer altitude must be picked. As derived in Ref. [11], the minimum holding altitude, hold_{min}, should be at an altitude sufficiently separated from TP activities, namely 1000 ft (∼300 m) above conventional TPA, which is at a maximum of 1500 ft (∼460 m) AGL. The maximum holding altitude, hold_{max}, is limited to 5500 ft (∼1680 m) AGL to avoid manned traffic flows in higher airspaces and to limit the descent time and distance of UAS from holding into TP. The initial terminal altitude of UAS, UAS_{occ}, will be set to the airport-specific recommended TPA plus an additional 1000 ft (∼300 m), as explained in the previous section. Note that, as explained in Section 3.1, 1000 ft (∼300 m) above the airport-specific recommended TPA is also the upper bound of the UAS TP integration area; see Figure 12.

The altitudes of active holding layers, $\text{hold}_{\text{occ},j}$, are vertically separated in 500 ft steps, Δ_{vertical}. The vertical separation step, Δ_{vertical}, also accounts for vertical separation from manned aircraft. The altitude of other manned aircraft present in airspace segments relevant for UAS integration is indicated as $\text{traffic}_{\text{occ},i}$. Here, $i = 1, \ldots, N_T$ indexes manned aircraft and $j = 1, \ldots, N_H$ indexes holding layers.

$$\begin{aligned}
\text{hold}_{\text{min}} &= 2500 \text{ ft AGL};\\
\text{hold}_{\text{max}} &= 5500 \text{ ft AGL};\\
\text{UAS}_{\text{occ}} &= \text{Recommended TPA} + 1000 \text{ ft};\\
\text{traffic}_{\text{occ},i} &: \text{Altitude of manned traffic } i, \quad i = 1, \ldots, N_T;\\
\text{hold}_{\text{occ},j} &: \text{Altitude of occupied holding layer } j, \quad j = 1, \ldots, N_H;\\
\Delta_{\text{vertical}} &: \text{Vertical separation step (i.e., 500 ft).}
\end{aligned}$$

Equation (1) gives the baseline altitude for holding, $\text{hold}_{\text{base}}$, to be at least hold_{min} and vertically separated from the highest observed manned altitude below the UAS, UAS_{occ}.

$$\text{hold}_{\text{base}} = \max\Big(\text{hold}_{\text{min}},\ \max\left\{\text{traffic}_{\text{occ},i} : \text{traffic}_{\text{occ},i} \le \text{UAS}_{\text{occ}}\right\} + \Delta_{\text{vertical}}\Big). \tag{1}$$

For example, with the TPA being at 1200 ft AGL ($\text{UAS}_{\text{occ}} = 2200$ ft AGL), $\Delta_{\text{vertical}} = 500$ ft and an exemplary maximum manned traffic altitude of 2100 ft AGL below UAS_{occ}, the resulting baseline holding altitude is $\text{hold}_{\text{base}} = \max(2500,\ 2100 + 500) = 2600$ ft AGL. This ensures selecting an appropriate holding altitude while maintaining vertical separation from manned traffic, even tough the recommended TPA can be expected to be at or below 1000 ft (∼300 m) AGL for most non-towered airports.

Equation (2) shows the options to choose the altitude of the initial holding layer (i.e., L_0) under conditions "assigned" (i.e., multiple UAS are allowed to hold above TP; one UAS per layer) and "not assigned" (i.e., other UAS in the terminal airspace are ignored by the arriving UAS; multiple UAS holdings are not possible).

$$L_0 = \begin{cases} \max\Big(\text{hold}_{\text{base}},\ \max(\text{hold}_{\text{occ},j}) + \Delta_{\text{vertical}}\Big), & \text{assigned},\\ \text{hold}_{\text{base}}, & \text{not assigned}. \end{cases} \tag{2}$$

Equation (3) shows the variable L, which denotes the current candidate holding layer altitude and is initialized as $L \leftarrow L_0$. For UAS under "assigned" condition, L_0 is set to the greater of $\text{hold}_{\text{base}}$ and the highest occupied layer plus a separation threshold Δ_{vertical}; otherwise, $L_0 = \text{hold}_{\text{base}}$.

$$L \leftarrow L_0. \tag{3}$$

In the next step, the algorithmic conflict resolution logic of the UAS decision "pick holding layer" is explained in Equations (4)–(7). Note that Equations (4)–(7) conceptually read as algorithmic rules rather than mathematical equations and the decision logic is only valid for condition "assigned". Equation (4) shows if the candidate holding layer, L, has an altitude band conflict, for example, with manned aircraft crossing the candidate layer. Similarly to the safety volume placed around the UA itself, the holding layer is also protected by a standard safety volume with the same HMD and VMD as the volume around the UA; see Section 3.3.1. If there is a projected altitude band conflict (i.e., manned traffic in the holding layer plus the safety volume), the algorithm moves the holding layer search upwards by one layer step, Δ_{vertical}. The search continues until the altitude band conflict is resolved or hold_{max} is reached.

If no vertical holding layer is available due to conflicting altitude bands (i.e., manned aircraft interaction), then the UAS cannot safely hold above TP and holding is denied; see Equation (5). Consequently, the UAS will end its TP approach, for example, by leaving the terminal airspace; see Figure 11c. This part of the UAS trajectory is not simulated; once a UAS receives the command "holding denied", the simulation run for the UAS ends.

If a suitable holding layer is identified, then the UAS trajectory towards the holding layer is checked for potential conflicts with manned aircraft trajectories. Consequently, similar to Equation (4), Equation (6) performs the same upward search logic, but for conflict-free UAS trajectories. If a conflict-free UAS trajectory towards L is identified, then $\text{hold}_{\text{final}} = L$. Else, if the projected trajectory conflict cannot be resolved by moving to higher holding layers, the UAS receives the command "holding aborted" and the simulation run for the UAS ends; see Equation (7).

$$\begin{aligned}
\text{bandConflict}(L): &\ \text{Search for potential manned aircraft conflict with candidate UAS holding layer } (L);\\
\text{trajConflict}(L): &\ \text{Search for potential manned aircraft conflict with UAS trajectory towards candidate UAS holding layer } (L).
\end{aligned}$$

$$\text{while bandConflict}(L) \wedge (L + \Delta_{\text{vertical}} \leq \text{hold}_{\text{max}}): \quad L \leftarrow L + \Delta_{\text{vertical}}, \tag{4}$$

$$\text{if bandConflict}(L) \wedge (L + \Delta_{\text{vertical}} > \text{hold}_{\text{max}}): \quad \text{holding denied,} \tag{5}$$

$$\text{else proceed to trajectory check,}$$

$$\text{while trajConflict}(L) \wedge (L + \Delta_{\text{vertical}} \leq \text{hold}_{\text{max}}): \quad L \leftarrow L + \Delta_{\text{vertical}}, \tag{6}$$

$$\text{if trajConflict}(L) \wedge (L + \Delta_{\text{vertical}} > \text{hold}_{\text{max}}): \quad \text{holding aborted.} \tag{7}$$

Equation (8) provides a summary of the algorithmic conflict resolution logic. After initializing L with L_0, the simulation algorithm incrementally increases the holding layer altitudes by Δ_{vertical} to identify conflict-free holding altitudes and resolve projected UAS trajectory conflicts towards the candidate holding layer, L. If there is no conflict-free holding layer below hold_{max} or the UAS cannot safely reach the candidate holding layer, UAS holding is denied or aborted, otherwise $\text{hold}_{\text{final}}$ is set to the resulting L.

$$\text{hold}_{\text{final}} = \begin{cases} \text{deny}, & \text{bandConflict}(L) \wedge (L + \Delta_{\text{vertical}} > \text{hold}_{\text{max}}),\\ \text{abort}, & \neg\text{bandConflict}(L) \wedge \text{trajConflict}(L) \wedge (L + \Delta_{\text{vertical}} > \text{hold}_{\text{max}}),\\ L, & \neg\text{bandConflict}(L) \wedge \neg\text{trajConflict}(L). \end{cases} \tag{8}$$

In short, "holding denied" is issued if a manned aircraft trajectory conflicts with the candidate UAS holding layer (L plus safety buffers HMD and VMD) by the time the UAS

reaches L; see Figure 11c. "Holding aborted" is provided if L was eligible for holding but the UAS trajectory towards L has a manned aircraft conflict; see Figure 11d.

Figure 17 provides the flow chart that shows the decision logic on how the UAS holding layer altitude, L, is chosen and how the UAS will react if no holding layer above TP is available.

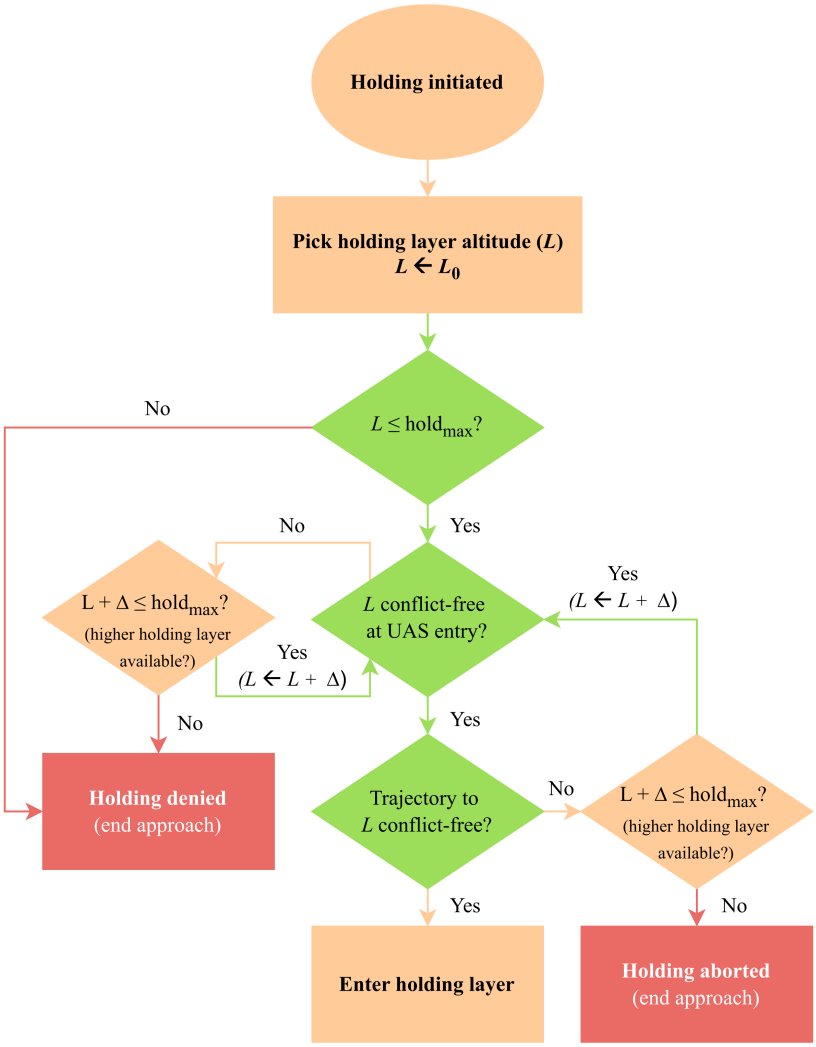

Figure 17. UAS decision-making flow chart "pick holding layer above TP".

After the UAS commits to enter holding at $\texttt{DIR}_{\texttt{WP1}}$ (i.e., "holding initiated"; see Figure 17), $\texttt{DIR}_{\texttt{WP1}}$ becomes $\texttt{EHLD}_{\texttt{WP1}}$ and EHLD is flown towards the beginning of the holding trajectory, HLD. Here, the final EHLD WP, $\texttt{EHLD}_{\texttt{WP4}}$, becomes the initial HLD WP, $\texttt{HLD}_{\texttt{WP1}}$ (i.e., "enter holding layer"; see Figure 17).

3.3.3. Decision-Making Process "Rejoin TP from Holding"

After entering the holding layer at $\texttt{HLD}_{\texttt{WP1}}$ (i.e., "holding layer entered"; see Figure 18), the UAS is provided with information on when and where the UAS will be allowed to descend to a lower holding altitude or into TP for landing. At every gate WP of the holding (i.e., $\texttt{HLD}_{\texttt{WP2}}$, $\texttt{HLD}_{\texttt{WP5}}$, $\texttt{HLD}_{\texttt{WP8}}$, and $\texttt{HLD}_{\texttt{WP11}}$; see Figure 14), the UAS can descend to a new lower holding layer altitude, L, provided that L and the UAS trajectory to L are conflict-free using a determined look-ahead time (i.e., 60/120/180 s) and the specified minimum vertical separation, Δ_{vertical}, from other holdings and manned aircraft is maintained. Otherwise, the UAS will continue to orbit in its current holding layer.

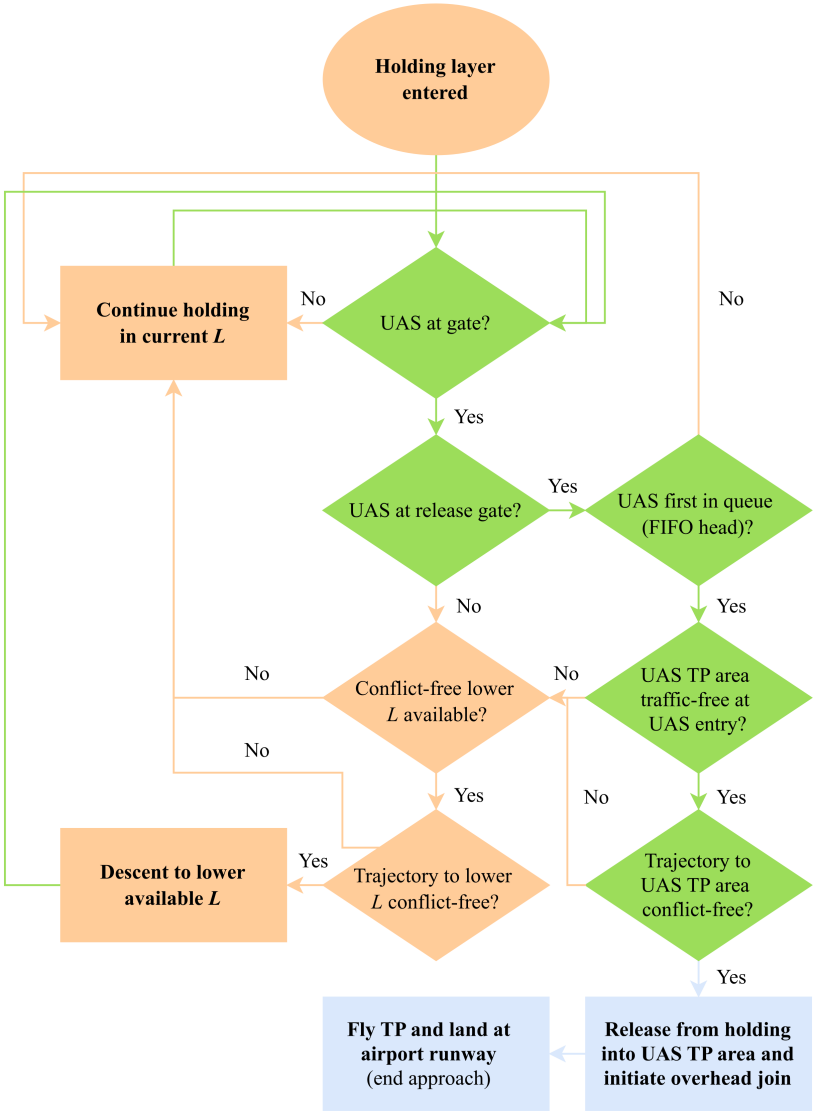

Figure 18. UAS decision-making flow chart "rejoin TP from holding".

Figure 18 provides the flow chart that shows the decision logic on how the UAS will transition from its holding layer to lower holding layers or the airport TP towards landing. At the gate release WP (i.e., $\texttt{HLD}_{\texttt{WP8}}$), if the UAS is first in sequence order (i.e., FIFO head; lowest UAS in hold), the UAS can descend towards TP, provided that the UAS TP integration area (i.e., airspace around TP) is traffic-free using a specified look-ahead time and the UAS trajectory to TP is conflict-free. From $\texttt{HLD}_{\texttt{WP8}}$, which becomes $\texttt{REJ}_{\texttt{WP1}}$ in case of gate release towards TP, the UAS will steadily descend to $\texttt{REJ}_{\texttt{WP3}}$ at UAS_{occ} (i.e., recommended TPA + 1000 ft), before integrating into the TP via overhead join approach towards runway at $\texttt{REJ}_{\texttt{WP3}}$, which becomes $\texttt{DIR}_{\texttt{WP2}}$ at UAS_{occ} altitude.

4. Data Analysis and Results

Based on the algorithmic simulation approach discussed in the previous sections, Table 2 provides an overview of the baseline altitudes relevant for the UAS simulation study using the airspace environments of Juist (EDWJ) and Egelsbach (EDFE).

Table 2. Overview of baseline altitudes relevant for UAS integration.

	Juist (EDWJ)	**Egelsbach (EDFE)**
Airport-specific recommended TPA	600 ft MSL (592 ft AGL)	1300 ft MSL (915 ft AGL)
Height of UAS TP integration area	TPA [1] + 1000 ft = 1592 ft AGL	TPA [1] + 1000 ft = 1915 ft AGL
UAS integration altitude (UAS_{occ})		
Standard min. holding altitude ($hold_{min}$)	2500 ft AGL	2500 ft AGL

[1] Note that TPA refers to the airport-specific recommended TPA, not the conventional TPA.

UAS_{occ} is based on the airport-specific recommended TPA plus an additional buffer altitude of 1000 ft (∼300 m) to have sufficient separation from potential traffic in the TP; see Section 3.1. Since the recommended TPA at Juist (EDWJ) and Egelsbach (EDFE) varies, different UAS TP integration area altitudes and UAS_{occ} are obtained for each airport.

4.1. Analysis of Temporal Traffic Distribution in the UAS TP Integration Area

To better understand manned traffic behaviors in the TP airspace segment relevant for UAS integration, different statistical metrics are analyzed and visualized in the following Figures 19 and 20. Figure 19 provides an overview of daily historical flights at Juist (EDWJ) and Egelsbach (EDFE) using the daily total unique flight count (see Total_d in Equation (9)), the daily median of hourly unique flight counts (see Median_d in Equation (10)) and the daily mean of hourly unique flight counts (see Mean_d in Equation (11)).

Let D be the number of days per year (i.e., $D = 365$) and $h \in \{8, 9, \ldots, 17\}$ denote daily airport operating hours, $d \in \{1, \ldots, D\}$, for a standard time window from 8:00 AM to 6:00 PM local time. The hourly unique flight count, $\text{count}_{d,h}$, is defined as the number of unique flights present during hour h on day d.

$$\text{Total}_d = \text{number of unique flights present on day } d \quad [\text{flights}]. \tag{9}$$

$$\text{Median}_d = \text{median}\Big(\text{count}_{d,8}, \text{count}_{d,9}, \ldots, \text{count}_{d,17}\Big) \quad [\text{flights}]. \tag{10}$$

$$\text{Mean}_d = \frac{1}{10} \sum_{h=8}^{17} \text{count}_{d,h} \quad [\text{flights}]. \tag{11}$$

Significant deviations in flight counts can be observed throughout the year in the UAS TP integration area for both airports; see Figure 19. In 2022, at Juist (EDWJ), fewer than five daily flights occurred in the months of January and February, while flight counts increased significantly in spring and summer, especially during May. For flights in the UAS TP integration area, the busiest day at Juist (EDWJ) was on May 18, with 43 daily flights between 8:00 AM and 6:00 PM local time. In addition, taking into account the median and mean values provides insight into traffic distributions over the year and within the day and how that traffic is spread over hours. During the year, a median of 3.0 and a mean of ∼5.6 daily flights occurred in the TP airspace segment relevant for UAS integration at Juist (EDWJ). The higher mean value indicates recurring traffic peaks in certain times of the day rather than uniformly high traffic throughout the day. A higher mean value compared to the median daily flight counts can also be observed at Egelsbach (EDFE). However, compared to Juist (EDWJ), traffic activities peak in the months of January to March, with a maximum of 68 daily flights on January 6, and the TP area of Egelsbach (EDFE) was significantly busier than Juist (EDWJ) with a median of 14.0 and a mean of ∼15.9 daily flights.

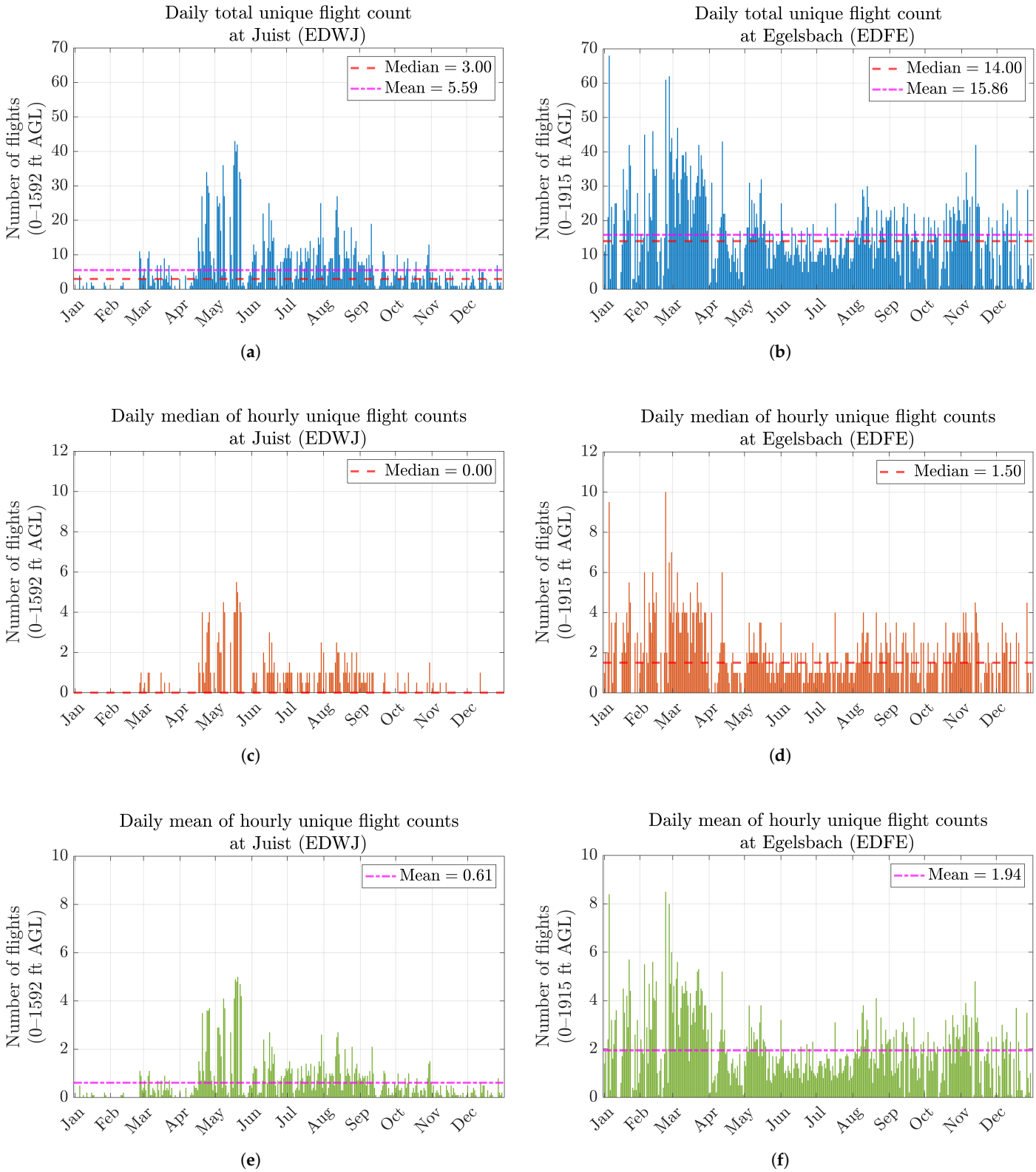

Figure 19. Statistics of flights in the UAS TP integration area for ten airport operating hours from 8:00 AM to 6:00 PM local time: Daily total unique flight count (Total_d) at (**a**) Juist (EDWJ) and (**b**) Egelsbach (EDFE). Daily median of hourly unique flight counts (Median_d) at (**c**) Juist (EDWJ) and (**d**) Egelsbach (EDFE). Daily mean of hourly unique flight counts (Mean_d) at (**e**) Juist (EDWJ) and (**f**) Egelsbach (EDFE).

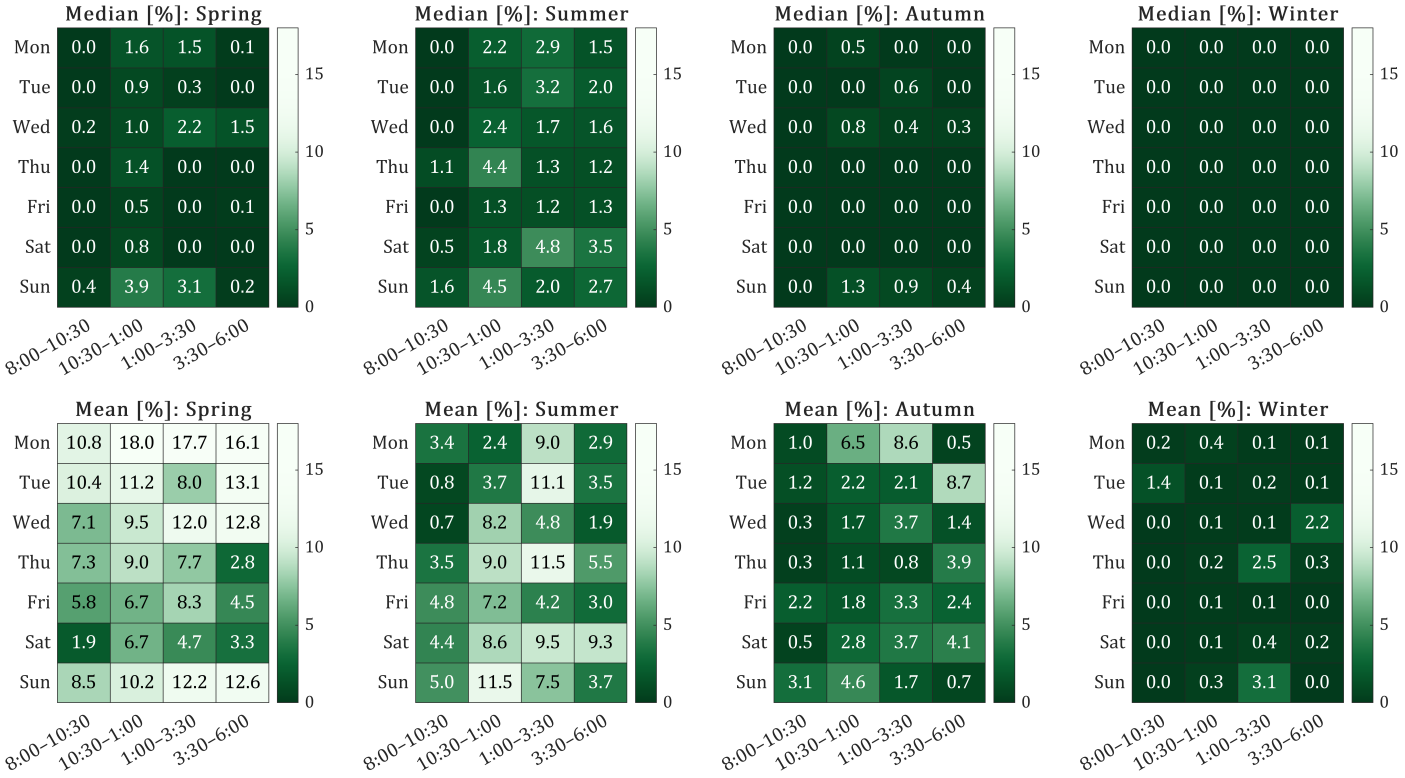

(**a**)

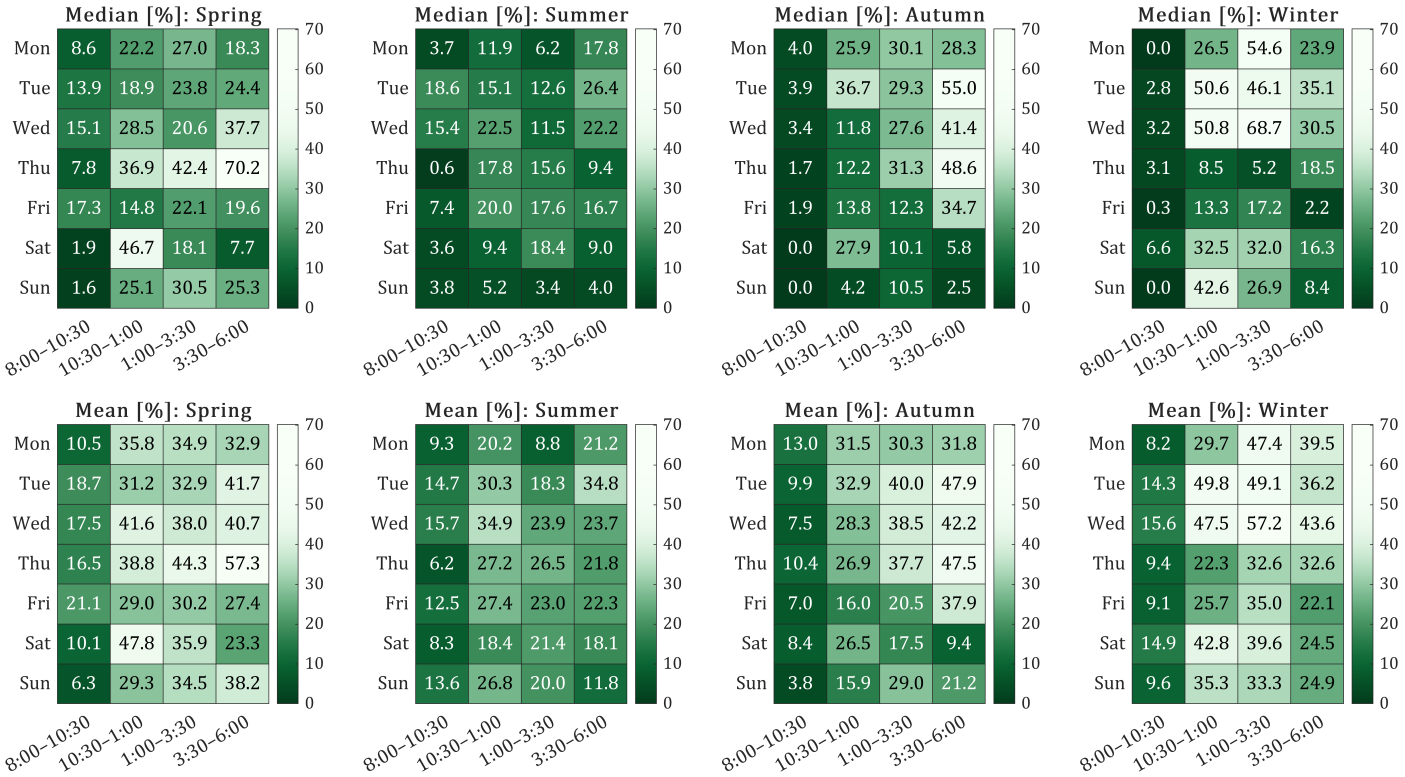

(**b**)

Figure 20. Temporal airspace occupancy of at least one manned aircraft present in the UAS TP integration area for ten airport operating hours from 8:00 AM to 6:00 PM local time of (**a**) Juist (EDWJ) and (**b**) Egelsbach (EDFE). Spring covers the months of March, April, and May, summer covers June, July, and August, autumn covers September, October, and November, and winter covers December, January, and February.

During the day, on average, there were less than one flight (i.e., median of 0.00 flights and mean of 0.61 flights) per airport operating hour at Juist (EDWJ) and less than two flights (i.e., median of 1.50 flights and mean of 1.94 flights) on average per hour at Egelsbach (EDFE). The busiest hourly flight count at Juist (EDWJ) occurred in May, with a median of 5.5 flights on May 20 and a mean of 5.0 flights on May 19. At Egelsbach (EDFE), February was considered the busiest month in terms of average hourly flight counts, with a median of 10.0 flights on February 23 and a mean average of 8.5 flights on February 23.

To better understand recurring traffic peaks in certain times of the day and throughout the annual seasons of each airport, Figure 20 provides information on the temporal airspace occupancy of at least one manned aircraft present in the UAS TP integration area. At Juist (EDWJ), the mean temporal occupancy peaks on Mondays in spring between 10:30 AM and 1:00 PM with an average airspace occupancy of 18.0% of at least one present aircraft. On all other days of the week, airspace occupancy during that time window ranges from 6.7% to 11.2%. The mean airspace occupancy stays below 8.7% in autumn and below 3.1% in winter. Again, compared to the lower values of the median airspace occupancy, the higher mean values indicate recurring traffic peaks in certain time windows, for example due to good weather conditions.

At Egelsbach (EDFE), the highest temporal airspace occupancy can be seen on Thursday afternoons in spring, with a 70.2% rate between 3:30 PM and 6:00 PM, whereas the occupancy of other days of the week only ranges from 7.7% to 37.7% in the afternoon. This pattern could be explained by the usual increase in business aviation activities on Thursday evenings, as end-of-week return travel brings people back from business trips.

In summary, analysis of average flight counts and temporal airspace occupancies directly affect UAS airspace accessibility by assessing the probability of conflicts with manned aviation, interaction risk, and expected waiting times during high-traffic periods. Identifying off-peak time windows that reduce queuing and in-flight encounters with manned aircraft can therefore be considered an important early enabler for safe UAS integration. In contrast, peak hours are likely to increase the probability and duration of UAS holdings, as well as fuel consumption and the overall risk of conflicts.

4.2. Analysis of Spatial Traffic Distribution in the UAS TP Integration Area

In addition to the temporal airspace availability at non-towered airports, spatial airspace availability needs to be considered for safe and efficient UAS integration. Figure 21 provides information on manned flight behavior of different aircraft categories in the UAS TP integration area of Juist (EDWJ) and Egelsbach (EDFE) over the course of a year. The following aircraft types are investigated:

LA: "Light-weight" civilian fixed-wing aircraft with <2.0 t MTOW;
MA: "Medium-weight" civilian fixed-wing aircraft with 2.0–5.7 t MTOW;
HA: "Heavy-weight" civilian fixed-wing aircraft with >5.7 t MTOW;
GLI: Non-motor-driven civilian fixed-wing aircraft such as gliders;
HEL: Civilian rotary-wing aircraft such as helicopters;
MIL: Military fixed-wing and rotary-wing aircraft;
OTH: Other aircraft such as balloons or gyrocopters;
N/A: Aircraft without a type designator.

In Figures 21 and 22, the occurrence of historical manned flights is shown in the UAS TP integration area. Each data point in Figure 21 indicates a unique flight, the color of the data points represents the aircraft type, the *y*-axis shows the initial integration altitude, and the *x*-axis provides information on the flight distance of each flight. Figure 22 sorts aircraft types by their initial airspace integration altitude and provides the flight count per aircraft type and the total flight count for each altitude band.

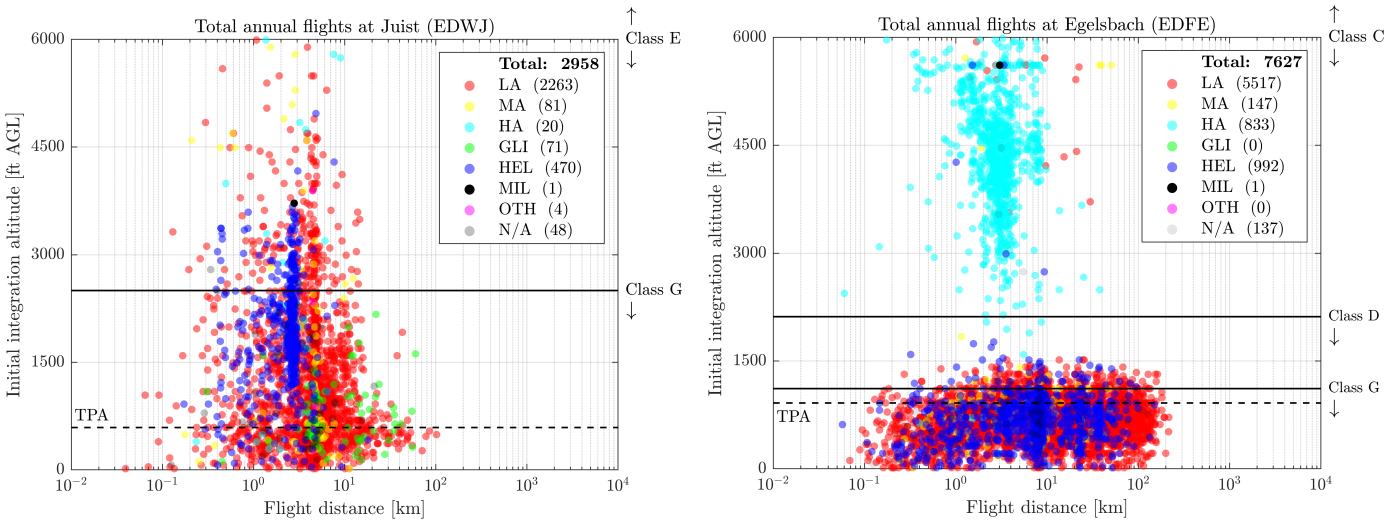

Figure 21. Scatter plots for airports of interest for annual flights in the UAS TP integration area and above up to 6000 ft (∼1830 m) AGL. Each data point indicates the initial airspace integration altitude (*y*-axis), the operated flight distance (*x*-axis), and the aircraft type (color) for all flights at (**a**) Juist (EDWJ) and (**b**) Egelsbach (EDFE). Note that arriving and departing aircraft are shown.

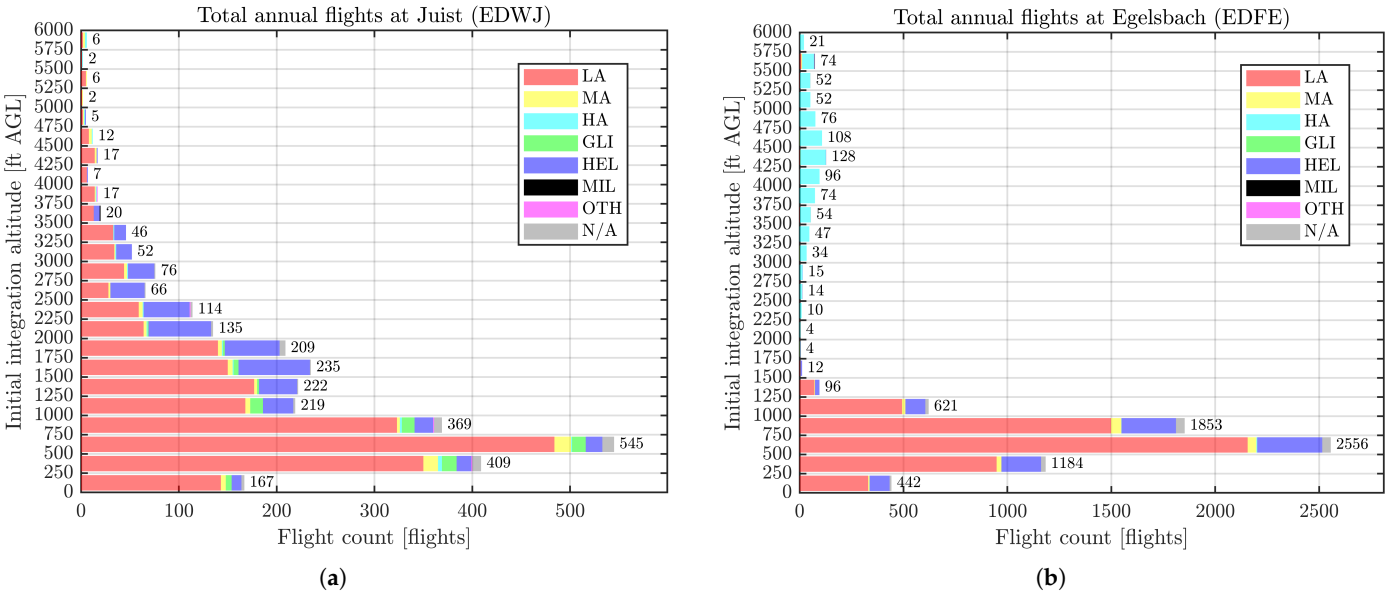

Figure 22. Bar plots for airports of interest for annual flights in the UAS TP integration area and above up to 6000 ft (∼1830 m) AGL. Each bar sorts aircraft types (color) by their initial airspace integration altitude (*y*-axis) and provides the flight count per aircraft type and total flight count for each altitude band (*x*-axis) at (**a**) Juist (EDWJ) and (**b**) Egelsbach (EDFE). Note that arriving and departing aircraft are shown.

The vertical distribution of flights indicates where manned aircraft have historically integrated into the TP and which types of manned aircraft the UAS has to expect in different altitude bands in and around the UAS TP integration area. At Juist (EDWJ), aircraft types are more evenly distributed vertically than at Egelsbach (EDFE); see Figure 21. Most helicopter occurrences ("HEL" designator) are found between ∼1500 and 3000 ft (∼460–910 m) AGL at Juist (EDWJ), likely crossing the terminal airspace on their way to offshore wind parks located north of the island. At Egelsbach (EDFE) within Class D airspace, mainly aircraft with >5.7 t MTOW ("HA" designator) to or from Frankfurt (EDDF) occur, likely IFR-flying

aircraft. Here, it can be expected that ATC restricts VFR-flying aircraft from entering Class C and Class D airspace to avoid interfering with arriving or departing aircraft to or from the German main airport Frankfurt (EDDF). Note that, at Egelsbach (EDFE) in contrast to Juist (EDWJ), more aircraft ("LA" designator) have relatively long flight distances in the TP area, even over 100 km. Looking at individual historical flights, some aircraft flew repeated TP circuits for more than an hour, probably training flights by one of the local flight schools.

Recalling that the recommended TPA for Juist (EDWJ) and Egelsbach (EDFE) is at 600 ft MSL (592 ft AGL) and 1300 ft MSL (915 ft AGL), most aircraft integrated between 500 and 750 ft (∼150–230 m) AGL at both airports (545 and 2556 aircraft); see Figure 22. It can be summarized that both conflict risk and intent predictability are likely to change throughout altitude bands, as different aircraft types tend to fly different speeds and TP integration maneuvers. Some altitude bands are under-utilized (e.g., 1500–2500 ft (∼460–760 m) AGL at Egelsbach (EDFE)) and may offer feasible approach corridors for UAS, while other altitude bands are more saturated and effectively reduce UAS accessibility. For example, dense altitude bands with faster traffic likely require earlier detection of airspace users and more conservative separation thresholds to safely integrate UAS or even necessitate UAS holding if occupied.

4.3. Analysis of Fast-Time Simulation Results for Procedural UAS TP Area Integration

This section presents the simulation-based analysis of UAS terminal integration procedures that employ tactical holding decisions to enable short-term deconfliction between UAS and manned traffic in uncontrolled terminal airspaces.

Table 3 provides information on the theoretical flight times and distances of UAS in certain simulation scenarios, which were derived in Section 3.2. Based on airport-specific TP schemes, theoretical flight times and distances vary for UAS trajectories at Juist (EDWJ) and Egelsbach (EDFE). At Juist (EDWJ), a single holding orbit (i.e., $\texttt{HLD}_{\texttt{WP1}}$ to $\texttt{HLD}_{\texttt{WP1}}$), for example, requires 4.1 min flight time and ∼11.3 km flight distance, while at Egelsbach (EDFE) a holding orbit requires 6.4 min and ∼17.6 km.

Table 3. Theoretical UAS trajectory times and distances for airports of interest.

	Juist (EDWJ)			**Egelsbach (EDFE)**		
	Time [s]	**Time [min]**	**Distance [km]**	**Time [s]**	**Time [min]**	**Distance [km]**
Full trajectory (no holding) $\texttt{DIR}_{\texttt{WP1}}$ to RWY	418.9	7.0	19.40	473.6	7.9	21.93
Pre-overhead join trajectory $\texttt{DIR}_{\texttt{WP1}}$ to $\texttt{DIR}_{\texttt{WP2}}$	205.8	3.4	9.53	171.0	2.9	7.92
Holding trajectory (one orbit) $\texttt{HLD}_{\texttt{WP1}}$ to $\texttt{HLD}_{\texttt{WP1}}$	244.8	4.1	11.33	380.7	6.4	17.63
Trajectory to holding gate release [1] $\texttt{DIR}_{\texttt{WP1}}$ to $\texttt{HLD}_{\texttt{WP8}}$	597.1	10.0	27.65	801.3	13.4	37.10
Holding gate release trajectory $\texttt{HLD}_{\texttt{WP8}}$ to RWY	285.6	4.8	13.23	381.7	6.4	17.67
Full trajectory (with holding) [1] $\texttt{DIR}_{\texttt{WP1}}$ to RWY via HLD	882.8	14.7	40.87	1183.0	19.7	54.77

[1] Note that the trajectory includes an entire holding orbit.

Tables 4 and 5 provide information on the simulation results for Juist (EDWJ) and Egelsbach (EDFE) to quantify how predictive safety constraints (i.e., conflict detection within 60/120/180 s) and UAS stacking principles might impact terminal capacity at non-towered airports. For each scenario, a total of 14,600 flights were simulated over the course

of a year for Δt_{UAS} = 15 min (i.e., four UAS per hour over ten airport operating hours over 365 days) and 7300 simulated flights were conducted for Δt_{UAS} = 30 min.

Table 4. Simulation statistics for Juist (EDWJ): "Not assigned" and "assigned" conditions. Note that percentages are based on "total UAS flights" if not indicated differently.

Juist (EDWJ): "Not Assigned" Condition						
Look-ahead time for conflict detection	60 s		120 s		180 s	
UAS traffic rate (Δt_{UAS})	15 min	30 min	15 min	30 min	15 min	30 min
Total UAS flights	14,600 (100.0%)	7300 (100.0%)	14,600 (100.0%)	7300 (100.0%)	14,600 (100.0%)	7300 (100.0%)
Flights without holding	13,814 (94.6%)	6919 (94.8%)	13,634 (93.4%)	6814 (93.3%)	13,461 (92.2%)	6724 (92.1%)
Holding flights required	786 (5.4%)	381 (5.2%)	966 (6.6%)	486 (6.7%)	1139 (7.8%)	576 (7.9%)
Holding flights conducted [1]	648 (82.4%)	316 (82.9%)	826 (85.5%)	419 (86.2%)	996 (87.4%)	507 (88.0%)
Holding flights aborted [1]	138 (17.6%)	65 (17.1%)	140 (14.5%)	67 (13.8%)	143 (12.6%)	69 (12.0%)
Holding flights denied [1]	0 (0.0%)	0 (0.0%)	0 (0.0%)	0 (0.0%)	0 (0.0%)	0 (0.0%)
Mean orbit count per holding	1.7	1.8	1.9	1.9	2.2	2.2
Median orbit count per holding	1.0	1.0	1.0	1.0	1.0	1.0
Mean holding altitude [ft AGL]	2500	2500	2500	2500	2500	2500
Median holding altitude [ft AGL]	2500	2500	2500	2500	2500	2500
Juist (EDWJ): "Assigned" Condition						
Look-ahead time for conflict detection	60 s		120 s		180 s	
UAS traffic rate (Δt_{UAS})	15 min	30 min	15 min	30 min	15 min	30 min
Total UAS flights	14,600 (100.0%)	7300 (100.0%)	14,600 (100.0%)	7300 (100.0%)	14,600 (100.0%)	7300 (100.0%)
Flights without holding	13,724 (94.0%)	6915 (94.7%)	13,473 (92.3%)	6805 (93.2%)	13,241 (90.7%)	6708 (91.9%)
Holding flights required	876 (6.0%)	385 (5.3%)	1127 (7.7%)	495 (6.8%)	1359 (9.3%)	592 (8.1%)
Holding flights conducted [1]	737 (84.1%)	320 (83.1%)	985 (87.4%)	428 (86.5%)	1214 (89.3%)	523 (88.3%)
Holding flights aborted [1]	139 (15.9%)	65 (16.9%)	141 (12.5%)	67 (13.5%)	144 (10.6%)	69 (11.7%)
Holding flights denied [1]	0 (0.0%)	0 (0.0%)	1 (0.1%)	0 (0.0%)	1 (0.1%)	0 (0.0%)
Mean orbit count per holding	1.8	2.0	2.3	1.9	2.6	2.7
Median orbit count per holding	1.0	1.0	1.0	1.0	2.0	2.0
Mean holding altitude [ft AGL]	2607	2522	2668	2500	2715	2542
Median holding altitude [ft AGL]	2500	2500	2500	2500	2500	2500
UAS holding count touching altitude band [1,2]						
2500–<3000 ft AGL	716 (97.3%)	317 (99.1%)	932 (94.6%)	425 (99.3%)	1117 (92.2%)	517 (98.9%)
3000–<3500 ft AGL	3 (0.4%)	0 (0.0%)	16 (1.6%)	1 (0.2%)	30 (2.5%)	2 (0.4%)
3500–<4000 ft AGL	16 (2.2%)	2 (0.6%)	49 (5.0%)	4 (0.9%)	89 (7.3%)	7 (1.3%)
4000–<4500 ft AGL	6 (0.8%)	1 (0.3%)	21 (2.1%)	1 (0.2%)	43 (3.6%)	2 (0.4%)
4500–<5000 ft AGL	2 (0.3%)	0 (0.0%)	6 (0.6%)	0 (0.0%)	12 (1.0%)	0 (0.0%)
5000–<5500 ft AGL	3 (0.4%)	0 (0.0%)	10 (1.0%)	0 (0.0%)	18 (1.5%)	0 (0.0%)

[1] Percentages are based on "holding flights required". [2] Note that an individual flight can hold in multiple altitude bands.

Simulation statistics for Juist (EDWJ) show consistent trends in the evaluated temporal look-ahead horizons (60/120/180 s) and the UAS traffic rates Δt_{UAS} (15/30 min). In Table 4, under the "not assigned" condition, where UAS plan and fly their approach as if other UAS were not present, the majority of simulation flights are completed without holding (∼95% at 60 s to ∼92% at 180 s), while the fraction of holding flights increases with longer look-ahead horizons (from ∼5% at 60 s to ∼8% at 180 s). At the same time, the share of aborted holding flights decreases with increasing look-ahead horizon (from ∼17–18% to ∼12–13%), whereas no holding is denied. This combination indicates that longer look-ahead horizons trigger UAS holdings more frequently (i.e., more preventive interventions to avoid interaction with manned aircraft), but yield more stable holding executions once holding is initiated. Consistent with that interpretation, the mean holding orbit count increases from approximately 1.7 to 2.2 while the median remains at 1.0 across all configurations, suggesting a distribution in which most holding cases require only a single holding orbit, but a smaller subset of holdings requires multiple orbits. Under the "not assigned" condition, both mean and median holding altitudes remain fixed at 2500 ft (∼760 m) AGL, implying that holding procedures are essentially realized at hold_{min}.

Under the "assigned" condition, see Table 4, where interactions with other UAS are considered and holdings can be stacked, the trends with look-ahead horizons remain similar, but holdings become more prevalent and are more sensitive to UAS traffic rates. Holding flights increase from 5.3–6.0% at 60 s to 8.1–9.3% at 180 s, with consistently higher values for higher UAS traffic rates (i.e., Δt_{UAS} = 15 min). Aborted holdings again decrease with longer look-ahead times (from ∼16–17% to ∼11–12%), and holding denials remain negligible (near 0%). Importantly, the holding demand becomes more prevalent as the mean holding orbit count reaches ∼2.6–2.7 at 180 s and the median increases from 1.0 to 2.0 compared to the "not assigned" condition. This indicates that multi-layer holdings are not infrequent outliers but become more typical under the most conservative traffic detection setting of the simulation (i.e., 180 s).

Still, altitude band statistics further show that holdings remain strongly concentrated in the lowest possible altitude band (2500–<3000 ft (∼760–<910 m) AGL, typically ∼92–99% of holding flights), while higher altitude bands are used only occasionally. This is also reflected by the median holding altitudes, which remain at 2500 ft (∼760 m) AGL in all configurations, while the mean holding altitudes slightly increase (e.g., ∼2600–2700 ft (∼790–820 m) AGL).

Overall, the results suggest that increasing look-ahead times to detect manned traffic and/or increasing UAS traffic volumes affect the frequency and duration of holdings (more holdings and more holding orbits), while holding altitude diversification at Juist (EDWJ) remains a rarely used mechanism to balance occasional peaks in holding demand. In addition, for Juist (EDWJ), holdings can largely be considered an effective conflict management mechanism, as holding denials are negligible, and most holdings complete successfully, predominantly using the lowest altitude band (2500–<3000 ft (∼760–<910 m) AGL).

In Table 5, simulation statistics for the non-towered airport with the highest traffic volume in Germany, Egelsbach (EDFE), show an operating environment that is significantly more characterized by holding demands than Juist (EDWJ). For Egelsbach (EDFE), consistent sensitivities can be observed using temporal look-ahead windows (60/120/180 s) and different UAS traffic volumes, Δt_{UAS} (15/30 min). Under the "not assigned" condition, holdings are already frequent at the shortest look-ahead time horizon with ∼34–35% of all flights require holding at 60 s, increasing to ∼39–40% at 180 s. In parallel, the fraction of aborted holding flights decreases with longer look-ahead times (from ∼14% to ∼12%), indicating that longer look-ahead times not only trigger holding more often, but also tend to enable more stable holding executions. The holding rate at Egelsbach (EDFE) is considerable with mean holding orbit counts increasing from ∼6.6–6.7 to ∼7.4–7.5 with longer look-ahead times, while the median holding orbit count remains at 3.0 in all settings. Finally, under the "not assigned" condition, where other UAS are ignored, mean and median holding altitudes remain fixed at 2500 ft (∼760 m) AGL, implying that, despite the high prevalence of holdings, holdings are largely realized at $\mathrm{hold}_{\mathrm{min}}$.

Under the "assigned" condition in Table 5, similar look-ahead trends persist with holdings remaining high in demand and increasing with look-ahead times, but holding denials occur significantly more often, particularly for higher UAS traffic rates. For Δt_{UAS} = 15 min, holding denial rates reach ∼14–17% (increasing with look-ahead times), while, for Δt_{UAS} = 30 min, they remain substantially lower (∼4–5%). At Egelsbach (EDFE), this indicates that a significant subset of UAS approaches reaches conditions where holding is not feasible (e.g., due to capacity constraints) and that this effect is strongly amplified by higher UAS traffic volumes.

Table 5. Simulation statistics for Egelsbach (EDFE): "Not assigned" and "assigned" conditions. Note that percentages are based on "total UAS flights" if not indicated differently.

Egelsbach (EDFE): "Not Assigned" Condition						
Look-ahead time for conflict detection	60 s		120 s		180 s	
UAS traffic rate (Δt_{UAS})	15 min	30 min	15 min	30 min	15 min	30 min
Total UAS flights	14,600 (100.0%)	7300 (100.0%)	14,600 (100.0%)	7300 (100.0%)	14,600 (100.0%)	7300 (100.0%)
Flights without holding	9488 (65.0%)	4793 (65.7%)	9106 (62.4%)	4627 (63.4%)	8799 (60.3%)	4473 (61.3%)
Holding flights required	5112 (35.0%)	2507 (34.3%)	5494 (37.6%)	2673 (36.6%)	5801 (39.7%)	2827 (38.7%)
Holding flights conducted [1]	4407 (86.2%)	2159 (86.1%)	4787 (87.1%)	2325 (87.0%)	5092 (87.8%)	2477 (87.6%)
Holding flights aborted [1]	705 (13.8%)	348 (13.9%)	707 (12.9%)	348 (13.0%)	709 (12.2%)	350 (12.4%)
Holding flights denied [1]	0 (0.0%)	0 (0.0%)	0 (0.0%)	0 (0.0%)	0 (0.0%)	0 (0.0%)
Mean orbit count per holding	6.6	6.7	7.0	7.2	7.4	7.5
Median orbit count per holding	3.0	3.0	3.0	3.0	3.0	3.0
Mean holding altitude [ft AGL]	2500	2500	2500	2500	2500	2500
Median holding altitude [ft AGL]	2500	2500	2500	2500	2500	2500
Egelsbach (EDFE): "Assigned" Condition						
Look-ahead time for conflict detection	60 s		120 s		180 s	
UAS traffic rate (Δt_{UAS})	15 min	30 min	15 min	30 min	15 min	30 min
Total UAS flights	14,600 (100.0%)	7300 (100.0%)	14,600 (100.0%)	7300 (100.0%)	14,600 (100.0%)	7300 (100.0%)
Flights without holding	9543 (65.4%)	4717 (64.6%)	9284 (63.6%)	4552 (62.4%)	9096 (62.3%)	4420 (60.5%)
Holding flights required	5057 (34.6%)	2583 (35.4%)	5316 (36.4%)	2748 (37.6%)	5504 (37.7%)	2880 (39.5%)
Holding flights conducted [1]	3685 (72.9%)	2136 (82.7%)	3826 (72.0%)	2284 (83.1%)	3911 (71.1%)	2396 (83.2%)
Holding flights aborted [1]	683 (13.5%)	344 (13.3%)	671 (12.6%)	344 (12.5%)	669 (12.1%)	345 (12.0%)
Holding flights denied [1]	689 (13.6%)	103 (4.0%)	819 (15.4%)	120 (4.4%)	924 (16.8%)	139 (4.8%)
Mean orbit count per holding	6.3	7.2	6.6	7.7	7.0	8.1
Median orbit count per holding	3.0	3.0	3.0	3.0	3.0	4.0
Mean holding altitude [ft AGL]	3100	2911	3128	2945	3159	2972
Median holding altitude [ft AGL]	2500	2500	2897	2500	3000	2500
UAS holding count touching altitude band [1,2]						
2500–<3000 ft AGL	2450 (57.3%)	1523 (68.9%)	2438 (53.8%)	1551 (65.4%)	2391 (50.8%)	1558 (62.4%)
3000–<3500 ft AGL	1025 (24.0%)	481 (21.8%)	1094 (24.1%)	514 (21.7%)	1129 (24.0%)	572 (22.9%)
3500–<4000 ft AGL	695 (16.3%)	279 (12.6%)	746 (16.5%)	303 (12.8%)	763 (16.2%)	347 (13.9%)
4000–<4500 ft AGL	694 (16.2%)	252 (11.4%)	743 (16.4%)	278 (11.7%)	800 (17.0%)	307 (12.3%)
4500–<5000 ft AGL	373 (8.7%)	129 (5.8%)	379 (8.4%)	147 (6.2%)	395 (8.4%)	157 (6.3%)
5000–<5500 ft AGL	506 (11.8%)	169 (7.6%)	527 (11.6%)	196 (8.3%)	573 (12.2%)	212 (8.5%)

[1] Percentages are based on "holding flights required". [2] Note that an individual flight can hold in multiple altitude bands.

Consistent with increasing holding demand, holding intensity also increases with mean holding orbit counts reaching ∼7.7–8.1 under Δt_{UAS} = 15 min, and the median increases from 3.0 to 4.0, suggesting that multi-orbit holdings become increasingly typical. Although a "typical" holding event may remain moderate (median of 3–4 orbits), a subset of days exhibits substantially longer holding sequences that increase the mean. Together with the significant share of UAS flights that require holding, compared to Juist (EDWJ), this indicates that there are operating periods in which holding becomes the dominant mode of UAS flow management. In practice, this means that UAS spend a large fraction of their time in the holding stack, waiting for conflict-free entry windows while holdings accumulate, rather than UAS progressing directly to the runway.

The altitude band statistics further show that, at Egelsbach (EDFE), UAS holdings are more distributed across altitudes than at Juist (EDWJ) under the "assigned" condition. Although the lowest band (i.e., 2500–<3000 ft (∼760–<910 m) AGL) still captures the largest share of holding flights, it accounts for only ∼51–69% of use by UAS, with a substantial share of UAS holdings occupying 3000–<5500 ft (∼910–<1680 m) AGL. This is also reflected by mean holding altitudes consistently exceeding 2500 ft (∼760 m) AGL and by median holding altitudes that occasionally exceed hold_{min}.

Overall, the results for Egelsbach (EDFE) show that UAS holdings are a frequently used mechanism for conflict management, while longer look-ahead times increase both

the frequency and duration of holdings, and the "assigned" condition increases holding denials that become significant under higher UAS traffic volumes (i.e., Δt_{UAS} = 15 min). Compared to Juist (EDWJ), Egelsbach (EDFE) exhibits a significantly higher demand for UAS holdings. While Juist (EDWJ) requires holding in only ∼5–9% of flights under the "assigned" condition, Egelsbach (EDFE) requires holding in ∼35–40% of flights, and the holding intensity is substantially higher (mean holding orbit counts of ∼6–8 at Egelsbach (EDFE) versus ∼2–3 at Juist (EDWJ)). Moreover, denied holdings remain negligible at Juist (EDWJ) but become a notable mechanism at Egelsbach (EDFE) under the "assigned" condition, implying reduced operational flexibility that limits traffic capacity at Egelsbach (EDFE) under the simulated conditions. Note that statistics for gate releases at $\mathtt{HLD}_{\mathtt{WP8}}$ by altitude bands can be found for both airports in Appendix A.2 in Table A1.

Figures 23 and 24 summarize the temporal and vertical characteristics of UAS holdings using the rule-based terminal deconfliction logic presented in Section 3.2, shown for different look-ahead times (60/120/180 s) and UAS traffic volumes (Δt_{UAS} = 15/30 min). For each configuration, the upper bar plot shows the accumulated holding minutes per time bin (i.e., 15 min), with the color indicating the daily mean holding occurrence in that time bin. The lower heatmap displays the same holding minutes across time and altitude bins as well as the weighted mean holding altitude.

In all configurations for Juist (EDWJ), the results illustrate a clear trade-off. Increasing the look-ahead horizon generally increases total holding minutes, particularly for higher UAS traffic volumes (i.e., Δt_{UAS} = 15 min). This indicates that more predictive look-ahead times trigger UAS holdings more frequently and/or earlier, thereby generating UAS throughput delays but providing an additional tactical separation margin. Similarly, shortening the UAS traffic rate from 30 min to 15 min increases holding demand throughout the day.

In summary, higher UAS throughput generates more frequent interactions with existing manned traffic and more frequent activation of UAS holdings and stacking. The holding heatmaps for Juist (EDWJ) further show that UAS holdings are conducted predominantly in the lowest available altitude band (i.e., 2500–<3000 ft (∼760–<910 m) AGL) for most time bins. Higher altitude bands for holding appear rarely, suggesting that a vertical holding distribution is used as a mechanism to manage local traffic peaks rather than as a default holding strategy.

Finally, time-of-day considerations reveal that holding demand concentrates on the main traffic periods (∼11:00 AM–4:00 PM), providing time windows for the integration availability of UAS into the terminal airspace. Time and altitude bins with low holding minutes correspond to periods when the UAS TP integration area is more frequently accessible for UAS approaches.

For Egelsbach (EDFE), the heatmap in Figure 24 depicts a more holding intensive and vertically diversified UAS holding scheme than for Juist (EDWJ), which is consistent with the simulation statistics in the previous Tables 4 and 5. Again, the upper bar charts show large numbers of accumulated holding minutes throughout the day, particularly for Δt_{UAS} = 15 min, indicating that UAS holdings are not used occasionally but as a dominant deconfliction mechanism over extended time periods.

Similarly, increasing the look-ahead time generally increases the total holding minutes, reflecting the expected safety versus throughput trade-off by triggering holdings more frequently and/or earlier and increasing throughput delay while providing additional tactical separation margins.

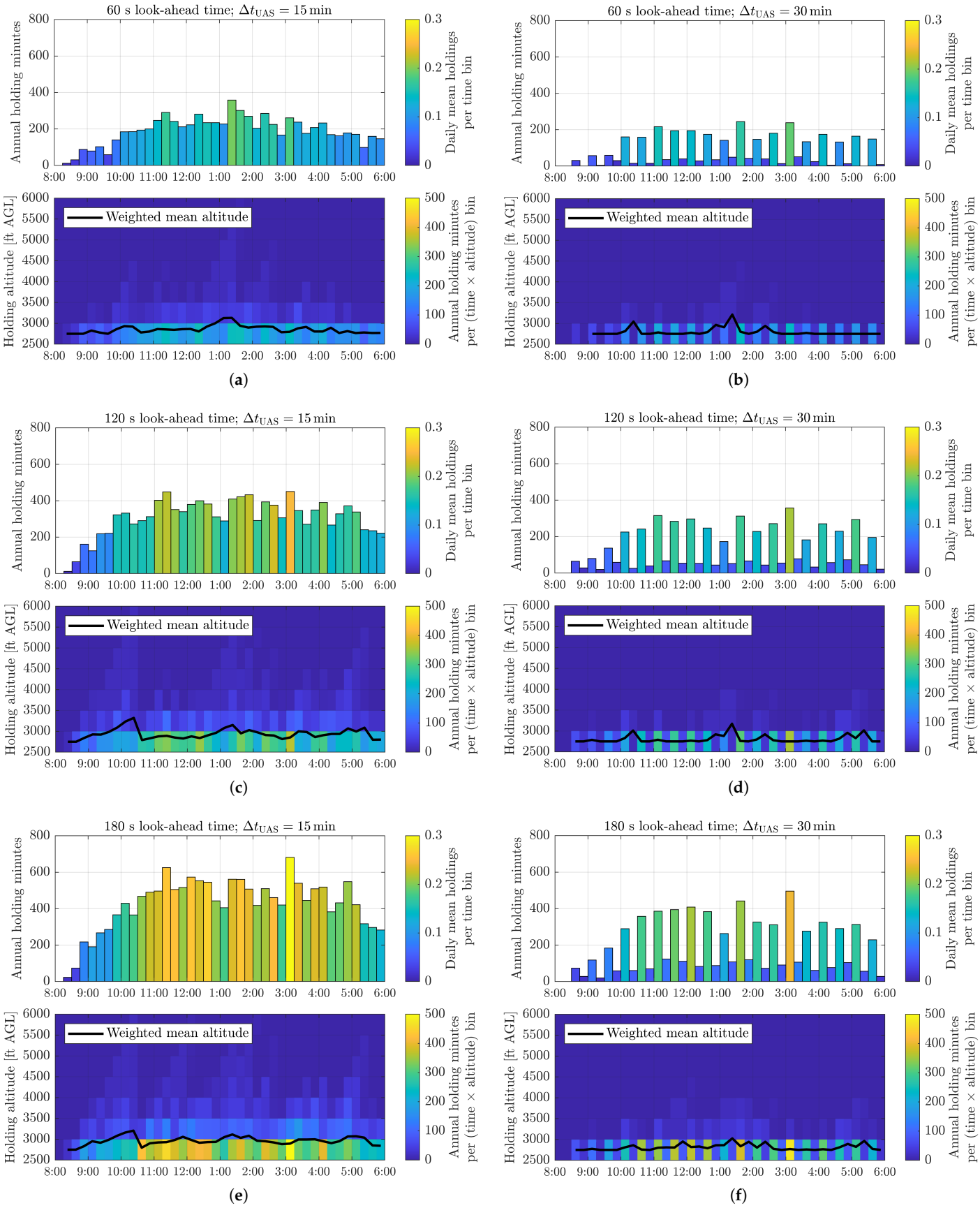

Figure 23. UAS holding heatmaps with 15 min bins for Juist (EDWJ): 60 s look-ahead time with (**a**) Δt_{UAS} = 15 min and (**b**) Δt_{UAS} = 30 min. 120 s look-ahead time with (**c**) Δt_{UAS} = 15 min and (**d**) Δt_{UAS} = 30 min. 180 s look-ahead time with (**e**) Δt_{UAS} = 15 min and (**f**) Δt_{UAS} = 30 min.

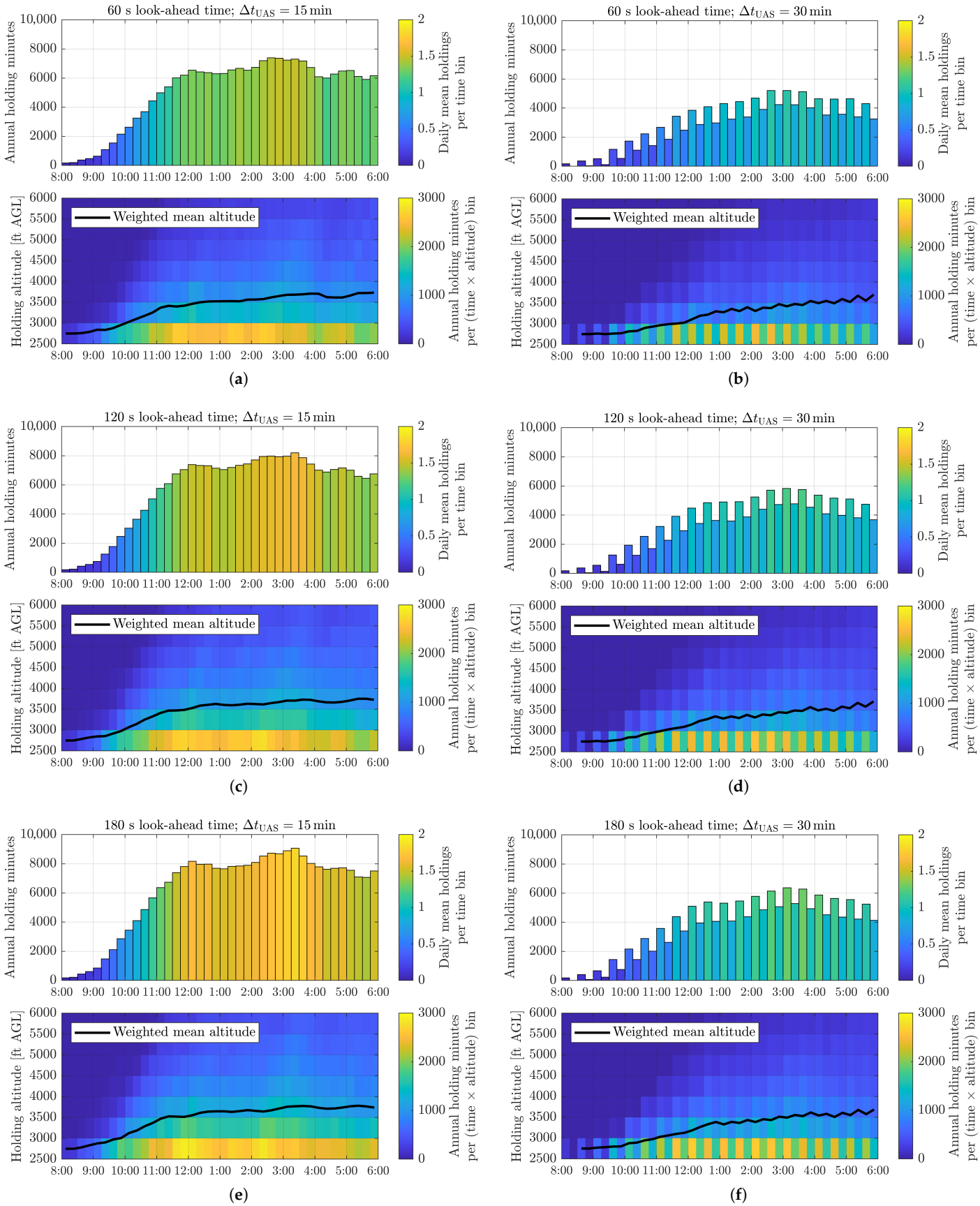

Figure 24. UAS holding heatmaps with 15 min bins for Egelsbach (EDFE): 60 s look-ahead time with (**a**) Δt_{UAS} = 15 min and (**b**) Δt_{UAS} = 30 min. 120 s look-ahead time with (**c**) Δt_{UAS} = 15 min and (**d**) Δt_{UAS} = 30 min. 180 s look-ahead time with (**e**) Δt_{UAS} = 15 min and (**f**) Δt_{UAS} = 30 min.

In contrast to Juist (EDWJ), the lower heatmaps highlight that Egelsbach (EDFE) does not rely on a single dominant holding altitude band, such as 2500–<3000 ft (∼760–<910 m) AGL at Juist (EDWJ). Still, holding activities are high at the lowest available altitude band at Egelsbach (EDFE), but the vertical distribution of holdings increasingly spreads into higher altitude bands and the weighted mean holding altitude rises over the course of the day up to 3500–<4000 ft (∼1070–<1220 m) AGL. This can also be observed under the higher UAS traffic volume (i.e., t_{UAS} = 15 min), where both the magnitude of holding minutes and the vertical distribution of holdings are highest. However, even at lower UAS traffic volumes, multi-layer holdings are frequently used to assure deconfliction from manned aviation.

In operational terms, the heatmaps imply that for Egelsbach (EDFE) the UAS TP integration area is rarely "free" and that the proposed UAS operating scheme increasingly depends on vertical distribution of holdings. Compared to Juist (EDWJ), Egelsbach (EDFE) shows markedly higher holding minutes throughout the day and much broader altitude band utilization of UAS holdings with an increased weighted mean holding altitude, highlighting a more constrained airspace environment for UAS integration using the proposed deconfliction principles.

5. Conclusions

The introduction of UAS around non-towered airport environments, where ATC services are usually unavailable and non-cooperative VFR traffic is increasingly present, remains one of the most challenging UAS integration problems. Initial UAS operations, such as for the commercial cargo use case, must be feasible without degrading safety, fairness, or capacity for existing manned traffic present in terminal airspace. However, a central integration dilemma is that increasing predictive separation thresholds to avoid UAS interaction with manned aircraft likely reduces operational efficiency. Conservative deconfliction decisions may reduce conflict risk, but can increase delay, reduce throughput, and restrict general airspace accessibility. Addressing this dilemma requires an initial conceptual approach to quantitatively assess airspace accessibility of UAS in uncontrolled terminal environments.

In this work, historical temporal and spatial manned traffic distributions are assessed and a fast-time simulation framework is developed to evaluate tactical deconfliction procedures for UAS approaching non-towered airport TPs with manned aviation in their vicinity. The simulation framework applies historical manned flight track data, fixed terminal flight procedures for UAS (such as standard TP overhead join procedures and holding maneuvers for deconfliction), and rule-based operational decision-making that represent an exemplary UAS operation scheme. The simulation logic includes look-ahead detection of manned traffic activities, a FIFO queuing logic for approaching UAS, minimum separation principles, and airspace capacity constraints. The simulation design can be used across varying scenario configurations to derive metrics that assess UAS throughput (share of holding flights), delay propagation (holding minutes and holding orbit counts), fairness among UAS interaction (FIFO queuing), concept feasibility (aborted/denied holdings), and vertical altitude band usage above non-towered airports.

In all simulation scenarios investigated, the results consistently show a safety versus throughput trade-off. Increasing the look-ahead time (i.e., from 60 s to 120 s to 180 s) to detect manned traffic interaction generally increases the share of simulated flights requiring holding and the accumulated holding minutes. This indicates that more predictive look-ahead times trigger earlier or more frequent preventive interventions, such as UAS holdings in this operating scheme. At the same time, longer look-ahead times reduce the share of aborted holding flights, suggesting that earlier deconfliction decisions enable more stable holding executions once holding is initiated. Varying UAS traffic volumes (i.e.,

one UAS every 15 min or 30 min) further demonstrate that higher UAS traffic rates can increase holding demand and delay propagation. Importantly, the simulation study also provides insight into when the terminal airspace relevant for UAS integration is effectively "accessible" for UAS utilization and which day times and altitude bands are required for holding.

The comparative analysis of two German non-towered airports, Juist (EDWJ) and Egelsbach (EDFE), relevant for initial commercial cargo UAS operations further emphasizes that it is unlikely that there will be a "one size fits all" approach for UAS holding placements and terminal integration procedures. Juist (EDWJ) exhibits a relatively low demand for holdings to deconflict UAS with manned aviation, while most holdings are executed successfully, predominantly within minimum holding altitude (i.e., 2500 ft (∼760 m) AGL). Based on the simulated design, this indicates that UAS holdings can serve as an effective tactical conflict management mechanism with limited complexity in the vertical distribution of holding layers. In contrast, Egelsbach (EDFE), the busiest non-towered airport in Germany, exhibits substantially higher holding prevalence, broader altitude band utilization of holdings, and higher shares of holding denials. This indicates a more constrained airspace environment where vertical allocation of holdings becomes an important mechanism to manage holding demand. A deconfliction strategy using only holdings may not scale well at Egelsbach (EDFE), because high holding demand and limited release opportunities can trap UAS in the holding stack and increase the probability of infeasible outcomes. However, the proposed simulation framework can be used to identify time windows with lower traffic density and higher predicted accessibility, enabling operating schedules in which UAS access is feasible at Egelsbach (EDFE). These differences highlight that terminal airspace accessibility and operational feasibility are strongly context-dependent, driven by airport-specific TP layouts and related integration procedures, and constraint settings (e.g., safety thresholds).

This work relies on several important conceptual assumptions. First, it is assumed that DAA capabilities on board the UAS will be certified and functional in uncontrolled terminal airspace environments. Second, because IFR operations for UAS may not be feasible in many non-towered airport environments, the proposed operating scheme implies a setting in which UAS must integrate under procedural rules that are compatible with today's or "new" sets of flight rules. Third, and most importantly, the simulation study assumes perfect traffic information and intent knowledge. Manned traffic trajectories and near-term intent are treated as known without reflecting different states of intent uncertainty. In operational reality, historical traffic data can provide knowledge on common TP usage and spatio-temporal airspace occupancies, but historical data alone is insufficient for real-time integration of UAS. Tactical decisions will largely depend on where aircraft are likely to go next, instead of relying on where they have been. UAS integration frameworks therefore require intent prediction concepts that constrain the set of reachable conflict-free UAS options without perfect intent knowledge. Future work will have to include intent uncertainty consistent with observed manned traffic variability, such as unexpected turns, speed changes, or altitude deviations, to quantify how these intent uncertainties impact conflict alerts and the resulting holding decisions.

Consequently, limitations and research needs follow from these assumptions. Using static historical flight tracks neglects trajectory negotiation between manned aircraft and UAS, as manned aircraft do not adapt their flight behavior in response to UAS appearances in the simulation setup. This can bias estimated conflicts, deconfliction procedures, and efficiency considerations, since real-world operations may involve interaction maneuvers (e.g., self-sequencing, TP leg extensions, and missed approaches). Future work should extend the simulation framework with cooperative decision-making mechanisms, including

dynamic sequencing, trajectory negotiation, or priority-based allocation of arrival slots, to improve UAS throughput and delay propagation while maintaining the same deconfliction and separation constraints.

Moreover, in this paper, "safety" is addressed in an operational sense by evaluating whether the proposed procedures maintain separation and avoid detected conflicts under realistic traffic conditions. Measures such as holding frequency, holding duration, and aborted UAS operations are safety-relevant indicators rather than probabilistic risk metrics such as loss-of-separation probability or collision risk. Future work will have to move from these indicators to probabilistic risk metrics by combining separation principles (i.e., VMD/HMD) with different states of manned intent uncertainty and encounter-rate modeling, for example.

Furthermore, the proposed simulation framework evaluates tactical deconfliction performance, but does not establish regulatory safety thresholds that distinguish between different levels of safety-critical traffic volumes or terminal look-ahead times to detect conflicts. To date, these safety margins, as well as robust UAS integration capabilities such as merging and spacing around an airport TP, have not yet been defined and standardized in regulations. In addition, UAS integration decisions will depend on whether the operation is in a nominal or off-nominal state (e.g., contingency situations such as an LC2L). Although the proposed concept suggests that a UAS in an LC2L state, for example, unable to integrate into holding would execute a missed approach or divert to an alternative airport, the simulation study does not include specific off-nominal procedures due to the current lack of standardizations. Addressing these gaps requires the development of safety regulations and operational concepts for contingency handling, along with simulation studies that incorporate intent uncertainty, surveillance errors, and communication delays, such as between the RP and the UA.

In addition, the simulation study assumed that the relevant airspace segment of the TP for UAS integration must be "free" before the UAS can integrate into the airport TP. With the introduction of advanced DAA systems, it can be expected that UAS will be able to space and merge with (multiple) manned aircraft present in the TP. However, this "traffic-free" access rule is a conservative baseline and is expected to overestimate UAS holding demand while underestimating UAS throughput. Future work will have to incorporate spacing and merging logic to quantify their impact on holding rates, UAS throughput, and predicted conflicts to improve operational realism.

The simulation results are derived from two German non-towered airport environments and should therefore be interpreted within the bounds of comparable non-towered terminal airspaces. In particular, the proximity of Egelsbach (EDFE) to the CTR of Frankfurt (EDDF) and the resulting traffic and airspace constraints may not be representative to other non-towered environments. Moreover, the findings provide simulation-based evidence under the assumptions of this study and do not constitute operational validation or implementation readiness. Future work will have to extend the analysis to a broader set of non-towered airport types (e.g., varying proximity to controlled airspace, traffic mixes, and TP geometry) and will have to complement the simulation with human-in-the-loop, for example, to test the transferability of the proposed procedures.

Moreover, holding capacity is intentionally constrained to one UAS per holding layer, consistent with conventional IFR holding level assignment. Future work could extend the holding framework to quantify layer capacity by allowing multiple UAS per layer using additional sequencing and separation logic, and to evaluate saturation measures such as delaying entry or diverting to an alternate airport.

In addition, the analysis of this paper focuses on operational feasibility and does not quantify economic impacts (e.g., energy consumption of UAS or cost of time). However, the UAS holding times translate into additional operational times, increased energy use, and increased operating cost. Future work could couple delay outputs to operational cost measures (e.g., cost per minute of delay in holding) to estimate the economic tradeoffs of different deconfliction and spacing settings.

Finally, neglecting wind and meteorological conditions likely makes the results optimistic, as UAS trajectories and arrival times are perfectly repeatable in the simulation. In reality, wind can shift flight tracks and affect maneuver timing, increasing uncertainty and typically requiring more conservative spacing, which in turn can increase holding demand. Meteorological uncertainty (e.g., wind-driven TP variations and weather-related operational constraints) should therefore be incorporated in future work, for example, by extending the simulation with stochastic weather scenarios and assessing the resulting impacts on UAS accessibility, holding demand, and conflict risk.

Funding: This research received no external funding.

Data Availability Statement: Relevant data can be found in the manuscript. Restrictions apply to the availability of raw data sets used from Flightradar24. Raw data obtained from Flightradar24 are available at https://www.flightradar24.com (accessed on 21 June 2023) with the permission of Flightradar24. Selected processed data sets are available from the author on reasonable request.

Acknowledgments: The author wants to thank Gunnar Schwoch, Jordan Sakakeeny, Franz Knabe, and Enno Nagel for discussion and feedback on the concept and the simulation work. During the preparation of this study, the author used ChatGPT-5 for the purpose of providing support in coding the Matlab script for the simulation study and to enhance readability and language of the manuscript. The author has carefully reviewed and edited the output and takes full responsibility for the content of this publication.

Conflicts of Interest: The author declares no conflicts of interest.

Abbreviations

The following abbreviations are used in this manuscript:

ACAS	Airborne Collision Avoidance System
ADS-B	Automatic Dependent Surveillance-Broadcast
AFR	Automated Flight Rules
AGL	Above Ground Level
ATC	Air Traffic Control
ATM	Air Traffic Management
ATZ	Aerodrome Traffic Zone
BFR	Basic Flight Rules
BVLOS	Beyond Visual Line Of Sight
C2	Command and Control
CNS	Communication, Navigation, and Surveillance
ConOps	Concept of Operations
DAA	Detect And Avoid
DAIDALUS	Detect and Avoid Alerting Logic for Unmanned Systems
DAR	Dynamic Airspace Reconfiguration
DFR	Digital Flight Rules
DLR	German Aerospace Center
EASA	European Union Aviation Safety Agency
EFR	Enhanced Flight Rules
EU	European Union
eVTOL	electric Vertical Takeoff and Landing

FIFO	First-In/First-Out
FL	Flight Level
HFR	High-Level Flight Rules
HMD	Horizontal Miss Distance
IAP	Instrument Approach Procedure
ICAO	International Civil Aviation Organization
IFR	Instrument Flight Rules
IMC	Instrument Meteorological Condition
GBSS	Ground-Based Surveillance System
LC2L	Lost Command and Control Link
LFR	Low-Level Flight Rules
MFR	Managed Flight Rules
MLAT	Multilateration
MOPS	Minimum Operational Performance Standards
MSL	Mean Sea Level
MTOW	Maximum Takeoff Weight
NASA	National Aeronautics and Space Administration
RAM	Regional Air Mobility
RMZ	Radio Mandatory Zone
RP	Remote Pilot
RWY	Runway
SARPs	Standards and Recommended Practice
SATS	Small Aircraft Transportation System
SID	Standard Instrument Departure Route
STAR	Standard Terminal Arrival Route
TaFR	Tailored Flight Rules
TCAS	Traffic Alert and Collision Avoidance System
TMA	Terminal Control Area
TMZ	Transponder Mandatory Zone
TP	Traffic Pattern
TPA	Traffic Pattern Altitude
TTM	Tailored Trajectory Management
UA	Unmanned Aircraft
UAM	Urban Air Mobility
UAS	Unmanned Aircraft System
UFR	U-Space Flight Rules
US	United States
USSP	U-Space Service Provider
VFR	Visual Flight Rules
VHF	Very High Frequency
VLOS	Visual Line Of Sight
VMC	Visual Meteorological Condition
VMD	Vertical Miss Distance
VOC	Visual Operating Chart
WP	Waypoint

https://doi.org/10.3390/drones10020141

Appendix A

Appendix A.1

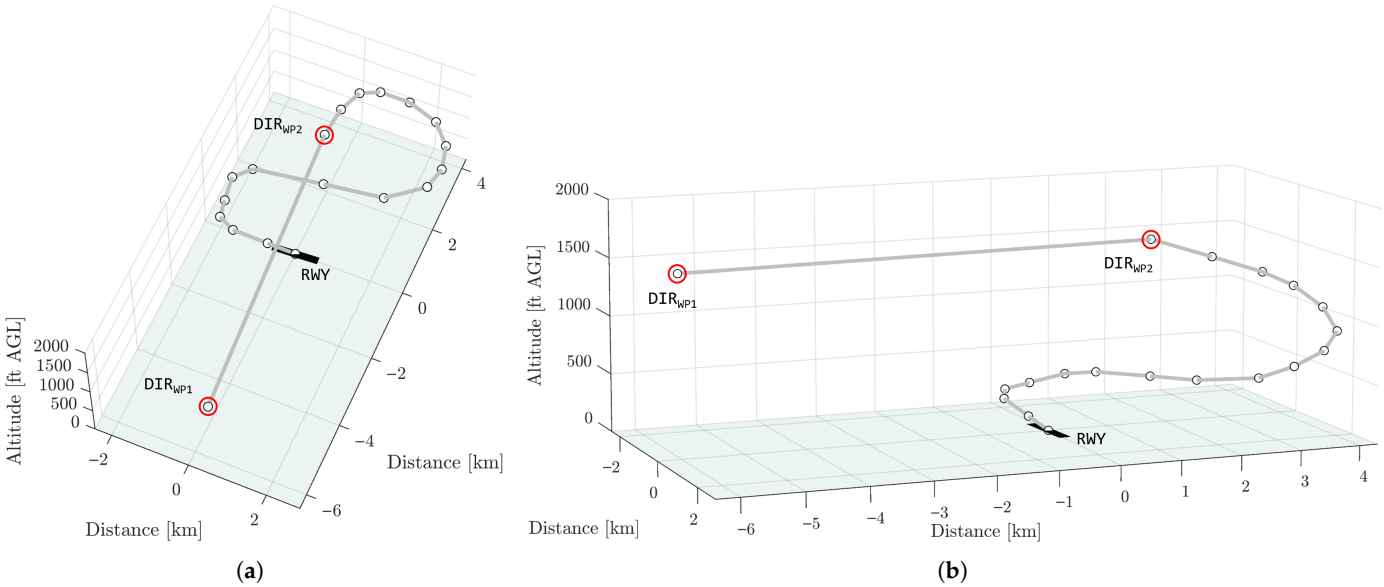

Figure A1. UAS trajectory and key WPs from terminal airspace entry via overhead join into airport TP downwind leg towards runway, using the dimensions of Egelsbach (EDFE): (**a**) top view and (**b**) side view.

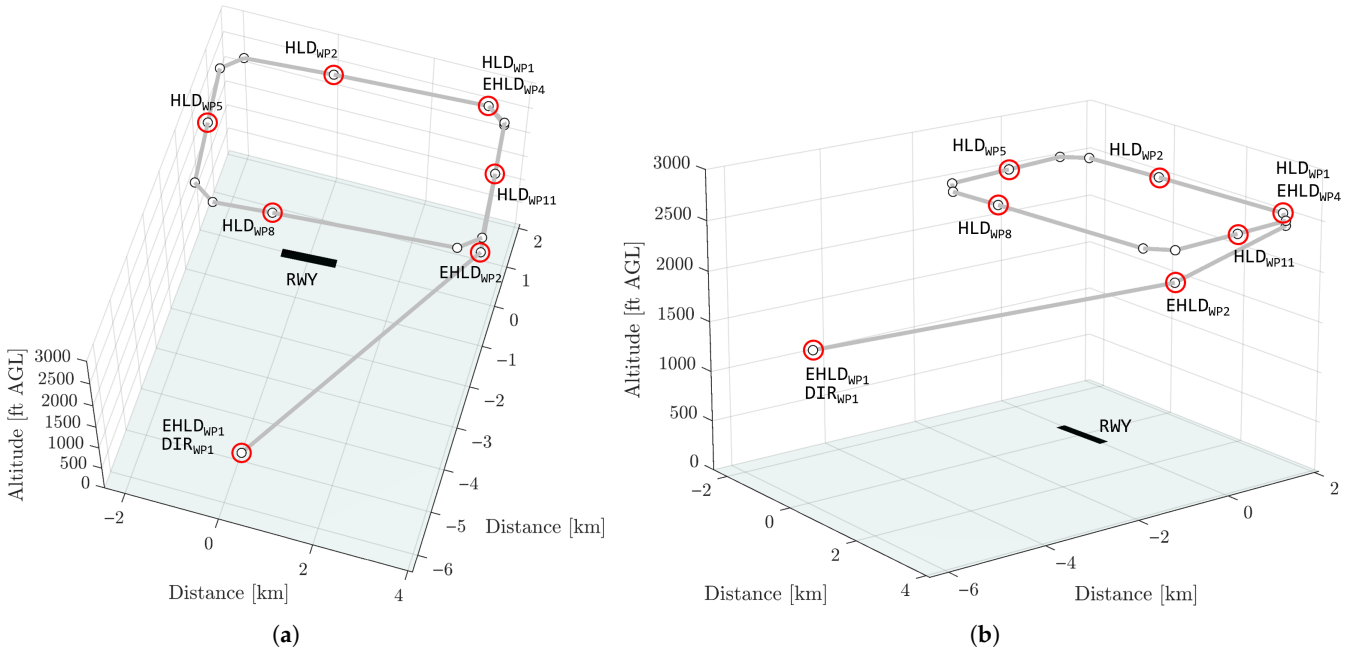

Figure A2. UAS trajectory and key WPs from terminal airspace entry via holding entry into holding above TP, using the dimensions of Egelsbach (EDFE): (**a**) top view and (**b**) side view.

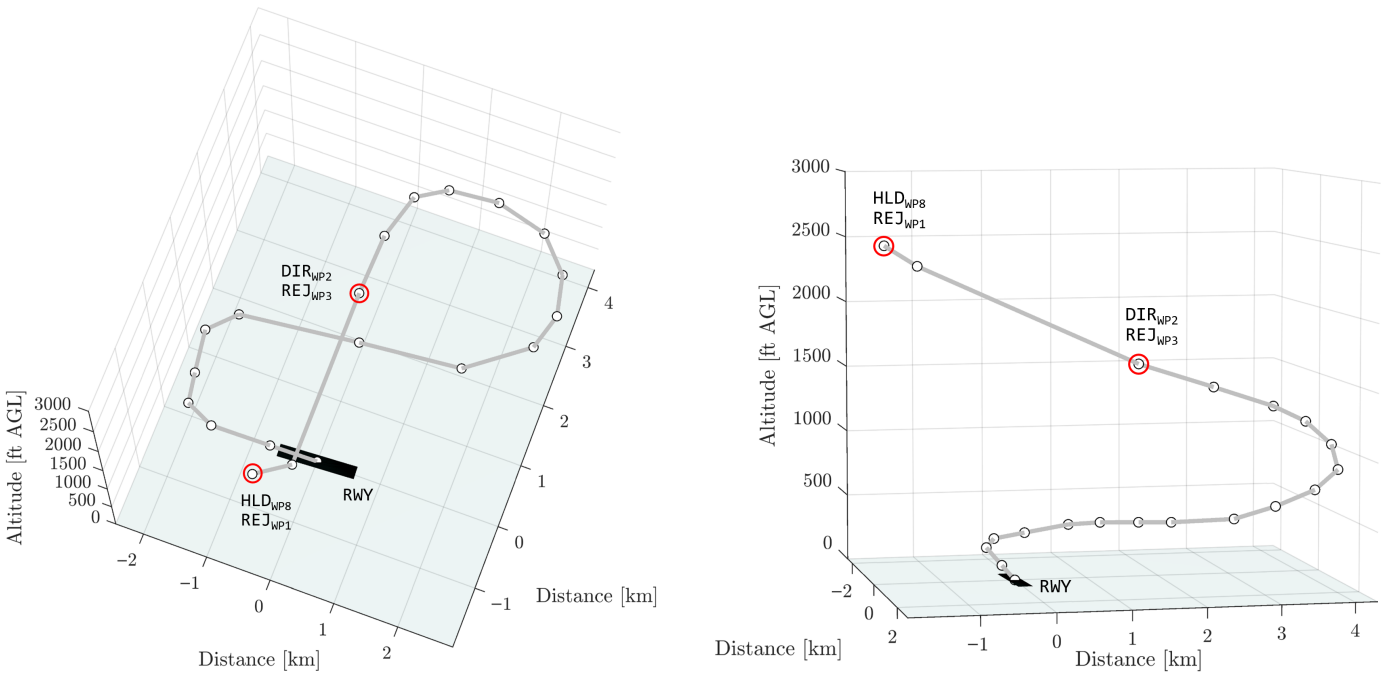

Figure A3. UAS trajectory and key WPs from holding via overhead join into airport TP downwind leg towards runway, using the dimensions of Egelsbach (EDFE): (**a**) top view and (**b**) side view.

Appendix A.2

Table A1. Holding gate release counts (at HLD$_{WP8}$) by altitude band under "assigned" condition. Note that percentages are based on holding flights per altitude band as shown in Tables 4 and 5.

Juist (EDWJ): "Assigned" Condition						
Look-ahead time for conflict detection	60 s		120 s		180 s	
UAS traffic rate (Δt_{UAS})	15 min	30 min	15 min	30 min	15 min	30 min
Gate releases by holding altitude band						
2500–<3000 ft AGL	716 (100.0%)	317 (100.0%)	932 (100.0%)	425 (100.0%)	1117 (100.0%)	517 (100.0%)
3000–<3500 ft AGL	0 (0.0%)	0 (0.0%)	1 (6.3%)	0 (0.0%)	4 (13.3%)	0 (0.0%)
3500–<4000 ft AGL	13 (81.2%)	2 (100.0%)	33 (67.4%)	3 (75.0%)	59 (66.3%)	5 (71.4%)
4000–<4500 ft AGL	6 (100.0%)	1 (100.0%)	15 (71.4%)	0 (0.0%)	26 (60.5%)	1 (50.0%)
4500–<5000 ft AGL	0 (0.0%)	0 (0.0%)	0 (0.0%)	0 (0.0%)	0 (0.0%)	0 (0.0%)
5000–<5500 ft AGL	2 (66.7%)	0 (0.0%)	5 (50.0%)	0 (0.0%)	9 (50.0%)	0 (0.0%)
Egelsbach (EDFE): "Assigned" Condition						
Look-ahead time for conflict detection	60 s		120 s		180 s	
UAS traffic rate (Δt_{UAS})	15 min	30 min	15 min	30 min	15 min	30 min
Gate releases by holding altitude band						
2500–<3000 ft AGL	2451 (100.0%)	1523 (100.0%)	2438 (100.0%)	1551 (100.0%)	2391 (100.0%)	1558 (100.0%)
3000–<3500 ft AGL	778 (75.9%)	338 (70.3%)	885 (80.9%)	393 (76.5%)	958 (84.9%)	455 (79.6%)
3500–<4000 ft AGL	439 (63.2%)	154 (55.2%)	511 (68.5%)	191 (63.0%)	563 (73.8%)	222 (64.0%)
4000–<4500 ft AGL	464 (66.9%)	154 (61.1%)	541 (72.8%)	185 (66.6%)	611 (76.4%)	205 (66.8%)
4500–<5000 ft AGL	8 (2.1%)	2 (1.6%)	9 (2.4%)	3 (2.0%)	6 (1.5%)	2 (1.3%)
5000–<5500 ft AGL	234 (46.3%)	67 (39.6%)	261 (49.5%)	81 (41.3%)	306 (53.4%)	93 (43.9%)

References

1. Thipphavong, D.P.; Apaza, R.D.; Barmore, B.E.; Battiste, V.; Burian, B.K.; Dao, Q.V.; Feary, M.S.; Go, S.; Goodrich, K.H.; Homola, J.R.; et al. Urban Air Mobility Airspace Integration Concepts and Considerations. In Proceedings of the AIAA 2018 Forum, Atlanta, GA, USA, 25–29 June 2018. [CrossRef]
2. Pak, H.; Asmer, L.; Kokus, P.; Schuchardt, B.I.; End, A.; Meller, F.; Schweiger, K.; Naeem, N.; Papenfuß, A.; Pertz, J.; et al. Can Urban Air Mobility Become Reality? Opportunities and Challenges of UAM as Innovative Mode of Transport and DLR Contribution to Ongoing Research. *CEAS Aeronaut. J.* **2025**, *16*, 665–695. [CrossRef]

3. Walsh, R. *Regional Air Mobility: Infrastructure Challenges, Passenger and Cargo Market Potential, and Sustainability Strategies for Underserved Airports*; NASA Technical Reports Server (NTRS) Document ID 20250002542; NASA Langley Research Center: Hampton, VA, USA, 2025.
4. Antcliff, K.; Borer, N.; Sartorius, S.; Saleh, P.; Rose, R.; Gariel, M.; Oldham, J.; Courtin, C.; Bradley, M.; Roy, S.; et al. *Regional Air Mobility: Leveraging Our National Investments to Energize the American Travel Experience*; White Paper; NASA Langley Research Center: Hampton, VA, USA, 2021.
5. Hayashi, M.; Idris, H.; Sakakeeny, J.; Jack, D. *PAAV Concept Document*; White Paper; NASA Ames Research Center: Moffett Field, CA, USA, 2022.
6. EUROCONTROL. *UAS ATM Integration Operational Concept*; Conceptual Report; EUROCONTROL: Brussels, Belgium, 2018.
7. International Civil Aviation Organization (ICAO). *Unmanned Aircraft Systems Traffic Management (UTM): A Common Framework with Core Principles for Global Harmonization*, 4th ed.; Conceptual Report; ICAO: Montréal, QC, Canada, 2023.
8. Teutsch, J.; Petersen, C.C.; Schwoch, G.; Bos, T.; Lieb, J.; Zon, R. On the Impact of UAS Contingencies on ATC Operations in Shared Airspace. In Proceedings of the 2023 Integrated Communications, Navigation and Surveillance Conference (ICNS), Dulles, VA, USA, 18–20 April 2023. [CrossRef]
9. Mühlhausen, T.; Peinecke, N. Capacity and Workload Effects of Integrating a Cargo Drone in the Airport Approach. In *Automated Low-Altitude Air Delivery*; Dauer, J.C., Ed.; Springer: Cham, Switzerland, 2021; pp. 449–461.
10. Sakakeeny, J.; Idris, H.; Jack, D.; Bulusu, V. A Framework for Dynamic Architecture and Functional Allocations for Increasing Airspace Autonomy. In Proceedings of the AIAA Aviation 2022 Forum, Chicago, IL, USA, 27 June–1 July 2022. [CrossRef]
11. Sievers, T.F.; Sakakeeny, J.; Idris, H.; Peinecke, N.; Bulusu, V.; Nagel, E.; Jack, D. Conceptual Development of Terminal Airspace Integration Procedures of Large Uncrewed Aircraft Systems at Non-Towered Airports. *Drones* **2025**, *9*, 858. [CrossRef]
12. European Union Aviation Safety Agency (EASA). i-Conspicuity: Interoperability of Electronic Conspicuity Systems for General Aviation. Available online: https://www.easa.europa.eu/en/research-projects/i-conspicuity-interoperability-electronic-conspicuity-systems-general-aviation (accessed on 22 December 2025).
13. RTCA, Inc. *DO-381: MOPS for Ground-Based Surveillance Systems (GBSS) for Traffic Surveillance*; RTCA, Inc.: Washington, DC, USA, 2020.
14. Bulusu, V.; Idris, H.; Chatterji, G. Analysis of VFR Traffic Uncertainty and Its Impact on Uncrewed Aircraft Operational Capacity at Regional Airports. In Proceedings of the AIAA Aviation 2023 Forum, San Diego, CA, USA, 12–16 June 2023; p. 3553. [CrossRef]
15. Acharya, A.; Bulusu, V.; Idris, H. VFR Trajectory Forecasting Using Deep Generative Model for Autonomous Airspace Operations. In Proceedings of the 43rd Digital Avionics Systems Conference (DASC), San Diego, CA, USA, 29 September–3 October 2024. [CrossRef]
16. RTCA, Inc. *DO-365B: Minimum Operational Performance Standards (MOPS) for Detect and Avoid (DAA) Systems*; RTCA, Inc.: Washington, DC, USA, 2021.
17. Rorie, R.C.; Smith, C.L. Detect and Avoid and Collision Avoidance Flight Test Results with ACAS Xr. In Proceedings of the 43rd Digital Avionics Systems Conference (DASC), San Diego, CA, USA, 29 September–3 October 2024. [CrossRef]
18. Reliable Robotics Corporation. Flight Testing for ACAS X Detect and Avoid (DAA) Standards. Available online: https://reliable.co/blog/flight-testing-for-acas-x-detect-and-avoid-daa-standards (accessed on 18 September 2025).
19. International Civil Aviation Organization (ICAO). *ICAO Doc 8168: Aircraft Operations—Volume II: Construction of Visual & Instrument Flight Procedures (Sixteenth Edition)*; ICAO: Montréal, QC, Canada, 2020.
20. Sievers, T.F.; Sakakeeny, J.; Dimitrova, N.; Idris, H. Operational Integration Potential of Regional Uncrewed Aircraft Systems into the Airspace System. *CEAS Aeronaut. J.* **2025**, *16*, 1037–1059. [CrossRef]
21. Andrews, J.; Lara, M.; Yon, R.; Del Rosario, R.; Block, J.; Davis, T.; Hasan, S.; Weingart, D.; Frankel, C.; Spitz, B.; et al. *LMI Automated Air Cargo Operations Market Research and Forecast*; NASA Contractor Report; NASA Ames Research Center: Moffett Field, CA, USA, 2021.
22. Sakakeeny, J.; Sievers, T.F.; Idris, H. Potential of United States and European Regional Air Cargo Operations for Uncrewed Aircraft Systems. In Proceedings of the 15th USA/Europe Air Traffic Management Research and Development Seminar (ATM2023), Savannah, GA, USA, 5–9 June 2023.
23. Reliable Robotics Corporation. Reliable Robotics—Company. Available online: https://reliable.co/company (accessed on 21 January 2025).
24. Merlin Labs. Merlin—Home. Available online: https://merlinlabs.com/ (accessed on 21 January 2025).
25. Pipistrel. Cargo Reimagined. Available online: https://www.pipistrel-aircraft.com/air-cargo/ (accessed on 5 December 2025).
26. Textron Aviation Inc. Textron Aviation—Grand Caravan EX Photos. Available online: https://media.txtav.com/assets/225573/ (accessed on 9 May 2023).
27. European Union Aviation Safety Agency (EASA). Certified Category—Civil Drones. Available online: https://www.easa.europa.eu/en/domains/drones-air-mobility/operating-drone/certified-category-civil-drones (accessed on 3 March 2025).
28. International Civil Aviation Organization (ICAO). *Annex 2 to the Convention on International Civil Aviation: Rules of the Air*, 10th ed.; ICAO: Montréal, QC, Canada, 2005.

29. Federal Aviation Administration (FAA). Aeronautical Information Manual (AIM) (Basic with Change 1, Change 2, and Change 3). Available online: https://www.faa.gov/air_traffic/publications/ (accessed on 27 March 2025).
30. Federal Aviation Administration (FAA). Airplane Flying Handbook: FAA-H-8083-3C. 2024. Available online: https://www.faa.gov/regulations_policies/handbooks_manuals/aviation/airplane_handbook (accessed on 24 March 2025).
31. DFS Deutsche Flugsicherung. Luftfahrthandbuch Deutschland. Available online: https://aip.dfs.de/basicAIP/ (accessed on 15 September 2025).
32. Viken, S.A.; Brooks, F.M.; Johnson, S.C. Overview of the Small Aircraft Transportation System Project Four Enabling Operating Capabilities. *J. Aircr.* **2006**, *43*, 1602–1612. [CrossRef]
33. Pastor, E.; Royo, P.; Delgado, L.; Perez, M.; Barrado, C.; Prats, X. Depart and Approach Procedures for UAS in a VFR Environment. In Proceedings of the 1st International Conference on Applications and Theory of Automation in Command and Control Systems (ATACCS), Barcelona, Spain, 26–27 May 2011; pp. 27–37.
34. Bulusu, V.; Idris, H.; Acharya, A. Analysis and Prediction of VFR vs. IFR Traffic Behavior to Support Uncrewed Aircraft Flight Operations at Regional Airports. In Proceedings of the AIAA Aviation 2024 Forum, Las Vegas, NV, USA, 29 July–2 August 2024; p. 4551. [CrossRef]
35. European Union. *Commission Implementing Regulation (EU) 2021/664 of 22 April 2021 on a Regulatory Framework for the U-Space*; Implementing Regulation; European Union: Brussels, Belgium, 2021.
36. German Aerospace Center (DLR). AREA U-Space (Air Space Research Area U-Space). Available online: https://www.dlr.de/en/uc/research-and-transfer/projects-and-missions/area-u-space (accessed on 9 January 2025).
37. SESAR Joint Undertaking. *U-Space ConOps and Architecture (Edition 4)*; SESAR Joint Undertaking: Brussels, Belgium, 2023.
38. Sievers, T.F.; Geister, D.; Schwoch, G.; Peinecke, N.; Schuchardt, B.I.; Volkert, A.; Lieb, J. *DLR Blueprint—Initial ConOps of U-Space Flight Rules (UFR)*; Blueprint; German Aerospace Center (DLR), Institute of Flight Guidance: Braunschweig, Germany, 2024. [CrossRef]
39. Schwoch, G.; Geister, R.; Geister, D.; Sangermano, V.; Löhr, F.; Fas-Millán, M.A.; Gómez, M.; Sunil, E.; Reuber, E.; Rocchio, R.; et al. *INVIRCAT Final ConOps 'RPAS in the TMA'*; Final Report; SESAR Joint Undertaking: Brussels, Belgium, 2022.
40. Hoekstra, J.M.; Ellerbroek, J. Aerial Robotics: State-Based Conflict Detection and Resolution (Detect and Avoid) in High Traffic Densities and Complexities. *Curr. Robot. Rep.* **2021**, *2*, 297–307. [CrossRef]
41. Lee, S.M.; Park, C.; Thipphavong, D.P.; Isaacson, D.R.; Santiago, C. *Evaluating Alerting and Guidance Performance of a UAS Detect-and-Avoid System*; Technical Memorandum; NASA Ames Research Center: Moffett Field, CA, USA, 2016.
42. Herencia-Zapana, H.; Jeannin, J.; Muñoz, C. Formal Verification of Safety Buffers for State-Based Conflict Detection and Resolution. In Proceedings of the 27th International Congress of the Aeronautical Sciences (ICAS 2010), Nice, France, 19–24 September 2010.
43. Ribeiro, M.; Ellerbroek, J.; Hoekstra, J. Analysis of Conflict Resolution Methods for Manned and Unmanned Aviation Using Fast-Time Simulations. In Proceedings of the 9th SESAR Innovation Days, Athens, Greece, 2–6 December 2019.
44. Tadema, J.; Theunissen, E.; Kirk, K.M. Self-Separation Support for UAS. In Proceedings of the AIAA Infotech@Aerospace 2010 Conference, Atlanta, GA, USA, 20–22 April 2010. [CrossRef]
45. Idris, H.; Shen, N.; Wing, D.J. Complexity Management Using Metrics for Trajectory Flexibility Preservation and Constraint Minimization. In Proceedings of the 11th AIAA Aviation Technology, Integration, and Operations (ATIO) Conference, Virginia Beach, VA, USA, 20–22 September 2011. [CrossRef]
46. Pasaoglu, C.; Akcam, N.; Koyuncu, E.; Tarhan, A.F.; Inalhan, G. Collaborative Intent Exchange Based Flight Management System with Airborne Collision Avoidance for UAS. *J. Intell. Robot. Syst.* **2016**, *84*, 665–690. [CrossRef]
47. Zeng, F.; Idris, H.; Clarke, J. Trajectory Planning for Mission Survivability of Autonomous Vehicles in Moderately to Extremely Uncertain Environments. In Proceedings of the 14th USA/Europe Air Traffic Management Research and Development Seminar (ATM2021), Virtual, 20–23 September 2021.
48. Zeng, F.; Clarke, J.; Idris, H. A Methodology to Develop Survivability Maps for Autonomous Aerial Vehicles. In Proceedings of the AIAA Aviation 2023 Forum, San Diego, CA, USA, 12–16 June 2023. [CrossRef]
49. Alexandrov, N.M.; Ozoroski, T.A. Design for Survivability: An Approach to Assured Autonomy. In Proceedings of the 16th AIAA Aviation Technology, Integration, and Operations Conference, Washington, DC, USA, 13–17 June 2016. [CrossRef]
50. Ghasri, M.; Maghrebi, M. Factors Affecting Unmanned Aerial Vehicles' Safety: A Post-Occurrence Exploratory Data Analysis of Drones' Accidents and Incidents in Australia. *Saf. Sci.* **2021**, *139*, 105273. [CrossRef]
51. Patrikar, J.; Moon, B.; Oh, J.; Scherer, S. Predicting Like a Pilot: Dataset and Method to Predict Socially-Aware Aircraft Trajectories in Non-Towered Terminal Airspace. In Proceedings of the IEEE International Conference on Robotics and Automation (ICRA), Philadelphia, PA, USA, 23–27 May 2022; pp. 2525–2531. [CrossRef]
52. Murça, M.C.R. Identification and Prediction of Urban Airspace Availability for Emerging Air Mobility Operations. *Transp. Res. Part C Emerg. Technol.* **2021**, *131*, 103274. [CrossRef]

53. Burke, P.J. Small Unmanned Aircraft Systems (SUAS) and Manned Traffic near John Wayne Airport (KSNA) Spot Check of the SUAS Facility Map: Towards a New Paradigm for Drone Safety near Airports. *Drones* **2019**, *3*, 84. [CrossRef]
54. Hill, D.R.; Patterson, A.P.; Gregory, I.M. Simple Pattern Traffic Generation for Automated Flight Research in Non-Towered Traffic Patterns. In Proceedings of the AIAA Aviation 2025 Forum, San Diego, CA, USA, 21–25 July 2025. [CrossRef]
55. Thipphavong, D.P.; Lauderdale, T.A.; Windhorst, R.D.; Arneson, H.M.; Idris, H.; Coppenbarger, R.A.; Sakakeeny, J.; Dimitrova, N.; Bulusu, V.; Chatterji, G.; et al. Initial Study of Tailored Trajectory Management for Multi-Vehicle Uncrewed Regional Air Cargo Operations. In Proceedings of the 42nd Digital Avionics Systems Conference (DASC), Barcelona, Spain, 1–5 October 2023. [CrossRef]
56. Geister, D.; Korn, B. *Concept for Urban Airspace Integration: DLR U-Space Blueprint*; Blueprint; German Aerospace Center (DLR), Institute of Flight Guidance: Braunschweig, Germany, 2017.
57. Corraro, G.; Corraro, F.; Ciniglio, U.; Filippone, E.; Peinecke, N.; Theunissen, E.; Pastor, E.; Frau, G.; Shaw, C. Fast Time and Real Time Validation of a Remain Well Clear Function for Airspace Classes D to G. In Proceedings of the 12th SESAR Innovation Days, Budapest, Hungary, 5–8 December 2022.
58. EUROCONTROL. *ACAS Guide: Airborne Collision Avoidance Systems (March 2022)*; EUROCONTROL: Brussels, Belgium, 2022.
59. Federal Aviation Administration (FAA). *Airworthiness Approval of Traffic Alert and Collision Avoidance Systems (TCAS II), Versions 7.0 & 7.1 and Associated Mode S Transponders (AC 20-151C)*; FAA: Washington, DC, USA, 2017.
60. EUROCAE. *ED-275 Vol. I: Minimum Operational Performance Standard (MOPS) for ACAS Xu*; EUROCAE: Saint-Denis, France, 2020.
61. RTCA, Inc. *DO-386 Vol. I/II: MOPS for Airborne Collision Avoidance System Xu (ACAS Xu)*; RTCA, Inc.: Washington, DC, USA, 2020.
62. Gjersvik, A. Enhanced Parallel Simulation for ACAS X Development. In Proceedings of the 2020 IEEE High Performance Extreme Computing Conference (HPEC 2020), Waltham, MA, USA, 22–24 September 2020. [CrossRef]
63. Weinert, A.; Campbell, S.; Vela, A.; Schuldt, D.; Kurucar, J. Well-Clear Recommendation for Small Unmanned Aircraft Systems Based on Unmitigated Collision Risk. *J. Air Transp.* **2018**, *26*, 113–123. [CrossRef]
64. Pothana, P.; Joy, J.; Snyder, P.; Vidhyadharan, S. UAS Air-Risk Assessment in and Around Airports. In Proceedings of the 2023 Integrated Communications, Navigation and Surveillance Conference (ICNS), Herndon, VA, USA, 18–20 April 2023. [CrossRef]
65. Alvarez, L.E.; Jessen, I.; Owen, M.P.; Silbermanny, J.; Wood, P. ACAS sXu: Robust Decentralized Detect and Avoid for Small Unmanned Aircraft Systems. In Proceedings of the 38th Digital Avionics Systems Conference (DASC), San Diego, CA, USA, 8–12 September 2019. [CrossRef]
66. Airbus. *Blueprint for the Sky: The Roadmap for the Safe Integration of Autonomous Aircraft*; Blueprint; Airbus: San Jose, CA, USA, 2018.
67. Wing, D.; Lacher, A.; Ryan, W.; Cotton, W.; Stilwell, R.; John, M.; Vajda, P. *Digital Flight: A New Cooperative Operating Mode to Complement VFR and IFR*; Technical Memorandum; NASA Langley Research Center: Hampton, VA, USA, 2022.
68. Federal Aviation Administration (FAA). *Initial Concept of Operations for an Info-Centric National Airspace System*; Conceptual Report; FAA: Washington, DC, USA, 2022.
69. Joint Authorities for Rulemaking of Unmanned Systems (JARUS). *JARUS Whitepaper on Considerations for Automation of the Airspace Environment*; White Paper; JARUS: Vienna, Austria; Brussels, Belgium; Ottawa, ON, Canada, 2024.
70. The Boeing Company; SkyGrid; Wisk Aero. *Concept of Operations for Automated Flight Rules*; Conceptual Report; The Boeing Company: Chicago, IL, USA, 2025.
71. Flightradar24. Flightradar24: Live Flight Tracker—Real-Time Flight Tracker Map. Available online: https://www.flightradar24.com/ (accessed on 21 June 2023).
72. European Union Aviation Safety Agency (EASA). Horváth Second Workshop: Interoperability of E-Conspicuity Systems for GA. Available online: https://www.easa.europa.eu/en/downloads/139413/en (accessed on 24 May 2025).
73. European Union. Commission Implementing Regulation (EU) No 923/2012 of 26 September 2012 Laying Down the Common Rules of the Air and Operational Provisions Regarding Services and Procedures in Air Navigation. Consolidated Version of 1 May 2025. Available online: https://eur-lex.europa.eu/legal-content/EN/TXT/PDF/?uri=CELEX:02012R0923-20250501 (accessed on 9 December 2025).
74. Verma, S.A.; Tang, H.; Ballinger, D.; Chinn, F.C.; Kozon, T.E.; Farrahi, A.; Buchmann, E.; Walker, J.; Wooten, D.; Pfeiffer, J.; et al. Human Factors Evaluation of Conflict Detection Tool for Terminal Area: Terminal-Area Tactical Separation-Assured Flight Environment (T-TSAFE). In Proceedings of the 10th USA/Europe Air Traffic Management Research and Development Seminar (ATM2013), Chicago, IL, USA, 10–13 June 2013.
75. Carreño, V.A.; Masci, P.; Consiglio, M. Assistive Detect and Avoid for Pilots in the Cockpit. In Proceedings of the 41st Digital Avionics Systems Conference (DASC), Portsmouth, VA, USA, 18–22 September 2022. [CrossRef]